

THE CATAZONAL POLY-METAMORPHIC ROCKS OF CABO ORTEGAL (NW SPAIN),
A STRUCTURAL AND PETROFABRIC STUDY

BY

J. P. ENGELS

ABSTRACT

The petrological study of the southern part of the Cabo Ortegal area is a complement of Vogel's (1967) investigation of the northern half. The present investigations include a structural as well as a petrofabric study. The rocks belong to an eugeosynclinal sequence which during the Precambrian underwent prograde metamorphism from the staurolite-almandine-muscovite and the kyanite-almandine-muscovite sub-facies of the almandine-amphibolite facies through the clinopyroxene-pyralmandine (\pm hornblende) granulite facies into the eclogite facies (M_1). Several of these zones, bounded by isogrades, which are sometimes tectonic in nature, have been mapped. From the fact that the banded gneisses are only metatextitic and from the jadeite content of omphacite, the P/T conditions for the eclogite facies are estimated as: $T \approx 700^\circ - 750^\circ \text{C}$, $P \approx 11 - 13 \text{ Kb}$, and water vapour pressures: very low.

In the gneisses isoclinal folding (F_1) accompanied the metamorphism. The axial planes are subhorizontal and the fold axes plunge just west of north. The fabric analyses of eclogite (point-maximum for $[010]$) and basic granulite (point-maximum for $[001]$) show that the same stressfield which produced the F_1 -folds in the paragneisses, influenced the preferred orientation of clinopyroxene.

A second Precambrian metamorphic phase retrograded the rocks into the hornblende granulite facies (M_2). Before the onset of this phase pronounced cataclasis caused the formation of thick mylonitic horizons, followed by E-W trending drag folding (F_2). The fabric diagram for clinopyroxene does not show a preferred orientation. During this deformation phase the M_1 metamorphic zoning was turned upside down by a combined process of folding and thrusting. In the paragneisses the hornblende granulite metamorphism is marked by a second generation of kyanite. Gabbros, intruded along thrust planes, were partly metamorphosed into garnet-coronites. During this second metamorphic phase isoclinal folds (F_3) with subhorizontal axial planes and N-S axial directions were formed. The fabrics of these folds show a marked orientation of the c-axes of (metastable) diopside and brown-green hornblende parallel to the fold axis direction.

A third metamorphic phase caused further retrogradation of the rocks into the amphibolite facies (M_3). The characteristic amphibole of this phase is a blue-green hornblende. The former metabasites were metamorphosed into (garnet-)amphibolites. Intruded gabbros were transformed along their margins into 'flaser' amphibolites. Folds with vertical axial planes and N-S axial directions reflect the synchronous F_4 -deformation. The large syn- and antiform structures are products of this phase. The fabric of the hornblende in the amphibolites is determined by the stress field of F_4 . Older hornblende orientations were destroyed. Whether a Hercynian age should be attributed to the amphibolite facies is not certain; if so, F_4 is the first Hercynian deformation phase.

After the overthrusting of the complex over its low-grade country rocks, a phase of chevron folding (F_5) was active locally. On the thrust plane small folds of the second Hercynian folding phase can be discerned. A third Hercynian folding phase can be seen in the Paleozoic rocks but not in the Cabo Ortegal Complex proper.

Local greenschist retrogradation (M_4) and the emplacement of dolerite dykes are late Hercynian. The tectonic history ends with a phase of normal block faulting which caused the E-W faults.

RESUMEN

El estudio petrológica de la parte meridional de la región de Cabo Ortegal completa la investigación de la parte septentrional llevada a cabo por Vogel (1967). Las investigaciones actuales incluyen un estudio tanto estructural como un estudio óptico y estadístico de la orientación preferida de los elementos microestructurales ('petrofabrics'). Las rocas pertenecen a una secuencia eugeosinclinal que sufrió durante el Precámbrico un metamorfismo progresivo desde la subfacies de estaurolita-almandina-moscovita y la distena-almandina-moscovita pertenecientes a la facies de almandina-anfibolita, pasando por la facies granulítica de clinopiroxena-piralmantina (\pm hornblenda) hasta la facies eclogítica (M_1). Han sido cartografiadas diversas zonas limitadas por isogradas, que a veces son de naturaleza tectónica. Como los gneises bandeados son solamente metatextíticos y como del contenido de jadeita de la omfacita se estiman las condiciones de P/T para la facies eclogítica, por lo tanto: $T \approx 700^\circ - 750^\circ \text{C}$, $P \approx 11 - 13 \text{ Kb}$ y presiones de vapor de agua: muy bajas.

Un plegamiento isoclinal acompañó en los gneises el metamorfismo. Los planos axiales son subhorizontales y los ejes de plegamiento se inclinan justamente occidental del norte. La orientación preferida de piroxena en las eclogitas y en los granulitas básicas demuestra que el mismo campo de 'stress' que produjo los pliegues del tipo F_1 en los paragneises influyó en la recristalización sintectónica de la misma clinopiroxena.

Una segunda fase metamórfica Precámbrica metamorfoseó retrogradamente las rocas hasta la facies granulítica de hornblenda (M_2). Antes del comienzo de esta fase un cataclasis pronunciado causó la formación de horizontes anchos miloníticos seguidos por un plegamiento del tipo 'drag' orientada E-W (F_2). El diagrama microestructural para clinopiroxena no demuestra una orientación preferida. Durante esta fase de deformación el zonamiento metamórfico del tipo M_1 había dado una media vuelta por un proceso combinado de plegamiento y cabalgamiento. En los paragneises el metamorfismo de la granulita de hornblenda esta marcado por una segunda generación de distena. Gabros introducidos a lo largo de planos de cabalgamiento han sido metamorfoseados parcialmente en coronitas de granate. Durante esta

segunda fase metamórfica se han formado pliegues isoclinales (F3) con planos axiales subhorizontales y direcciones axiales N-S. Las microestructuras de estos pliegues demuestran una orientación clara de los ejes c de diopsida (metaestable) y de hornblenda marrón-verde paralelos a la dirección del eje de plegamiento.

Una tercera fase metamórfica causó otra retrogradación de las rocas hasta la facies anfibolítica (M3). El anfíbol característico de esta fase es una hornblenda de un color azul-verde. Las metabasitas primeramente mencionadas han sido metamorfoseadas en anfibolitas (de granate). Gabros introducidos se transformaron a lo largo de sus límites en anfibolitas del tipo 'flaser'. Pliegues con planos axiales verticales y direcciones axiales N-S reflejan la deformación sincrónica F4. Las estructuras grandes de sin- y antiformes son productos de esta fase. La microestructura de la hornblenda en las anfibolitas está determinada por el campo de 'stress' de F4. Orientaciones más antiguas de hornblenda han sido destruidas. No es seguro si se debe atribuir una edad Hercínica a la facies anfibolítica; en caso positivo F4 es la primera fase Hercínica de deformación.

Después del cabalgamiento del Complejo sobre sus rocas madres de grado bajo una fase de plegamiento de tipo 'chevron' (F5) ha sido localmente activa. Sobre los planes de cabalgamiento se pueden distinguir pliegues menores de la segunda fase del plegamiento Hercínico. Se puede ver una tercera fase de plegamiento en las rocas Paleozoicas, pero no en el Complejo de Cabo Ortegal mismo.

Una retrogradación local (M4) en la facies de los esquistos verdes y el emplazamiento de diques doloríticos son Hercínicos tardíos. La historia tectónica termina con una fase de fracturación en bloques que causo las fallas de una orientación E-W.

CONTENTS

I. Introduction	85	Outline of the deformation phases within Cabo Ortegal	102
Geography	85	Deformation phases	102
Geological setting	85	F1-deformation phase	102
The geology of Cabo Ortegal	85	F2-deformation phase	103
Gravity survey	85	F3-deformation phase	105
The present study	85	F4-deformation phase	105
Rock formations	85	Folding of eclogite	107
Paragneisses	87	F5-deformation phase	107
Basic rocks	87	Structural map	108
Ultramafic rocks	87	Behaviour of the metabasic rocks under stress	108
Dating of events	87	Interference patterns	109
Acknowledgements	88		
II. Petrography	88	IV. Petrofabrics	111
Introduction	88	Introduction	111
Division into metamorphic zones	88	Procedure	111
Nomenclature of eclogite and mafic granulite facies rocks	88	The diagrams	112
Explanation of terms	89	Sampling	112
A. Eclogite facies zone	89	Clinopyroxene in eclogite	113
Eclogites	89	Clinopyroxene in basic granulite	117
Atoll garnets	90	Fabrics of F2-folds	117
Staurolite-bearing eclogite	91	Fabrics of F3-folds	117
Paragneisses	92	Description of other clinopyroxene fabrics recorded in literature	117
B. Granulite facies zone	92	Amphibole fabrics	119
Metabasic rocks	93	Hornblende in an F2-fold	120
Leptynites	95	Hornblende in F3-folds	120
Segregated quartz veins containing kyanite and zoisite	95	Hornblende in F4-folds	120
Garnet-biotite-(muscovite) gneisses in the metabasites	95	The origin of preferred orientations	122
Calc-silicate rocks	95	Intracrystalline slip	124
Paragneisses	95	Recrystallization	124
Gabbros in the Chimparragneisses	96	The theories based on thermodynamic equilibrium	124
C. Amphibolite facies zone	96	The theory based on oriented nucleation	124
Metabasites	97	The theory based on oriented grain growth	124
The Purrido Amphibolite Formation	97	Preferred orientation observed within Cabo Ortegal	124
Paragneisses	97		
Metagabbros	98	V. Conclusions and synthesis of the results in the geological framework of the NW Iberian peninsula	125
Adaptation to granulite facies conditions	98	Geological history in the Precambrian	125
Adaptation to amphibolite facies conditions	99	Hercynian orogeny	126
The Carreiro zone of tectonic movement	99		
Physical conditions during metamorphism	99	Samenvatting	127
III. Tectonics	101	References	128
Introduction	101	Localities of the samples	132
Aim	101	Sample map (Appendix I)	133
Recent tectonic studies of the Hesperian massif	101	Enclosure (in back flap): Structural map	
Pre-Hercynian deformation phases	101		
Hercynian deformation phases	101		
Nomenclature	102		

CHAPTER I INTRODUCTION

GEOGRAPHY

The investigated area is situated in the northwestern corner of Spain; Cabo Ortegal is the cape just west of Estaca de Vares, the northernmost point of Spain. The Cabo Ortegal Complex forms a semi-elliptical outcrop of catazonal rocks which is limited to the north, and partly to the west, by the Atlantic Ocean. The inland boundary runs roughly through the townships of Valdoviño, Moeche and Santa Marta de Ortigueira, and further northwards to the ocean near Espasante.

The topographical data used for the preparation of the geological map of the area, which is published as plate I in Vogel's thesis (1967), were taken from the maps edited by the Cartografía Militar de España (scale 1:25,000): sheet 1 (quadrants I, II, III), sheet 2 (quadrant III) and sheet 7 (quadrants I, II, III, IV).

Enough roads cross the area to make it possible to approach most outcrops on foot; only the areas on the northwestern side, along the Atlantic, are not easily accessible with normal vehicles.

GEOLOGICAL SETTING

Tectonically the Cabo Ortegal Complex belongs to the axial zone of the Hercynian orogen of the western Iberian Peninsula: the Hesperian Massif. This zone has been designated by Capdevila (1965) as the 'domaines internes'. The general orogenic trend varies from NNE in the north to NNW in Portugal. The axial zone is characterized by the upthrust of several, mainly mafic, Precambrian massifs and by the occurrence of migmatitic and granitic rocks (the calcalkaline and alkaline series, Floor, 1970; Capdevila and Floor, 1970). The Lower Paleozoic is reduced and the Upper Paleozoic is absent in the axial zone. On both sides the axial zone is flanked by geosynclinal zones mainly consisting of Lower Paleozoic sediments. A map simplified from the 'Carte Géologique du Nord Ouest de la Péninsule Ibérique', published in 1969, is given in Fig. I-1.

One of the largest Precambrian massifs in the axial zone is that of Cabo Ortegal; comparable massifs are the Morais and Bragança-Vinhais Complexes in N Portugal and the massifs along the margin of the Ordenes 'basin', i.e. the mainly basic complexes near Agualada, Santiago, Mellid and Sobrado.

For a complete list of publications dealing with geological investigations in Galicia, the reader is referred to a review by Parga Pondal (1966).

THE GEOLOGY OF CABO ORTEGAL

The Cabo Ortegal rocks belong to a Precambrian geosynclinal episode: deposition of sediments (graywackes,

semipelitic rocks, arkoses, etc.) and the emplacement of an ophiolitic suite (basic lavas or tuffs, gabbros and ultramafics). Several metamorphic and orogenic phases transformed these rocks into their present form. During the Hercynian orogeny the catazonal rocks were presumably thrust into and over their Paleozoic country rocks, which are found in the greenschist facies. The thrusting was probably facilitated by the presence of serpentinites from a second ophiolitic suite which functioned as a 'lubricant' (Ho Len Fat et al. in press).

Gravity survey

During the summers of 1968 and 1969 the Department of Geophysics of Leyden University carried out a gravimetric survey of the area (van Overmeeren & van Riessen, to be published). Two sets of profiles, one from the centre of Cabo Ortegal toward the SSW and another toward the ESE, were interpreted. From the first set it is deduced that the Paleozoic dips 30°–90° (NE) under the Cabo Ortegal Complex; the second set indicates that the Cabo Ortegal Complex dips 15° ESE under the Paleozoic rocks.

The present study

Cabo Ortegal and its surroundings was recently mapped by the following graduate students: P. A. J. Coelwey, E. Romyn, D. E. Vogel, H. de Miranda, J. P. Engels, A. G. Ho Len Fat, G. H. T. C. Hoogervorst and W. F. Burgers. Two Ph. D. theses provide a more detailed investigation of the Complex. The northern part of the area was studied by Vogel (1967) who placed the emphasis on mineralogical and chemical analyses. The present study completes the petrography for the southern part and includes a structural analysis of the whole area.

The results of these investigations are presented in three chapters. The petrography is dealt with in chapter II. This is more or less a supplement to the study of Vogel. Chapter III contains the results of the structural investigations and in chapter IV, the connection between metamorphism and deformation is established through analysis of the micro-fabrics of the basic rocks.

Storage. — The location of the samples mentioned in the text is indicated on the sample map (Appendix I). The samples are numbered from RMG 162682 to 162741 and are stored at the Rijksmuseum van Geologie en Mineralogie (National Museum of Geology and Mineralogy) in Leiden.

Rock formations

In mapping the Cabo Ortegal Complex the rocks were grouped into several units. Their position is marked on the map in Figure I–2.

Paragneisses. — The paragneisses are divided into three separate units. The Cariñogneiss Formation (1) is located along the eastern border. These gneisses are not anatexitic and the alternation of leucocratic and melanocratic bands is thought to represent the original sedimentary banding. Graded bedding is perhaps still recognizable in some places. The Chimparragneiss Formation (2) occupies the central part of the Cabo Ortegal Complex. The gneisses are garnet- and biotite-bearing, and sometimes also contain kyanite. The gneisses show signs of incipient anatexis and often have a mylonitic texture. Outcrops of orthogneiss occur in the Chimparragneiss Formation. The Banded Gneiss Formation (3) is formed by the gneisses that enclose eclogitic rocks. The texture of the banded gneisses is comparable to that of the Chimparragneisses.

Basic rocks. — Eclogites (4) are exposed as large ridge-forming bodies and as small lenses in the Banded Gneiss Formation. The mafic rocks which underwent granulite facies metamorphism form several mappable units. The largest outcrop is the Bacariza Formation (5), west of the eclogite ridges. Another complex lies in the south and is called the Agudo Formation (6). The Agudo Formation continues underneath the Chimparragneisses and reappears as the Candelaria Granulite Formation (7).* The amphibolites form the periphery of the Cabo Ortegal Complex. At the western side a double series of

amphibolites occurs. The westernmost amphibolites belong to the Purrido Amphibolite Formation (8). These are separated from the Candelaria Amphibolite Formation (9) by the Carreiro zone of tectonic movement (a major tectonic zone with rock fragments derived from several complexes). The Candelaria Amphibolite Formation is believed to continue southwards as the Peña Escrita Formation (10) and in the form of several small outcrops along the eastern limit of the Cabo Ortegal Complex.

Ultramafic rocks. — Large plates of ultramafic rock cover the tops of the Herbeira (11) and Lima Mountains (12). Lenses of serpentinites are often found along the tectonic contacts. Of these the Uzal (13) is the largest. The ultramafics of Cabo Ortegal have been the subject of a detailed investigation by Maaskant (1970).

Dating of events

Only one isotopic age determination of a Cabo Ortegal rocks is available so far. A single sample of karinthic amphibole from an eclogite yielded an apparent age of 900 ± 30 m.y. for the eclogite facies metamorphism (Vogel and Abdel-Monem, 1971). More radiometric age determinations have been made for other parts of

*) In this paper Vogel's Candelaria Amphibolite Formation is divided into the Candelaria Amphibolite Formation forming the western part and the Candelaria Granulite Formation which comprises the eastern part. The parts are separated by a thrust zone.

Fig. 1-1. Geological map of the northwestern Iberian Peninsula. Simplified from the 'Carte Géologique du Nord Ouest de la Péninsule Ibérique' (1967). Cabo Ortegal is situated at the north coast of Galicia.

Legend:

1-7: Hercynian rocks
 1: gabbro
 2-3: calcalkaline granite series; 2: post-tectonic biotite granite; 3: older, mainly megacrystal-bearing, granodiorite
 4-7: alkaline granite series; 4: post-tectonic, megacrystal-bearing two-mica granites; 5: two-mica granites of varying age and texture; 6: inhomogeneous, migmatitic granites; 7: migmatites

8-12: Upper Precambrian and Lower Paleozoic (meta)sediments; 8: Ordovician (younger than armorican quartzite) and Silurian; 9: in Spain: Cambrian, Ordovician up to armorican quartzite inclusive; in Portugal: 'Complexo xisto-grauváquico anteordovícico'; 10: Upper Precambrian, fine-grained facies; 11: Upper Precambrian, 'Ollo de Sapo' facies; 12: undifferentiated metasediments

13: coarse-grained augengneiss
 14: probably younger Precambrian metasediments and Upper Ordovician orthogneiss, undifferentiated
 15: polymetamorphic metasediments
 16: metabasic rocks, partly polymetamorphic
 17: ultramafic rocks, partly polymetamorphic

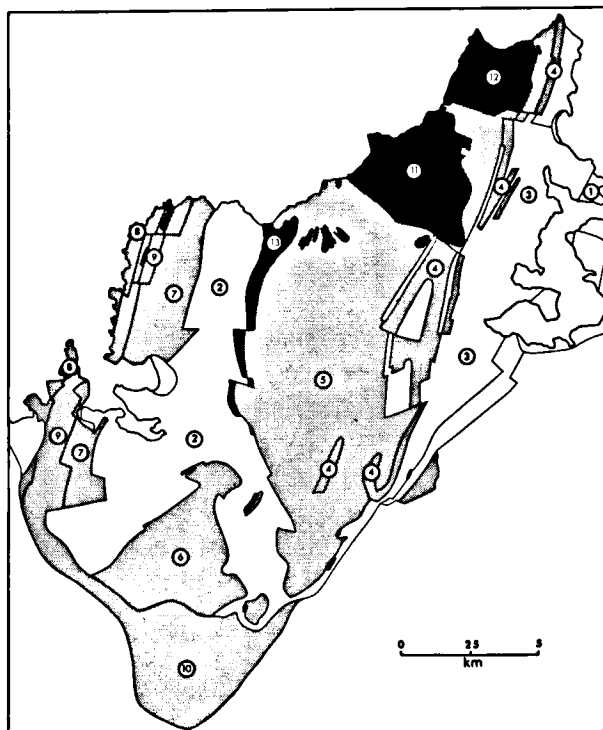


Fig. 1-2. Map of the Cabo Ortegal Complex showing the position of the significant formations. Paragneisses (not shaded): (1) Cariñogneiss Formation, (2) Chimparragneiss Formation, (3) Banded Gneiss Formation; metabasic rocks (shaded): (4) eclogites, (5) Bacariza Formation, (6) Agudo Formation, (7) Candelaria Granulite Formation, (8) Purrido Amphibolite Formation, (9) Candelaria Amphibolite Formation, (10) Peña Escrita Formation; ultramafic rocks (black): (11) Herbeira, (12) Limo and (13) Uzal.

western Galicia. Peralkaline and calcalkaline orthogneisses yielded ages of 460–430 m.y. These rocks show no evidence of polymetamorphism (Floor, 1966). Tentatively the augengneisses associated with the Precambrian polymetamorphic complexes of Sobrado-Mellid have been assigned to the same isochrons of 460–430 m.y. (Priem et al., 1970). The Hercynian amphibolite facies metamorphism and its associated granite series have yielded ages between 369 and 274 m.y. (Capdevila and Vialette, 1965; Priem et al., 1966, 1970). The end of the Hercynian orogenesis as indicated by the Rb/Sr whole rock ages of post-tectonic granites and by the regional cooling age of micas is estimated as 305–270 m.y. (Bonhomme et al., 1961; Capdevila and Vialette, 1965; Priem et al., 1965, 1970).

ACKNOWLEDGEMENTS

The author is greatly indebted to Professor E. den Tex for sharing his extensive knowledge of catazonal metamorphism and his experience in petrofabrics; his continuous interest and guidance were a great support. I wish to express my sincere thanks to Professor H. J. Zwart, Dr. C. J. L. Wilson and Mr. H. Koning for their critical reading of parts of the manuscript; their suggestions contributed greatly to its ultimate shape.

I am especially grateful to my former 'roommates' Dr. D. E. Vogel, Dr. J. R. Möckel and Dr. A. van Zuuren; references to their knowledge of petrology and

petrofabrics will often be found in this thesis. The many fruitful discussions of petrological problems with my colleagues, especially Dr. P. Floor, Dr. C. E. S. Arps, Mr. J. J. M. W. Hubregtse, Mr. J. Glass, Mr. J. D. Hilgen and Mr. E. J. van Scherpenzeel, were a great help during the preparation of this manuscript. Dr. P. Hartman, Mr. C. F. Woensdregt and Mr. R. O. Felius were always willing to help with crystallographic problems.

The instructive and pleasant evening discussions with Messrs. K. J. Roberti and J. A. Klein are well-remembered.

Without the cooperation of the entire technical and administrative staff of the Geological Institute this study would not have been possible. Nevertheless I want to record my special thanks to Mr. J. Bult for the drawing of the illustrations, Mr. A. Verhoorn who took the X-ray photographs, Messrs. W. C. Laurijssen and W. A. M. Devilé who took the many photographs, also those used for the petrofabric analyses, Messrs. M. Deyn, C. J. van Leeuwen and J. Schipper who made the thin sections and Misses C. M. Boer and C. C. Zuiderduin for typing parts of the manuscript.

I am especially thankful to my wife who retyped several drafts of the manuscript.

Thanks are also due to Mrs. G. P. Bieger-Smith for correcting the English manuscript and to Mr. and Mrs. Woensdregt for translating the abstract into Spanish.

The Saturday morning coffee of Mr. F. J. Schild was always excellent.

CHAPTER II

PETROGRAPHY

INTRODUCTION

Division into metamorphic zones

The northern half of the Cabo Ortegal Complex was the object of an extensive petrographic study by Vogel (1967). Most of the rock units mapped are also found in the southern part. Vogel divided Cabo Ortegal into two lithostratigraphic complexes: (1) the mixed mafic-felsic Concepenido Complex which contains the eclogites, the Banded Gneiss Formation, the Chimparragneiss Formation, the Cariñogneiss Formation, the Carreiro zone of tectonic movement and the Purrido Amphibolite Formation and (2) the massively mafic Capelada Complex which comprises the Bacariza Formation and the Candelaria Amphibolite Formation.

In this study a threefold metamorphic division is proposed (see Fig. II-1): (A) an eclogite facies zone (eclogites and Banded Gneiss Formation), (B) a granulite facies zone (Bacariza Formation, Chimparragneiss Formation, Agudo Formation and Candelaria Granulite Formation) and (C) an amphibolite facies zone

(Candelaria Amphibolite Formation, Peña Escrita Amphibolite Formation, Purrido Amphibolite Formation and Cariñogneiss Formation). This division is based on the metamorphic grade attained during the first metamorphic phase and covers the different metamorphic facies of the metabasites as well as the paragneisses. The Cabo Ortegal Complex shows a reversal of the metamorphic zoning since the highest grade now lies on top of the lowest (Fig. II-2).

Nomenclature of eclogite and mafic granulite facies rocks

Rocks consisting essentially of garnet and clinopyroxene are called eclogites by Haüy (1822). The clinopyroxene (omphacite) contains jadeite in solid solution and has a high jadeite/Tschermak's molecule ratio (White, 1964). According to de Waard (1965) the eclogite facies is characterized by the pair kyanite-clinopyroxene, which he regards as the critical assemblage for the eclogite facies. Thus in mafic rocks kyanite is only stable in the eclogite facies whereas plagioclase, garnet and clino-

Eclogites <i>Eclogites</i>		Purrido Amphibolite Formation <i>Purrido Amphibolite Formation</i>	CONCEPENIDO COMPLEX
Banded Gneiss Formation <i>Banded Gneiss Formation</i>	Chimparragneiss Formation <i>Chimparragneiss Formation</i>	Cariñogneiss Formation <i>Cariñogneiss Formation</i>	
	Bacariza Formation <i>Bacariza Formation</i> Agudo Formation	<i>Peña Escrita Formation</i>	CAPELADA COMPLEX
	Candelaria Amphibolite Formation <i>Candelaria Granulite Formation</i>	<i>Candelaria Amphibolite Formation</i>	
<i>eclogite facies zone</i>	<i>granulite facies zone</i>	<i>amphibolite facies zone</i>	Vogel (1967) <i>Engels</i>

Fig. II-1. Division of the several formations into two complexes according to Vogel (horizontal rows) and into three metamorphic zones as proposed in this study (vertical columns).

pyroxene form the critical mineral association for the high-pressure granulite facies. The presence of hornblende in the granulite facies depends on 'local' PH_2O conditions.

Granulite as a rock name is restricted to 'a metamorphic rock composed essentially of a fine-grained mosaic of feldspar, with or without quartz. Ferromagnesian minerals, if present, are predominantly anhydrous. Granulites typically contain lenticular (or elongated) grains or aggregates of grains'. This definition was given by the granulite work group (Behr et al., 1971). In this sense the name granulite was used for the first time by Weiss (see Naumann, 1850). The granulite work group suggested that all other rocks from the granulite facies with other textures should be named according to their texture (gneiss, granofels), with mineral names as prefixes. Special descriptive names for mafic granulites as proposed by Berthelsen (1960) or Vogel (1967) shall not be used here.

Explanation of terms

Grain sizes are subdivided as follows:

3 cm–5 mm	coarse-grained
1–5 mm	medium-grained
1/3–1 mm	fine-grained
1/100–1/3 mm	microcrystalline

To avoid any misunderstanding the following definitions are used for rocks with a planar texture. Layering is used to describe rocks with distinct layers; adjacent layers usually differ in composition (Hsu, 1955). Layered rocks do not necessarily have preferred mineral orientations. Massive is used as a textural term to describe rocks that are not layered. Foliation is used if there is a parallel orientation of the minerals in non-fissile rocks. Schistosity is the term used for parallelism in fissile rocks.

A. ECLOGITE FACIES ZONE

Eclogites

The eclogites in the southern part of the Cabo Ortegual Complex are a continuation of those found in the Sierra de Moles. Outcrops lie on three lines which extend N–S. Most eclogites are more or less retrogressive and exhibit features of retrograde metamorphism, i.e. development of a pyroxene-plagioclase symplectite, formation of kelyphitic rims around garnet and replacement of

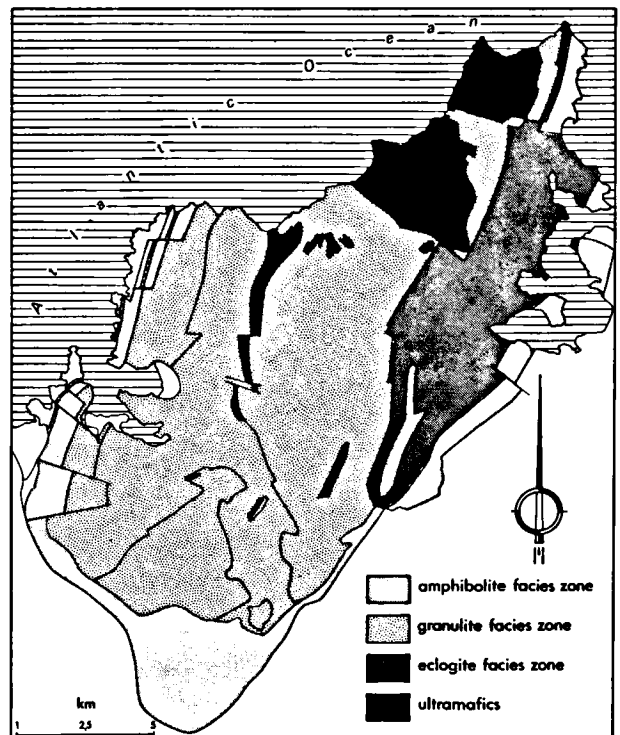


Fig. II-2. Map of the metamorphic facies zones in the Cabo Ortegual Complex.

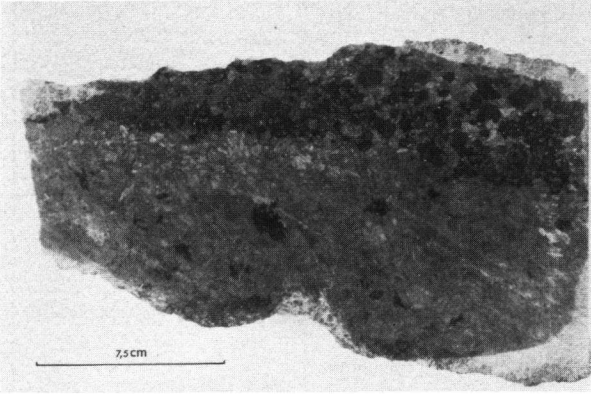


Fig. II-3. A layer of 'eclogite' without garnet, consisting only of omphacite in various stages of symplectitization. Dark spots mark the replacement of clinopyroxene by hornblende. Amphibolization is much stronger in garnetiferous parts. Thin section RGM 162682.

clinopyroxene by hornblende (Eskola, 1921; Lange, 1965; Vogel, 1967).

Although eclogite is a garnet-omphacite rock, it can be seen that one layer of eclogite, sample RGM 162682, contains no garnet (Fig. II-3). The thin section shows that this layer consists of omphacite in different stages of p.p. symplectite formation, as described by Vogel (1967). With the exception of rutile and a small amount of quartz with a narrow rim of clear pyroxene where no symplectite has formed (Fig. II-4), no other minerals are present; only local signs of amphibolization are seen in this layer. Where garnet is present, kelyphitic rims of blue-green hornblende have formed; beyond these rims, large hornblende crystals replace the clinopyroxene. Hornblende has a brownish colour around rutile. The anorthite content of plagioclase in hornblende is 11%.

Sample RGM 162683 was originally composed of garnet, omphacite, brown hornblende, quartz and small amounts of rutile. Omphacite is totally replaced by p.p.

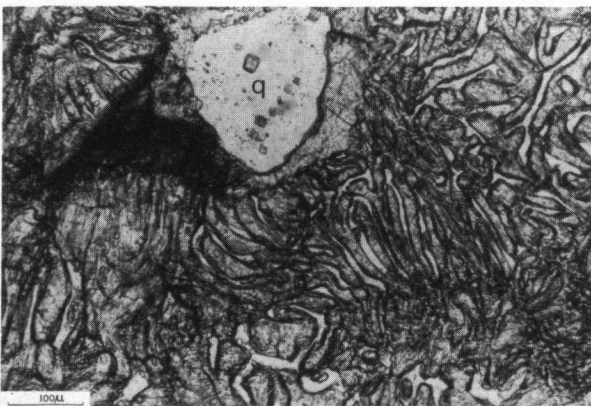


Fig. II-4. Coarse pyroxene-plagioclase symplectite. Around quartz (q) the pyroxene shows no symplectitic intergrowth. Thin section RGM 162682.

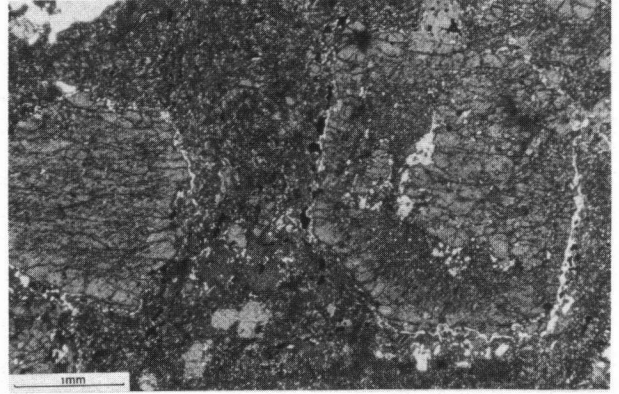


Fig. II-5. Three stages in the formation of garnet; the central part and the outer rim are almost devoid of inclusions; the middle zone is full of inclusions in parallel orientation. Thin section RGM 162683.

symplectite. The brown hornblende ($2 Va = 80^\circ$, $[001] \wedge \gamma = 16^\circ$) has a markedly preferred orientation in the thin section, which reveals only crystals with the $[001]$ -axes perpendicular to the section. It is interesting that the garnet ($\phi = 3.8$ mm) shows 3 definite stages of formation (Fig. II-5): a clear centre with corroded outlines, a zone with inclusions of quartz, clinopyroxene and rutile in parallel orientation and an outer rim free of inclusions with hypidiomorphic outlines. It is assumed that the eclogite facies was reached in steps during prograde metamorphism. After the second stage of garnet formation, a deformation took place since the S_j of different garnets are no longer parallel.

Atoll garnets. Retrogressive eclogites with atoll garnets, sometimes with 'barrier reef' garnets, are also found. This is clearly demonstrated in thin section RGM 162684 (Fig. II-6). Their eclogitic origin can be established by the occurrence of p.p. symplectite and

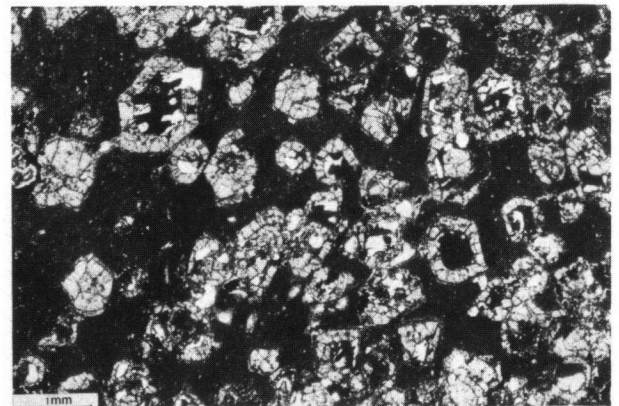


Fig. II-6. Atoll garnets in a retrograde eclogite. All of the omphacite is replaced by fine-grained pyroxene-plagioclase symplectite. Thin section RGM 162684.

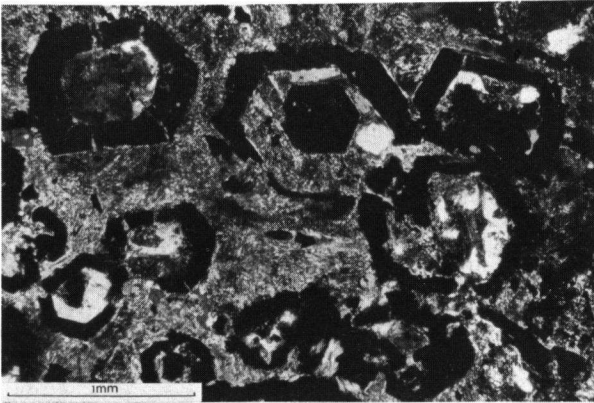


Fig. II-7. Atoll garnet with an idiomorphic garnet crystal in its centre; together they form the 'barrier reef' type garnet. Thin section RGM 162684.

the lack of original plagioclase. Garnet rims with hypidiomorphic outlines on the outside and idiomorphic faces inside surround kernels of quartz, sometimes quartz and p.p. symplectite, and in a few cases clinopyroxene. Occasionally an idiomorphic garnet crystal lies in the centre giving rise to the 'barrier reef' type of garnet (Fig. II-7).

Lange (1965) described atoll garnets in the retrogressive eclogites of Saxony. He stated that the inclusions could influence the breakdown of garnet. (See Scheumann (1924) for atoll garnets in garnet-clinzoisite-albite gneisses of the Fichtelgebirge in Saxony). An indication that the same process took place in Cabo Ortegal is perhaps the fact that the remains of inner zones full of inclusions have been found. Quartz is assumed to have migrated to the centre of the atoll which was the point of minimum stress.

If amphibolization of eclogites continues amphibolites are formed. Examples of this process are seen in samples RGM 162685 and RGM 162686. Thin section RGM 162686 is an amphibolite composed of blue-green hornblende and small amounts of highly twinned plagioclase (36% An). Kyanite relics bordered by



Fig. II-8. Staurolite relics as fine needles in kyanite in a highly retrograded eclogite. Thin section RGM 162687.

sericite, as well as a single garnet fragment with rutile inclusions and a kelyphitic rim, confirm the eclogitic origin. Folded streaks (3 mm wide) of fine-grained β -zoisite lie dispersed throughout the rock. Thin section RGM 162685 shows the same phenomena but here three types of hornblende formation are represented: 1. amphibolization of fine-grained clinopyroxene of the p. p. symplectite; 2. as a result of kelyphitization, garnet is no longer present but patches of radially oriented hornblende crystals ($\phi = 4$ mm) indicate the former presence of garnets; 3. hornblende blasts (3-4 mm). These hornblende blasts were deformed later. The anorthite content of the plagioclase is slightly lower (31% An). In both samples small rutile needles are found as inclusions in hornblende.

Staurolite-bearing eclogite. — A retrogressive eclogite with a significant mineralogy is sample RGM 162687, found just north of Forca Summit at a level of 300 m. Macroscopically it is a greyish rock with white specks and a weak foliation. Under the microscope the thin section shows a fine-grained garnet-bearing hornblende gneiss; the white specks are relics of kyanite ($\phi = 2-3$ mm) surrounded by a mass of sericite and an outer rim of clinzoisite. Frequently small garnet crystals lie at the border. Some biotite is present, particularly near and in the kyanite relics. Fine-grained plagioclase (core 26% An, rim 32% An) is dispersed throughout the sample. Quartz occurs as short polycrystalline ribbons; apatite, rutile, zircon and opaque minerals are accessories.

In one case staurolite relics are seen as fine needles in kyanite (Fig. II-8). Staurolite relics surrounded by kyanite have also been found by A. G. Ho Len Fat in a retrogressive eclogite in the Banded Gneiss Formation

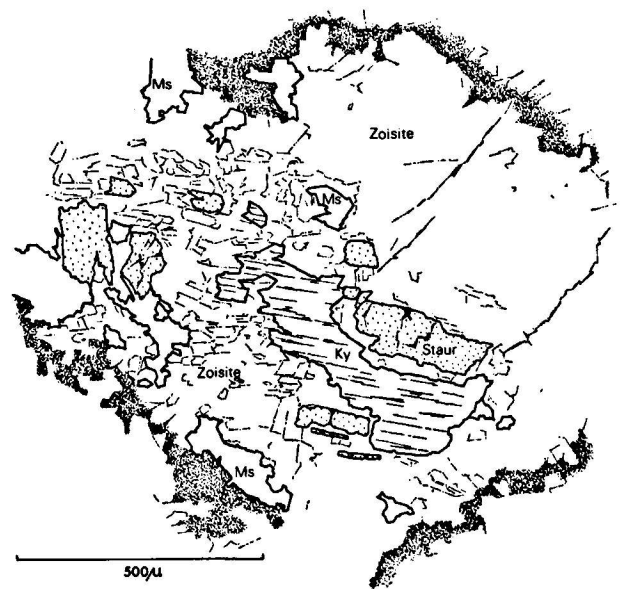


Fig. II-9. Relics of staurolite (stippled) and kyanite (ky) surrounded by a mass of zoisite in a retrograded eclogite. Ms = muscovite. Thin section RGM 162688.

north of Campo del Hospital (sample RGM 162688, Fig. II-9). The occurrence of staurolite in a mafic rock seems to be an 'impossibility', according to the facies concept: it should only be found in rocks of pelitic composition. However the same 'impossibility' is known elsewhere, e.g. the quartenschiefer at Frodalera, Lukmanier area, Switzerland (Frey, 1969). There staurolite is found together with garnet, hornblende, kyanite, biotite, plagioclase and quartz. The physical conditions assumed by Frey are $T = 500^{\circ} - 550^{\circ}\text{C}$ and $P = 6 - 8 \text{ Kb}$. Richardson (1968) states that staurolite is stable up to temperatures just below 700°C . The upper limit for the stability of staurolite is given by Hoschek (1969) as $675^{\circ} \pm 15^{\circ} \text{C}$ at 5.5 Kb PH_2O and $575^{\circ} \pm 15^{\circ} \text{C}$ at 2 Kb PH_2O . At higher temperatures staurolite breaks down forming biotite, Al-silicate and vapour or Al-silicate and garnet. All of these P/T conditions lie within the range of the almandine-amphibolite facies. This means that before the eclogite facies was reached, the rock passed through an amphibolite facies metamorphism (cf. the stages of garnet formation). After the eclogite facies (M_1), granulite facies (M_2) conditions prevailed causing the formation of p.p. symplectite; this was subsequently followed by amphibolite facies (M_3) conditions which were responsible for kelyphite formation and amphibolization, with amphibolites as ultimate products. Vogel found only local indications of a greenschist facies metamorphism (M_4) in the eclogites.

Paragneisses

The fact that many small lenses of (retrograded) eclogite are found in the Banded Gneiss Formation proves that it belongs to the eclogite facies zone. The Banded Gneiss Formation thins out rapidly to the south; near Francoy it is no wider than 250 m and is poorly exposed. Immediately east of the Banded Gneiss Formation lie the Cariñogneisses. At the contact of the two, there are lenses of serpentinite which simplify the mapping of the boundary. Samples RGM 162689, RGM 162690 and RGM 162691 are from the Banded Gneiss Formation in the south and demonstrate the variety to be found in these gneisses.

Sample RGM 162689 is from a gneiss between the eclogite ridges, just southwest of Campo del Hospital. Macroscopically the rock is finely schistose ($\phi = 0.5 - 1 \text{ cm}$) and brownish due to biotite, with some quartzofeldspathic augen and streaks parallel to the schistosity. The thin section of sample RGM 162689 shows a fine-grained granoblastic fabric of quartz and plagioclase with biotite in more or less parallel orientation; the plagioclase is zoned and frequently twinned (core 20%, rim 30% An). Muscovite is scarce. On the other hand large, broken and highly twinned plagioclase clasts are richer in sodium (10-15% An). Garnets with rutile inclusions, two generations of kyanite (the first of which is often bent and the second, fine-grained and needle-shaped) and the occurrence of rutile are indications of a catazonal origin. Apatite, zircon and opaque matter are

accessories. Along a crack, clinozoisite formed together with recrystallized muscovite; in a zone parallel to this crack, biotite and garnet altered into chlorite, and plagioclase is saussuritized. More muscovite is present than in the unaltered rock.

Sample RGM 162690 is a kyanite-garnet-biotite gneiss. The gneiss shows a mosaic texture, with weak preferred orientation of biotite. Plagioclase is twinned according to (010) and (001) and has an anorthite content of 14% An. Unstrained quartz has amoeboid outlines. Garnet is almost colourless and has corroded outlines. Growth of garnet in two stages is suggested by the presence of circularly dispersed quartz inclusions. Kyanite occurs in two generations. The older generation is found as corroded, sometimes slightly bent crystals (0.5 mm). This generation is occasionally enclosed in garnet. A second generation is seen as aggregates of microcrystalline needles along the borders of plagioclase, garnet or first generation kyanite. Biotite flakes (0.3 mm) have a light greenish-brown colour. Dispersed throughout the rock is fine-grained orthorhombic amphibole, in one place surrounded by garnet. The amphibole is slightly pleochroic, ranging from colourless to very light green. The birefringence is low (0,013) and $2 V\gamma = 74^{\circ}$. Biotite replaces the orthorhombic amphibole. Rutile is found dispersed throughout the rock and enclosed in garnet. Zircon, apatite and opaque matter are accessory constituents.

Sample RGM 162691 found SE of Campo del Hospital has a granitoid appearance. Plagioclase ($\approx 1.4 \text{ mm}$), with a core of 12% An and a rim of 18% An, shows Albite law twinning and is full of small flakes of muscovite oriented parallel to the cleavages planes. In the plagioclases are zones of broken and recrystallized crystals. Microcline with cross-hatching forms slightly larger crystals ($\approx 2.2 \text{ mm}$) and is replaced along the borders by plagioclase with myrmekitic quartz. Fine-grained quartz crystals occur together in clusters. Highly deformed biotite is usually brown but sometimes green and is dispersed in nests (4-5 mm) together with muscovite. Orthite in biotite, garnet, usually together with muscovite, apatite, zircon and hematite are accessories.

B. GRANULITE FACIES ZONE

The granulite facies rocks occupy the central part of Cabo Ortegal. Rocks of the Bacariza Formation, the Candelaria Granulite Formation, the Agudo Formation and the Chimparragneiss Formation were all metamorphosed during the first phase (M_1) under granulite facies conditions. The Bacariza Formation contains the largest proportion of remnants of this phase. The contact between the Bacariza Formation and the Chimparragneiss Formation is tectonic and is marked by serpentinite bodies (Uzal and several smaller outcrops) and the presence of mylonites; the same can be observed

deformation phase	mineral paragenesis		metamorphic facies	metamorphic phase
	metabasites	paragneisses		
F ₁	cpx + gt + qz ± α-zo ± ky ± ru	bi + gt ± ky ± ge ± ru	eclogite facies	M ₁
	cpx + gt + pl ± β-zo ± ru	ms + bi + gt ± ky ± ru	granulite facies	
	hbl + pl ± gt	ms ± bi + gt ± ky ± st	amphibolite facies	
F ₂				
F ₃	cpx + brgr hbl + gt + pl ± sc ± ru	ms + bi + gt ± ky	granulite facies	M ₂
F ₄	blgr hbl + pl ± ep ± gt ± ti	bi + ms ± gt ± ti	amphibolite facies	M ₃
	ac + ab + ep + chl ± ti	ms + ab + chl ± bi	greenschist facies	M ₄
F ₅ normal faulting				

Fig. II-10. Synopsis of the relationships between the metamorphic and deformation phases in the Cabo Ortegal Complex.

at the contact between the Chimparragneisses and the underlying Candelaria Formation.

Metabasic rocks

Retrogressive metamorphic and tectonic phases transformed the original metabasites into a variety of rocks ranging from clinopyroxene-garnet-plagioclase granulites to common hornblende gneisses. A synopsis of these phases is given in Fig. II-10. Judging from what little is left, the original mafic-granulite facies rocks must have been diopside-garnet-(hornblende)-plagioclase granulites without a distinct mineral orientation. Whether hornblende was initially present cannot be ascertained, but it seems likely. Granulites with brownish green hornblende are most common but in the Candelaria Formation granulites with brownish hornblende also occur (Vogel, 1967). There are no indications that the brownish hornblende represents an earlier stage of metamorphism than the brownish green. Microscopical appearance (sample RGM 162692): the rocks is medium to fine-grained hypidiomorphic granular, with no preferred orientation of the minerals. Light pink subhedral garnet (sometimes with fine rutile needles) and light green diopside ($2V\gamma = 66^\circ$, $[001] \wedge \gamma = 43^\circ$) with amoeboid forms make up 80% of the rock; small amounts of brownish green hornblende ($2V\epsilon = 78^\circ$) are present. Quartz and plagioclase (27% An) fill the interstices between the above-mentioned minerals. Rutile as droplets, rounded apatite and clinozoisite with orthite cores are accessory minerals. Later retrogressive influences are indicated by the alteration of hornblende along cracks into a bluish-green variety and rutile into titanite, as well as the growth of pistacite.

A penetrative deformation followed the first metamorphic phase and was in most cases accompanied by the injection of pegmatoid matter into the granulites. The second metamorphic phase (M₂) is characterized by the poikiloblastic growth of large brownish-green hornblende which are in stable association with garnet, clinopyroxene and plagioclase (high-pressure hornblende

facies). Scapolite occasionally occurs. Since scapolite is also found in the metarolites of Sanxiao, which were emplaced after the first metamorphic stage, and not in the original granulites it is assumed that scapolite belongs to the second metamorphic phase. Scapolite in basic granulites is also mentioned by v. Knorring and Kennedy (1958). Rocks of the second phase are sometimes massive but usually show a clear layering marked by an alternation of predominantly felsic and predominantly mafic strata. The creation of this layering is correlated with the second deformation phase.

Microscopical appearance of samples of the massive type: sample RGM 162694, taken from the Bacariza Formation, clearly shows a poikiloblastic texture. Large ($\phi \approx 1$ cm) brownish-green hornblende poikiloblasts ($2V\alpha = 81^\circ$, $[001] \wedge \gamma = 17^\circ$) enclose clinopyroxene, garnet, plagioclase, rutile and zircon. When quartz is also enclosed, there is a rim of plagioclase between quartz and hornblende. Diopsidic clinopyroxene ($2V\gamma = 66^\circ$, $[001] \wedge \gamma = 44^\circ$) is sometimes partly replaced by hornblende. Clear light pink anhedral garnet is evidently in stable association with clinopyroxene. Plagioclase (18% An) also grew as very large poikiloblastic grains; sometimes all the plagioclase in one thin section appears to be one single crystal. Twinning according to the Albite and Pericline laws can be seen. Quartz, rutile, orthite, broken apatite, zircon and opaque matter are minor constituents. A very weak foliation is marked by the parallel orientation of rutile needles. Yellow-green pistacite, an alteration of hornblende and clinopyroxene, is found in cracks. In sample RGM 162693, taken from the Candelaria Granulite Formation, little is left of the clinopyroxene as most of it is replaced by brownish hornblende ($2V\alpha = 88^\circ$, $[001] \wedge \gamma = 15^\circ$). The rock contains more plagioclase (35% An) and the hypidiomorphic spongy garnet is full of quartz inclusions. Quartz, β -zoisite, apatite and rutile (sometimes enclosed by titanite) are minor constituents. Clinozoisite fills cracks.

At the top of Mount Texón in the Bacariza Formation, a well-marked foliation plane occurs. Rotated boudins of foliated basic granulites are found between these hornblende gneisses. The same phenomena can be observed at the top of Mount Agudo (Fig. II-11). Sample RGM 162695 is from one of the boudins; the rock shows a layering due to bands and streaks rich in quartz and plagioclase (pegmatoid injection). Otherwise it contains the same minerals as sample RGM 162694. Elongated diopside crystals lie parallel to the layering. Before further retrogradation of the rocks into the amphibolite facies, a third deformation phase was active. Cataclasis and mylonitization enhanced mineralogical readjustment to the conditions of the subsequent third metamorphic phase. Characteristic is the formation of a new blue-green hornblende, titanite (instead of rutile) and clinozoisite (instead of zoisite). Biotite is not rare. The mafic rocks of this facies are (garnet-)hornblende gneisses or (garnet-) amphibolites.



Fig. II-11. Rotated boudins of basic granulite surrounded by garnet-bearing amphibole gneisses. Locality: summit of Mount Agudo.

Sample RGM 162696 is taken from the hornblende gneisses which surround blocks of the above-mentioned hornblende-clinopyroxene-garnet gneisses (RGM 162695). Blue-green hornblende blasts with rims bluer than the cores, poorly oriented biotite flakes and large epidote crystals, often with cores of orthite, lie in a mosaic of recrystallized plagioclase (22% An) and quartz. Larger plagioclase clasts have twinned centres with a higher calcium content (27% An) than the untwinned rims. A few colourless garnets are enclosed by hornblende. The garnets in the plagioclase-quartz matrix exhibit all stages of replacement by plagioclase. Titanite crystals measure approximately 1 mm; sometimes rutile kernels indicate the previous, higher metamorphic grade.

The breakdown of garnet can be seen in many cases. The stability of garnet in metabasites depends in part on the chemical composition of the metabasites. By plotting chemical analyses of Bacariza Formation rocks in an ACF-diagram for the almandine-amphibolite facies, Vogel (1967, p. 190) predicted that many 'plagiopyrigarnites' must convert to garnet-free amphibole gneisses. Garnet is replaced by hornblende or a combination of plagioclase and hornblende. The ultimate products of the retrogradation of the metabasic rocks in

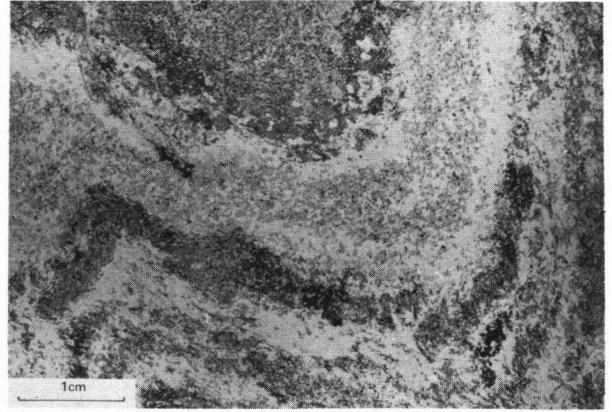


Fig. II-12. Folded leptynite layer between basic granulites. Locality: top of Mount Castrillon.

the amphibolite facies will be either garnet-free hornblende gneisses or amphibolites. The antiform with Mount Agudo at its centre shows clearly that retrograde metamorphism was more effective at the periphery of the formation. The centre is formed by pyroxene-bearing hornblende-garnet gneisses, overlain by hornblende-garnet gneisses; the outer zone is composed of hornblende gneisses.

Sample RGM 162697 (from the margin of the Agudo Antiform) is an example of a hornblende gneiss. Blue-green hornblende ($2 Va = 74^\circ$, $[001] \wedge \gamma = 17^\circ$) occurs in two generations: medium-grained clasts and fine-grained blasts. The latter, showing highly preferred orientation of their $[001]$ -axes, define a new foliation plane. Plagioclase (38% An), twinned according to (010) and (001), and quartz form a mosaic texture. A layering consists of alternating leucocratic bands. Rutile only occurs enclosed in hornblende, in the leucocratic parts it is replaced by titanite. Only one small grain of corroded garnet remains as an armoured relic in hornblende. Clinzoisite, apatite and zircon are minor constituents. Hornblende is replaced by chlorite along its rims.

In addition to the metabasites described above, these formations also contain certain typical rock types.

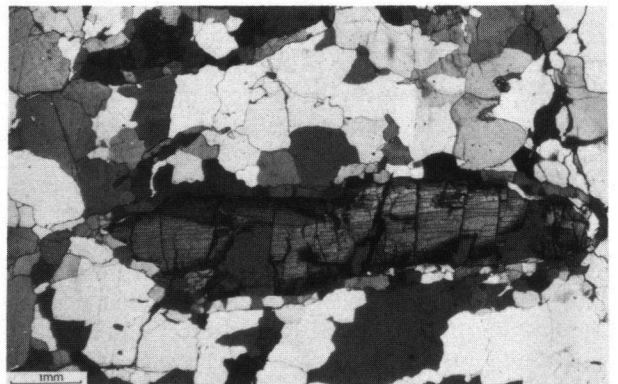


Fig. II-13. Crystal of kyanite surrounded by a rim of oligoclase in quartz segregation vein. Thin section RGM 162699.

Leptynites. — A highly characteristic feature of the metabasic granulites is the occurrence of leucocratic garnet-rich bands, a few cm to dm in width, which run more or less parallel to the foliation in the metabasites (Fig. II-12). These bands are composed of garnet + plagioclase + quartz. Clinzoisite with orthite kernels, hornblende and clinopyroxene can also occur in minor quantities. Rutile and zircon are accessories. The presence of these bands in the metabasites of the granulite facies zone and their absence in the metabasites of the amphibolite facies zone is a criterion for distinguishing retrograded granulite facies rocks.*

Segregated quartz veins containing kyanite and zoisite. — In the metabasic rocks are a few segregation veins of quartz. A good example was found on the northern slope of Mount Texón (sample RGM 162699). About 80% of the rock is coarse-grained undulose quartz which forms a mosaic texture with the elongated minerals, such as undulose kyanite and β -zoisite, lying in more or less parallel orientation. A few rounded and broken grains of light pink garnet are also present. Garnet, kyanite and zoisite have 0.2–0.3 mm wide coronas of fine-grained twinned plagioclase crystals. Muscovite is present as fine flakes in the quartz mosaic; but in some cases it also replaces kyanite, forming a rim between plagioclase and kyanite. β -zoisite has clinzoisite rims at the contact with plagioclase (Fig. II-13). Biotite is found as rims around muscovite flakes and as replacement of garnet. Zircon is an accessory.

Garnet-biotite-(muscovite) gneisses in the metabasites. — In the eastern part of the Bacariza Formation, bands of biotite-garnet gneisses alternate with hornblende-garnet-bearing gneisses. Most typical are the gneisses with large

*) Although the origin of leptynites remains a question to be solved, chemical analyses suggest a granophyric origin. Except for a higher Na₂O content, the chemical analysis of a hedenbergite granophyre from Dillsburg, Pennsylvania (Hotz, 1953) shows strong similarities to that of the leptynites of Cabo Ortegá.

	1	2	3
SiO ₂	69.56	63.26	61.69
Al ₂ O ₃	13.08	15.70	12.61
Fe ₂ O ₃	2.38	0.81	2.98
FeO	6.17	8.90	8.32
MnO	0.20	0.22	0.15
MgO	0.97	0.99	0.77
CaO	4.66	7.10	4.04
Na ₂ O	2.47	1.96	5.71
K ₂ O	tr.	0.03	0.57
H ₂ O	0.26	0.27	0.98
TiO ₂	0.57	0.77	1.46
P ₂ O ₅	0.17	0.22	0.50
total	100.49	100.23	99.78

1. Leptynite from the Bacariza Formation (Vogel G7-2).
2. Leptynite from the Candelaria Granulite Formation (RGM 162698).
3. Hedenbergite granophyre from Dillsburg.

'augen' or streaks of plagioclase porphyroclasts. The anorthite content of these clasts is higher in the rims (25–27% An) than in their cores (21–23% An). The augen are always surrounded by mortar structures.

Deep red-brown crystals of biotite, and sometimes also muscovite, lie in streaks that bend around the augen. The rest of the rock is made up of quartz, plagioclase, garnet, biotite, (hornblende) and epidote (pistacite). Apatite, tourmaline, rutile (always enclosed), titanite, zircon and opaque matter occur as accessories (sample RGM 162700). Where deformation was more pronounced, the augen (still rimmed by fine-grained crystals of quartz and plagioclase) are smaller and the rock has a more planar structure. Biotite seems to grow at the expense of garnet. Neither kyanite nor potash-feldspar was found. It is not clear whether these gneisses should be correlated with the Chimparragneisses or the Banded Gneisses.

Calc-silicate rocks. — These occur mostly in the western part of the Bacariza Formation, but also in the Agudo Formation. The calc-silicate rocks are macroscopically slightly darker in colour than the garnet-clinopyroxene rocks of the granulite facies. The mineral paragenesis is clinopyroxene-epidote or clinopyroxene-garnet-epidote. No rutile is present, but titanite is found in abundance. Both garnet and clinopyroxene have intense colours, the garnet being dark pink and the clinopyroxene dark green. Blue-green hornblende is secondary after clinopyroxene (sample RGM 162701).

Paragneisses

The Chimparragneiss Formation is situated between the metabasic Agudo and Bacariza Formations. This position suggests that the same (granulite facies) metamorphic conditions as in the metabasites could have prevailed. Such a correlation is confirmed by the fact that the few metabasic inclusions in the Chimparragneisses have a granulite facies paragenesis (gt+cpx+plag). Similar evidence is found in the dolerite dykes where garnet reaction rims occur between clinopyroxene and plagioclase. Although the map indicates the presence of paragneisses only, orthogneisses and granitoid rocks also occur in the Chimparragneiss Formation.

Most gneisses have planar or planolite, sometimes mylonitic, textures. The latter are concentrated near the contacts with the metabasic formations. Normally the Chimparragneisses are garnet-bearing biotite or two-mica gneisses. Quartz and plagioclase are frequently found to be concentrated in augen and streaks, indicating the incipient formation of a mobilizate. Coarse-grained muscovite-bearing pegmatoid bands also occur.

Quartz, plagioclase, garnet, biotite and (muscovite) are the main rock-forming minerals. Frequently the garnet-biotite gneisses also contain kyanite; in some cases two generations of kyanite can be discerned. Tourmaline, rutile, (titanite), clinzoisite, apatite and zircon are

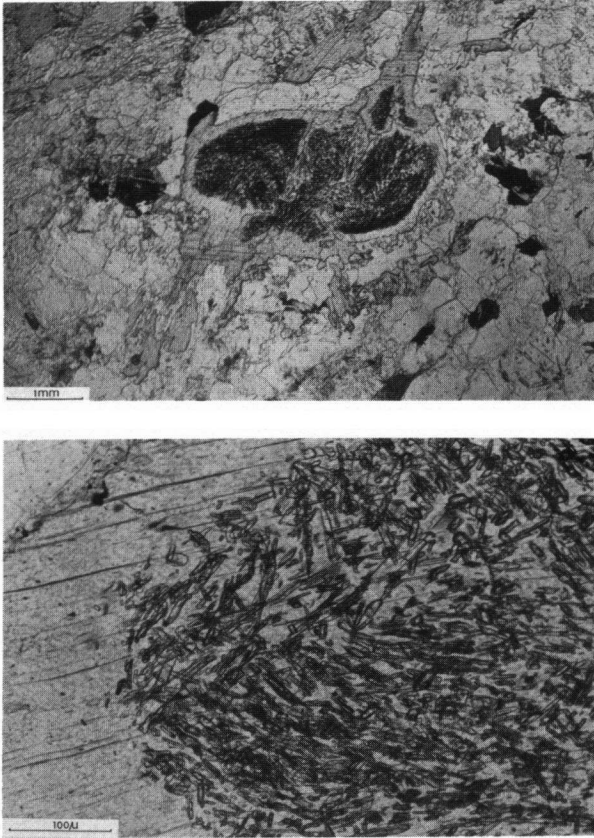


Fig. II-14. a. Large muscovite crystals containing sigmoidally oriented inclusions of kyanite needles. b. Detail of a. Thin section RGM 162703.

accessories. Quartz often forms the ribbon-like bands characteristic of the 'granulite' texture. Plagioclase (18–35% An) is sometimes antiperthitic, commonly twinned according to the Albite and Pericline laws. The fine-grained anhedral garnets show various stages of the replacement by biotite. Muscovite crystals, often bent or strained, are frequently bordered by fine biotites; this is especially true if a second generation of kyanite is present.

Interesting features are seen in thin section RGM 162702 (from the peninsula just S of Cedeira, near Esteiro). The fine- to medium-grained kyanite-garnet two-mica gneiss shows streaks richer in biotite and kyanite and parts richer in plagioclase and quartz with a mosaic texture. Medium-grained kyanite of the older generation is markedly deformed; the younger generation formed fine-grained aggregates. Garnet is also present in two generations: the older with corroded outlines and often bordered by kyanite, the younger surrounding biotite. Biotite has recrystallized in polygons. Muscovite, showing a more random orientation, is sometimes rimmed by biotite. Zircon with strong pleochroic haloes in biotite, apatite and olive-green tourmaline are accessories. Potash-feldspar is not present.

The granitoid rocks of this formation are well-repre-

sented by thin sections RGM 162703 and RGM 162704. Medium-grained quartz, microcline and plagioclase form a granitic texture. Muscovite and biotite are also rather abundant. Small relics of corroded garnet, surrounded by biotite, are still present. Biotite is replaced by muscovite; in some cases the biotite has disappeared completely. Along the borders of potash-feldspar myrmekite occurs. Large muscovite crystals contain very fine-grained sigmoidally oriented needles of kyanite (corroborated by X-ray diffraction, see Fig. II-14 a+b). In thin section RGM 162704 kyanite is concentrated along the borders of potash-feldspar (cf. Sturt, 1970). Chloritization of biotite and sericitization of feldspar are indications of a later retrograde metamorphism. Deformation of these granitic textures resulted in the formation of a wide range of orthogneisses with planar and linear textures.

Gabbros in the Chimparragneisses. — The top of Mount Castro, just south of Villarrube, contains gabbro. The gabbro is encountered in several places running in a NE direction. In addition dolerite is often found in the Chimparragneiss, but always as float. These rocks are of interest because they sometimes show metamorphic reaction rims between plagioclase and clinopyroxene. The gabbro of Mount Castro (sample RGM 162705) has a fine ophitic texture. It consists of plagioclase (40%), clinopyroxene (25%) and orthopyroxene (25%), biotite, hornblende, quartz and ore minerals. The plagioclase is zoned (core 58% An, rim 38% An). The orthopyroxene ($2 V\alpha = 74^\circ$) is a bronzite with 'schiller' inclusions; clinopyroxene has a small optic angle ($2 V\gamma = 46^\circ$). Both pyroxenes have borders of brown hornblende. Red-brown biotite is moulded on ore; rutile is an accessory. The rock is slightly strained. Sample RGM 162720 from the peninsula of Croya (S of Cedeira) is a medium-grained ophitic olivine (Fo 75 Fa 25) gabbro. Plagioclase is an unzoned bytownite (75% An). Olivine is surrounded by pyroxene and hornblende. Both ortho- and clinopyroxene are present and are rimmed by brown hornblende. Brown spinel occurs in olivine. Both these samples have a fresh appearance in contrast to the garnet-bearing sample RGM 162706. The latter is of the same type as sample RGM 162705 but the plagioclase is crowded with needle-like inclusions. Garnet coronas have formed around pyroxene and biotite (Fig. II-15), but this phenomenon is restricted to patches in the thin section. The formation of hornblende rims is more extensive than in the unaltered sample RGM 162705.

C. AMPHIBOLITE FACIES ZONE

The catazonal complex at Cabo Ortegal is surrounded by a more or less complete mantle of amphibolite facies rocks. The metabasites are represented by the Peña Escrita Formation and the Candelaria Amphibolite Formation, as well as some smaller outcrops on the eastern side. The Cariñogneiss Formation is the

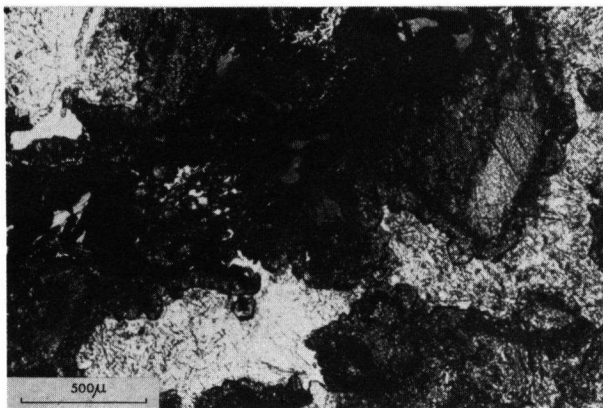


Fig. II-15. Garnet corona around pyroxene and biotite in a dolerite in the Chimparragneisses. Thin section RGM 162706.

amphibolite facies equivalent of the granulite facies Chimparragneiss Formation. The Cariñogneiss Formation lies to the east of the Banded Gneiss Formation. Locally small outcrops of banded gneisses also occur between the eclogite ridges.

Metabasites

Macroscopically the amphibolites are dark, fine-grained, schistose rocks. Sometimes a lamination is visible due to streaks richer in plagioclase. Occasionally the amphibolites contain garnet, although this is rare. In a quarry along the road from El Ferrol to Santa Marta de Ortigueira (km 62.5), one can discern thin calcite layers parallel to the lamination. Although the amphibolites are microfolded, they dip rather consistently (see Enclosure 1) towards the centre of the Cabo Ortegal Complex while in the south they lie subhorizontally, but still with inward dips.

Microscopically the amphibolites are essentially made up of fine-grained, dark green hornblende ($2 Va = 70^\circ - 78^\circ$, $[001] \wedge \gamma = 15^\circ - 17^\circ$) and fine-grained granular plagioclase. Sometimes larger porphyroblasts of hornblende are dispersed throughout the rock. Hornblende has a strong preferred orientation. A pink garnet is known from some samples in the west (RGM 162707) and south (RGM 162708). It formed as small subhedral crystals which are apparently unstable and is surrounded by plagioclase and hornblende. Plagioclase occurs as fine-grained anhedral crystals forming a mosaic with the hornblende. Its anorthite content ranges from 20 to 25% An. Fine-grained quartz occurs interstitially. Titanite is abundant as small spindles parallel to the foliation. Epidote is dispersed throughout the rock and in veinlets; it replaces hornblende near these veinlets. In the south and east near the greenschists, epidote becomes a rock-forming mineral. In thin sections of these rocks, one can discern non-pleochroitic epidote and pistacite with distinct greenish yellow tints for γ . The latter is supposed to be characteristic for the incipient retrograde metamorphism into the greenschist facies. Notable also

is that the hornblende in these slightly retrograde amphibolites is clearly more bluish in colour. The amphibolites in the south sometimes contain calcite in thin bands (3–6 mm) parallel to the foliation (sample RGM 162708) or as small crystals dispersed throughout the rock (sample RGM 162722). A chlorite with a distinctly green colour for γ replaces hornblende. Accessories are zircon, apatite, hematite and opaque matter.

In sample RGM 162709 from the Peña Escrita Formation (found near San Roman in the south), the amphibolite is crossed by a 1.5 cm thick vein. The centre of the vein (0.5–0.7 cm) consists of light green clinopyroxene ($2 V\gamma = 58^\circ$, $[001] \wedge \gamma = 36^\circ$) bordered on both sides by a zone. The zones are composed of saussuritized plagioclase, quartz, epidote and calcite and seem to be reaction zones between the amphibolite and the pyroxene vein, since the titanite crystals in both the zones and the amphibolite are in parallel orientation. Similar calc-silicate bands are described by Vogel from the Candelaria Amphibolite Formation.

The Purrido Amphibolite Formation. — Although separated from them by the Carreiro zone of tectonic movement, the Purrido Amphibolite Formation lies west of the Candelaria Amphibolite Formation. These amphibolites form macroscopically a rather monotonous greyish green series, consisting of a medium-grained hornblende and plagioclase, sometimes with a streaky appearance due to coarse-grained bands of plagioclase. The amphibolites show a highly developed foliation due to their planar nematoblastic texture. Now and again a lineation can be seen on the schistosity plane. About 80% of the rock is hornblende (α light yellowish green, β olive-green, γ bluish green; $[001] \wedge \gamma = 18^\circ - 20^\circ$, $2 Va = 80^\circ - 85^\circ$). A fabric of $[001]$ -axes in parallel orientation is notable. Plagioclase is heavily saussuritized; sometimes pronounced lamellar twinning is still recognizable. Slightly undulose quartz, epidote and titanite sometimes with cores of rutile occur in minor amounts. In all thin sections of the amphibolites one can see replacement of hornblende by chlorite. In places the rock is so rich in epidote that one can speak of an epidosite.

In several places (at the extremity of the Sanxiao peninsula) 10–40 cm wide bands extend parallel to the foliation; they consist of coarse-grained garnet-hornblende or garnet-chlorite schists (sample RGM 162719). In the garnet-bearing bands pennine replaces the hornblende, thus forming the garnet-chlorite schists. The idiomorphic garnets are light pink in colour and can be more than 4 cm across with parallel trails of inclusions of quartz, opaque matter and rutile.

Paragneisses

The Cariñogneisses are paragneisses of the amphibolite facies zone. A characteristic difference between these gneisses and the metasediments of higher metamorphic grade is the occurrence of staurolite in the former. This makes it possible to correlate the Cariñogneisses with the gneisses in the south near Balocos, where staurolite is



Fig. II-16. Detail from thin section RGM 162711 of a staurolite-bearing Cariñogneiss found between the eclogite ridges. Ky = kyanite; st = staurolite.

again found. The broad outcrop of the Cariñogneisses in the north narrows south of Campo del Hospital to a width of 250 m. The contact with the banded gneisses is sometimes marked by serpentinite outcrops. Staurolite-bearing gneisses are also found between the eclogite ridges, as reported by Vogel (1967) and H. A. de Miranda. The author found staurolite-bearing gneisses between the eclogites in the southern part of the Cabo Ortelal Complex near Felgosas de Abajo (Fig. II-16).

The gneisses near Balocos (sample RGM 162710) are well-laminated showing good cleavage. They lie almost horizontally. The rocks are fine-grained garnet-bearing muscovite-biotite gneisses (plagioclase 20% An) with large (6 mm) augen of bent muscovite flakes. In these augen relics of staurolite occur together with small, rounded, clear garnets. The garnets in the gneiss-matrix are elongated (long axis 1–1½ mm) with their long axis parallel to the schistosity. These garnets are encrusted with limonite, due to superficial alteration. Locally muscovite is replaced by chlorite. Zircon, tourmaline, hematite, apatite and opaque matter are minor constituents. No kyanite is found in this sample, but it is present in other samples. Other minerals which may occur in the Cariñogneisses are epidote, metamict orthite, titanite and rutile. No indications of incipient anatexis have been encountered in the Cariñogneisses.

Metagabbros

At the border between the Candelaria Amphibolite Formation and the Candelaria Granulite Formation are a number of lenses of gabbroic rocks. Gabbroic rocks also occur at the contact between the Peña Escrita Formation and the Agudo Formation. Vogel (1967, p. 186) also mentioned the presence of metagabbros in the centre of his Candelaria Amphibolite Formation without observing the fact that they lie on a metamorphic boundary. The gabbro lenses probably occupy a thrust plane between rocks of different metamorphic grade. Gabbro intrusion must have occurred at least twice; first

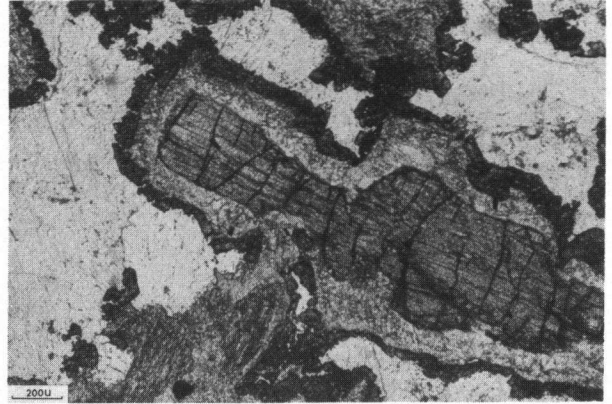


Fig. II-17. Garnet corona around hypersthene. Between the garnet and hypersthene is fine-grained hornblende. Large crystals of labradorite were broken and recrystallized as andesine in mortar zones. Thin section RGM 162712.

during granulite facies metamorphic conditions (M_2) and later during amphibolite facies conditions (M_3). This can be deduced from the adaptation of the gabbros to these different metamorphic conditions.

Adaptation to granulite facies conditions. — In sample RGM 162712 (Fig. II-17) two phenomena attract attention: (1) the formation of garnet coronas around hypersthene and (2) the presence of an older generation of coarse-grained labradorite (60% An) and a fine-grained aggregate of recrystallized andesine crystals (42% An). An inner reaction zone bordering the hypersthene consists of an aggregate of fine-grained, xenomorphic, light, bluish green crystals of actinolitic hornblende, interspersed with small quartz grains. Clinopyroxene has altered into brownish green hornblende. Here and there clusters of scapolite are found between the plagioclase crystals (Engels and Vogel, 1967).

Sample RGM 162713 from a locality west of Mount Agudo has an ophitic texture; plagioclase (39% An), twinned according to the Karlsbad, Albite and Pericline laws, is only partly saussuritized and contains epidote needles as inclusions. Relics of pyroxene are surrounded by fine-grained bluish green hornblende crystals, the pleochroism becoming more intense towards the plagioclase borders. Garnet seems to be restricted to rims around ore clusters. Zones of very fine-grained recrystallized crystals running through the plagioclase indicate the latter's deformation.

Sample RGM 162714 from a locality south of Mount Agudo shows the phenomena described in sample RGM 162712 but the deformation is slightly stronger; the texture is still recognizably ophitic.

Sample RGM 162715, an (olivine-bearing) two-pyroxene metagabbro, comes from a locality near Monte de Cabannela. In thin section a series of reaction rims is seen around former olivine crystals. In the centre olivine is replaced by an aggregate of ore minerals. The first inner rim consists of orthopyroxene with $2V\gamma = 60^\circ$.

Sometimes this rim is in turn replaced by a rim of actinolitic hornblende. The following rim is of very fine-grained olive-green hornblende; the outer rim consists of garnet. Clinopyroxene has a rim of fine-grained olive-green hornblende but the rim of garnet is often missing. Plagioclase shows Karlsbad, Albite and Pericline law twinning (60% An) and occasional undulose extinction. Mortar zones cut across the plagioclase. Fine-grained recrystallized plagioclase has a lower anorthite content (40% An).

The rock of sample RGM 162716 still shows some pyroxene relics, garnet rims and fine-grained brown-green hornblende. Plagioclase has recrystallized completely into an aggregate of oligoclase (25% An). It is remarkable that part of the magmatic clinopyroxene has recrystallized as clear diopsidic pyroxene. The sample is crowded with ore clusters. The rock is almost completely transformed into a granulite.

Adaptation to amphibolite facies conditions. — These gabbro lenses vary in diameter from about 100 m (a very coarse-grained gabbro lens, with crystals up to 4 cm, on the summit of the Sanxiao peninsula, west of Cedeira) to smaller lenses not exceeding a thickness of 10 cm. All of the lenses show a 'flaser' texture at their periphery. The smaller ones become 'flaser' amphibolites. Most of the undeformed cores of the lenses are medium-grained and have a gabbroic texture. The original gabbro must have consisted of labradorite, clinopyroxene with well-developed diallage parting, and orthopyroxene. Talc, surrounded by a rim of ore, reveals the former presence of olivine. Apatite, rutile, quartz and ore occur as accessories.

Sample RGM 162717 from the coarse-grained gabbro of Sanxiao is half pyroxene and half saussuritized plagioclase. The orthopyroxene is a bronzite with 'schiller' inclusions. Both clinopyroxene and orthopyroxene are replaced along their borders by a green hornblende which has a dusty appearance due to opaque inclusions. An aggregate of very fine-grained, newly formed, blue-green hornblende crystals borders the saussurite. Rims of ore suggest the former presence of some small olivine grains. Actinolite and chlorite are later products. A small cavity is filled with carbonate and quartz. The rock is not deformed.

In sample RGM 162718 saussurite is almost entirely replaced by epidote. There are no pyroxene relics; all pyroxene is replaced by uraltite and by an aggregate of very fine blue-green hornblende.

The Carreiro zone of tectonic movement

The Carreiro zone of tectonic movement lies just west of the Candelaria Amphibolite Formation. The zone is at its widest and is best exposed near the lighthouse at Punta Candelaria; it tapers out southwards. In addition to blastomylonites with inclusions of foliated amphibolites, lenses of highly deformed serpentinites and amphibolites are found in this zone. In the south, near Pantin, the zone is marked by the blastomylonites only.

The blastomylonites are probably the products of greatly deformed Chimparragneisses, rocks of the Candelaria Formations and serpentinites, as in the Uzal. This important movement zone was generated during the second deformation phase and was active during all later deformations. It was probably the sole of the overlying thrust planes.

Physical conditions during metamorphism

Small differences in physical conditions might be an explanation for the occurrence of zones with eclogites, mafic-granulites and (garnet-)amphibolites in close proximity. Experimental studies have shown that the transformation from the low-pressure gabbro assemblage to the high-pressure eclogite assemblage proceeds via a transitional mineral assemblage characterized by the co-existence of garnet, pyroxene and plagioclase (Ringwood and Green, 1966). This transitional zone has a slope of 21 bars/°C and in anhydrous environments, eclogite should be stable throughout large regions of the continental crust. However at high water vapour pressures, rocks of basaltic composition are converted into hydrated mineral assemblages: e.g. (garnet-)amphibolites.

Although the gabbro-eclogite transformation is gradual between the garnet-in and plagioclase-out isograds and the transformations eclogite-(garnet-)amphibolite and gabbro-(garnet-)amphibolite will also be gradual over a distinct P/T range, this means that the ranges over which eclogites, (garnet-)amphibolites and gabbros are stable join each other in a 'triple-point' (Essene and Fyfe, 1967). The position of this 'triple-point' on the slope of the gabbro-eclogite transformation is dependent upon the stability of amphibole. The breakdown of hornblende is reported by Lambert and Wyllie (1968) at pressures between 15 and 25 Kb. Essene et al. (1970) also found that hornblende disappears between 15–25 Kb and 700°–900°C. In both cases $P_{H_2O} \approx P_t$. If $P_{H_2O} < P_t$, the amphibole stability field would be reduced (Yoder and Tilley, 1962; Lambert and Wyllie, 1968). At high water vapour pressures, amphibolites would start to melt at $T \approx 650^\circ\text{C}$. There are some arguments to suppose that the metabasites reached a temperature above $\approx 650^\circ$ without melting and therefore $P_{H_2O} \ll P_t$ seems warranted.

The paragneisses of the amphibolite zone (Cariñogneisses) are not metatexitic in contrast to the gneisses of the granulite and eclogite zones (Chimparragneisses and the Banded Gneiss Formation). The Cariñogneisses contain staurolite. Fe-staurolite is stable to slightly below 700°C, almost independent of pressure according to Richardson (1968). If staurolite contains Mg it may persist even to slightly higher temperatures (Hoschek, 1967, 1969). The sporadically observed staurolite in eclogite shows distinct features of its instability.

The temperature at which a gneiss begins to melt depends on several factors, such as chemical composition, the normative Ab/An ratio, the presence or absence of potash-feldspar, the presence of volatile components

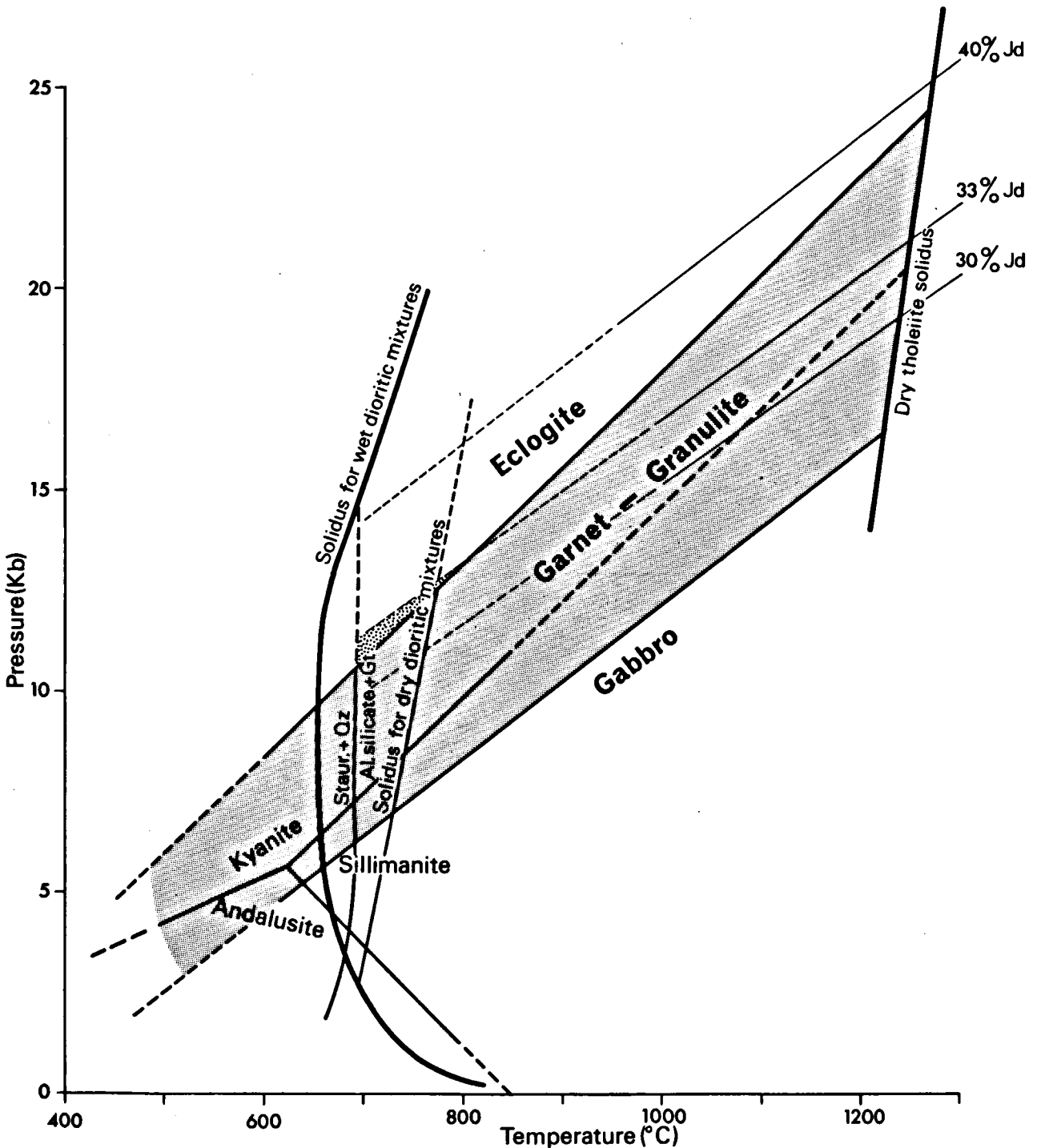


Fig. II-18. The position postulated for the field in which eclogite formation occurred in Cabo Ortegal (heavily shaded). Boundary curves for several metamorphic reactions are also shown. Data from Kushiro (1965), Green & Ringwood (1966), Richardson (1968), Richardson et al. (1969), Brown & Fyfe (1970).

and most important, the water vapour pressure (Tuttle and Bowen, 1958; Wyllie and Tuttle, 1959, 1961, 1964; Winkler and von Platen, 1961a, 1961b, 1962; Winkler, 1961, 1966, 1967; von Platen, 1965a, 1965b; Piwinski and Wyllie, 1968; Brown and Fyfe, 1970). Experimental

studies revealed that if $P_{H_2O} = P_t$ gneisses melt between 600° – 700° C. If $P_{H_2O} \ll P_t$ the temperatures at which the gneisses start to melt are higher. The Cabo Ortegal gneisses, which started to melt at temperatures above the stability T of staurolite, show predominantly forms of

metatexis (in the sense of Mehnert, 1968) and not anatexis; therefore on this basis rather 'dry' gneisses can also be postulated.

From the above considerations, $700^{\circ} < T < 750^{\circ}$ may be inferred for the first phase of metamorphism. The granulite-eclogite transition at these temperatures is found at pressures of 11–13 Kb. Experiments by Kushiro (1965) predicted a jadeite content for omphacites under these conditions of between 30–35%. This is in remarkable agreement with Vogel's analyses of omphacites in which the jadeite content was 31–33% (his lower values of 18% and 23% are for symplectitic omphacites which have already lost part of their Na_2O to form plagioclase). Noteworthy is also that Kushiro's curve for 30–35% jadeite lies in the high P/T conditions in the granulite field but in a lower P/T range in the eclogite field. The curve for 33% jd given in Fig. II-18 crosses the boundary at about 800° . The values of 700° – 750° C for T and 11–13 Kb for P differ from Vogel's values of 630° – 900° C and 14–19 Kb for the eclogites. Vogel inferred these values from the data of Pistorius et al. (1962) for the field in which kyanite and zoisite are mutually stable. Later experiments by Newton and Kennedy (1963) suggest that zoisite and kyanite can be stable together at much lower pressures and temperatures.

Bryhni et al. (1970) argued that if $P_{\text{H}_2\text{O}} \ll P_t$ the Norwegian eclogites could have formed under crustal conditions. They point out the fact that 'partial melting of crystalline rocks containing small amounts of water may lead to low values of $P_{\text{H}_2\text{O}}$ yielding a 'buffered' condition of $P_s = P_f > P_{\text{H}_2\text{O}}$ '. Fry and Fyfe (1969) concluded that 'crustal eclogites form in dry environ-

ments where $P_t \gg P_{\text{H}_2\text{O}}$. $P_{\text{H}_2\text{O}}$ is likely to be determined and buffered by incomplete hydration reactions'. They call attention to the 'not uncommon association of eclogites with partially serpentinized ultrabasic rocks'. Miller (1970) inferred for the gabbro-eclogite transformation in the Oetztaler Alps $T = 550^{\circ}$ – 700° C and $P = 6$ – 10 Kb. Dobretsov et al. (1970) in their classification of areal metamorphic formations give values of $P = 10$ – 15 Kb, $T = 750^{\circ}$ – 850° C and $P_{\text{H}_2\text{O}} \ll 0.3$ for the eclogite-gneiss formation.

The postulated values for Cabo Ortegal's first metamorphism of $T = 700^{\circ}$ – 750° C and $P = 11$ – 13 Kb (depth = 40–46 km) are in fair agreement with the opinion that eclogites can form under crustal conditions. The geothermal gradients of about 17° C/km would give regional metamorphism of a type between the intermediate- and high-pressure facies series (den Tex, 1971a).

The conditions of the second metamorphic phase are difficult to determine, because the growth of hornblende after clinopyroxene is mainly controlled by an increase in $P_{\text{H}_2\text{O}}$. The creation of 'retrograde' mineral assemblages by an increase in $P_{\text{H}_2\text{O}}$ is discussed, among many others, by Eskola (1952), Yoder (1952, 1955) and Dawes (1970). High P/T conditions are suggested by the formation of a second generation of kyanite in the paragneisses. The formation of garnet coronas in gabbros probably represents the cooling of a magma in the high-pressure granulite facies.

During the third metamorphic phase, low P/T conditions are inferred from the fact that gabbros are converted into 'flaser' amphibolites. The last metamorphic phase occurred under greenschist facies conditions.

CHAPTER III

TECTONICS

INTRODUCTION

Aim. — This chapter deals with the differentiation between several successive deformation phases within Cabo Ortegal, the description of the structures caused by these deformations and the relationship between deformation and metamorphism. Field investigations are supported by the petrofabric studies described in the next chapter.

Recent tectonic studies of the Hesperian massif

Pre-Hercynian deformation phases. — In the past few years, the tectonics of several catazonal complexes which closely resemble the Cabo Ortegal Complex have been described, i.e. the Bragança and Morais Complexes in N Portugal by Anthonioz (1968, 1969, 1970) and the Ordenes Complex, as defined in the study of an area near Santiago, by van Zuuren (1969). Both authors

recognized three pre-Hercynian deformation phases. Pre-Hercynian deformations in other areas of W Galicia have been reported briefly by Avé Lallemand (1965), Floor (1966), den Tex and Floor (1967) and Arps (1970).

Hercynian deformation phases. — The most extensive recent study of Hercynian deformations is a memoir by Matte (1968) dealing with the tectonics of the 'virgation hercynienne' or Hercynian arc in Galicia. Matte studied a large area of mainly Paleozoic rocks in E Galicia. According to Matte two Hercynian Deformation phases determined the structures; in W Asturia these same phases were followed by the formation of kink-bands. Marcos (1971) also reports the presence of both phases in W Asturia. Hercynian deformations in W Galicia have been described by the above-mentioned authors and by Floor et al. (in publication).

Nomenclature

For the description of folds, the following terms are used in the sense proposed by Fleuty (1964):

- hinge or fold axis: the line along a particular bed joining the points of greatest curvature in an infinite number of cross-sections (observed structure).
- axial direction: the nearest approximation to the line which, moved parallel to itself, generates (the folded) surface.
- axial plane: the locus of the hinges of all beds forming the fold.
- axial plane trace: the intersection of the axial plane with any surface other than those affected by the fold.
- profile plane: the cross-section normal to the hinge.
- fold limb: the part of the folded surface between one hinge and the next. (if unequal in length: long limb and short limb).

The following symbols are used for the description of deformation structures:

- F_1, F_2, F_3 etc.: phases of folding in chronological order.
- s_s : sedimentary stratification.
- s_1, s_2, s_3 etc.: s-surfaces in chronological order.
- l_1, l_2, l_3 etc.: lineations in chronological order.
- a: direction of translation by simple shear.
- B_1, B_2, B_3 etc.: directions of the fold axes formed during F_1, F_2, F_3 etc.

Outline of the deformation phases within Cabo Ortegal

Several deformation phases have been recognized in the Cabo Ortegal Complex. The earliest evidence of deformation is found as an F_1 -fold with a N-S fold hinge and a probably horizontal axial plane. The second deformation phase (F_2) was responsible for the mylonitization of the rocks and produced folds with E-W fold hinges and subhorizontal axial planes. The third deformation phase (F_3) is characterized by folds with N-S axial directions and by (again) subhorizontal axial planes; in contrast the folds of the fourth deformation phase (F_4) have vertical, N-S striking axial planes. Locally a fifth deformation phase (F_5) produced chevron folds. Normal faults which cross the complex constitute the latest phenomenon of deformation within Cabo Ortegal.

The chronology of the deformation phases could be established (1) by determining their relationship to the metamorphic phases and (2) by investigating their mutual relationships, as expressed by their interference patterns. Ramsay (1962c, 1967) states that there are only three types of basic patterns. Of these three types only type 1 is commutative, i.e. the same pattern results irrespective of which fold is impressed first (Carey,

1962), and therefore useless for determining the sequence of the deformation phases.

In general the metabasites reveal more evidence of tectonic history than the paragneisses. This is because they are more resistant to erosion and are less overgrown; in addition structures in the paragneisses were partly destroyed by incipient anatexis.

DEFORMATION PHASES

F_1 -deformation phase

Several possible F_1 -folds have been found in the paragneisses but the only clear-cut evidence of a folding phase before F_2 is found on one polished profile plane from an F_2 -fold hinge in the gneisses on the beach just north of Cariño. On this profile plane it is seen that an older fold was refolded by the F_2 -fold (Fig. III-1). The F_1 -deformation folded a pre-existing s-plane (perhaps s_s) isoclinally. It was found that the F_1 -axial direction lies almost parallel to the profile plane, i.e. it forms a large angle with B_2 , which means that the F_1 -axial direction trends approximately N-S. A N-S direction for B_1 is also confirmed by the preferred orientations of clinopyroxene in basic granulite (see chapter IV). It is assumed that the axial planes of F_2 -folds were subhorizontal since a steep axial plane should produce another interference pattern. F_1 -folding therefore may have substantially increased the thickness of the sequence, although no fold axes are seen. In thin section, biotite and muscovite flakes are oriented parallel to the axial plane of the F_2 -fold, i.e. parallel to s_2 . However, recrystallization along this plane could be a younger phenomenon because the axial planes of both F_2 - and F_3 -folds are subhorizontal.

No F_1 -folds have been observed in metabasic rocks. This may be due to the material since only heterogeneous rocks can be folded, e.g. when there is a difference in competence between the layers. If homogeneous basalts or gabbros are deformed and metamorphosed,

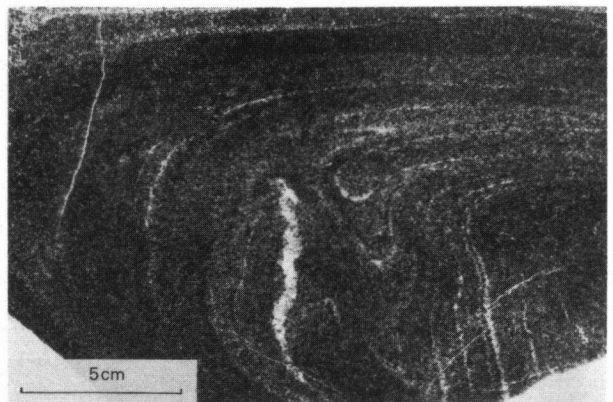


Fig. III-1. Profile plane of an F_2 -hinge in the paragneisses north of Cariño. An older F_1 -fold, refolded by F_2 , is seen in the centre.

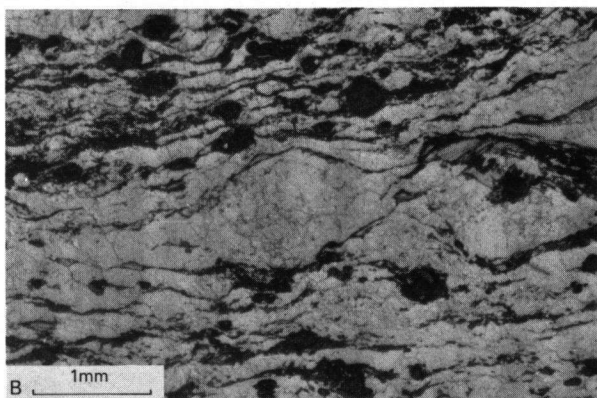
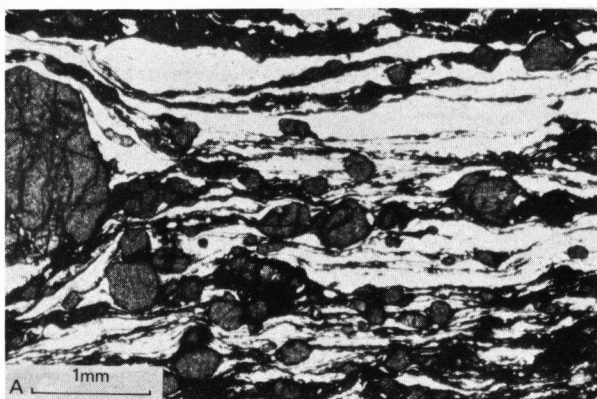


Fig. III-2. Part of a thin section of (a) a mylonitic mafic granulite from the Bacariza Formation and (b) a mylonitic Chimparragneiss.



Fig. III-3. Drag folds (F_2) in the basic granulites of the Bacariza Formation, near San Andres; looking S.

only a change in shape can be expected. In such a case an anisotropic mineral fabric is the only indication of previous differential stresses. Indeed, petrofabric analysis of the eclogites and basic granulites has revealed the presence of an F_1 -deformation phase (chapter IV).

F_2 -deformation phase

The second deformation phase produced only a few

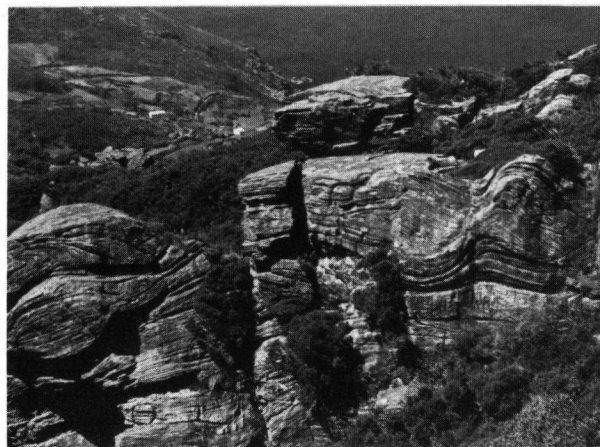


Fig. III-4. Rotated boudins surrounded by less competent, more mylonitic basic granulites. Same locality as in Fig. III-3. Looking N.

folde in the metabasic rocks. The process of cataclastic flow was the main mechanism of deformation. The granoblastic texture formed during the first metamorphic phase broke down as a result of intergranular sliding and marginal granulation. Practically all of the rocks of the granulite facies zone were deformed in this way. Cataclasis is most clearly evident at the contact between the Bacariza Formation and the Chimparragneiss Formation; this is seen in Fig. III-2a, a mylonitic mafic granulite, and in Fig. III-2b, a mylonitic paragneiss. The eclogites were more resistant to deformation, and cataclasis was restricted to narrow zones. Because of granulation and mylonitization as well as the introduction of pegmatoid matter, the mafic granulites were no longer homogeneous in composition. Thus a tectonic layering was formed.

This tectonic layering made the formation during F_2 of folds with E-W axial directions possible, such as the intrafolial folds (Turner and Weiss, 1963) found on a ridge between San Andres and Teixidelo in the Bacariza Formation (Fig. III-3). These tight to isoclinal folds have subhorizontal axial planes that dip gently to the north. These folds could be the products of the shearing stress exerted by more rigid blocks on a less competent interlayer (drag folds in the sense of Russell, 1955).

On the same hillcrest one can also observe that more rigid layers were broken and rotated relative to the layering in the less competent rocks (Fig. III-4). Both the drag folds and the rotated boudins might have been produced by the same stress field. Ramsay (1967, p. 109) shows in experiments that 'rotated' boudins are the result of asymmetric arrangement of the competent band within the strain ellipse.

Fabric analysis of an F_2 -fold with a moderately plunging hinge found north of Viciñeiro proves that the second deformation phase was active after the first metamorphic phase (M_1), which probably coincided with F_1 (see chapter IV). Folded cataclastic zones found in loose blocks of eclogite (Fig. III-5) are also believed to have been formed as drag folds.

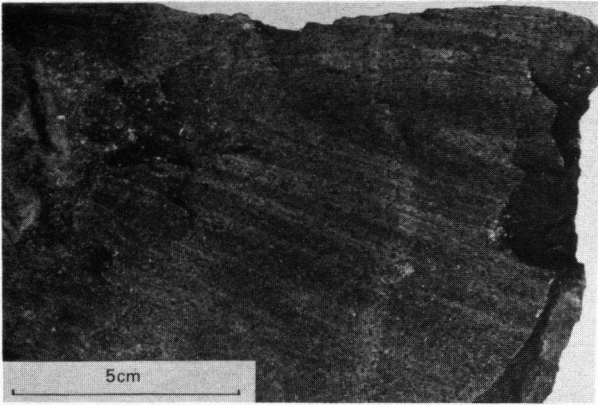


Fig. III-5. Isoclinal folding of cataclastic zones in eclogite found in the quarry at the top of Mount Castrillon.

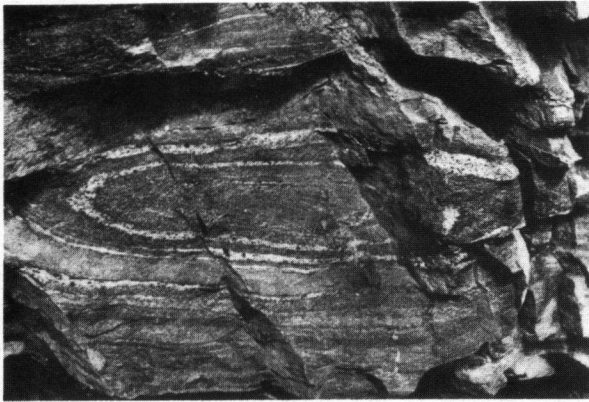


Fig. III-6. Elliptical outcrop pattern of an F₂-fold axis, found in the retrograded basic granulites of the Candelaria Amphibolite Formation; centre of the outcrop is formed by leptynite.



Fig. III-7. Two hinges of F₂-folds in paragneisses; the one on the left is the same as in Fig. III-1.



Fig. III-8. Folding of Carifogneisses at the beach north of Cariño. Three phases of folding can be seen. The F₂-folds have been formed on the E flank of an F₂-fold.

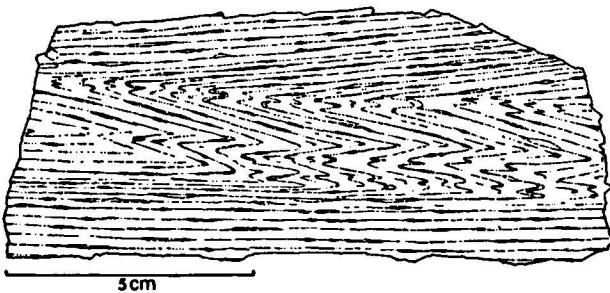


Fig. III-9. Narrow zone of F_3 -folds in Purrido amphibolites.

An elliptical outcrop pattern, seen on a vertical E-W surface near the weir in the Forcadas River, is probably due to an F_2 -hinge which was curved slightly by differential flattening (Ramsay, 1962a; Fig. III-6). It may also have been caused by a difference in the velocity-gradient of the flow (Howard, 1968). Similar elliptical outcrop patterns are also found in the (retrograded) mafic granulites near Trasmonte (Candelaria Granulite Formation) and near Porto do Cabo (Agudo Formation).

The rocks of the amphibolite facies zone were more ductile, and here deformation caused less cataclasis and more folding. In the paragneisses near Cariño, similar folds were formed with E-W axial directions and horizontal axial planes (Fig. III-7). Steeply plunging hinges in the Purrido amphibolites near Punta de Candelaria and Pantin should also be attributed to the second deformation phase. Here the fold axes were steepened by later deformation. F_2 -folds involved in interference outcrop patterns will be discussed separately.

F_3 -deformation phase

A third deformation phase (F_3) was responsible for the formation of usually small folds with hinges striking N-S (or NNW-SSE) and subhorizontal axial planes. The existence of this third phase is proven beyond doubt by the Cariño gneisses exposed on the beach north of Cariño. Here it is possible to distinguish F_1 -, F_3 - and F_4 -folds, all with N-S axial directions but refolding each other in the sequence indicated. In other areas where the full sequence cannot be established, the question may arise whether a certain N-S fold belongs to F_1 or to F_3 . One expedient is the fact that F_3 -folding was synchronous with M_2 (hornblende granulite) metamorphism, which is characterized in the basites of the granulite facies zone by the metablastic growth of a brown-green hornblende. Refolding of F_3 -folds by the almost co-axial F_4 -folds may have steepened the originally horizontal axial planes (s_3) into vertical positions. When this has happened, it is difficult to establish whether the folds resulted from the F_3 - or the F_4 -deformation phase. F_3 -folds are generally restricted to narrow zones. In the Cariño gneisses F_3 -folds are isoclinal folds on the limbs of an older F_2 -fold (Fig. III-8).

The same kind of folding produced small slip folds in the amphibolites of the Purrido Formation. Here too folding is concentrated in zones only cm to dm wide

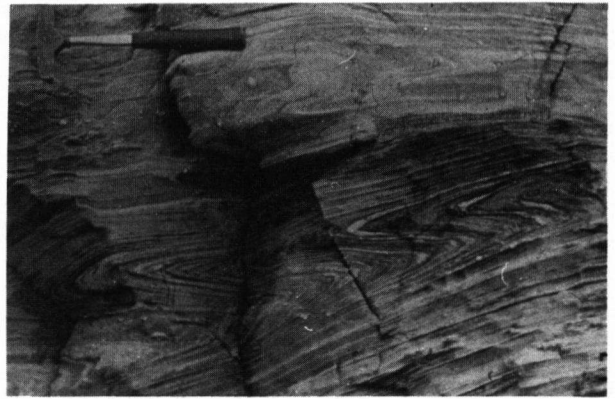


Fig. III-10. F_3 -folding of amphibolites in the Peña Escrita Formation; folding is restricted to a narrow zone.

(Fig. III-9). In addition the F_3 -folding is accompanied by a mineral lineation (l_3), which was caused by a strong preferred growth of hornblende parallel to the axial direction of the folds. The l_3 -lineation should not be confused with the l_4 -lineation that may also be seen in the same foliation plane.

Zones of F_3 -folding are also known to occur in the Agudo Formation (Fig. III-10) as well as in the metabasites of the Candelaria Granulite Formation. On the drawing it is seen that small F_3 -folds were refolded by a later F_4 -fold (Fig. III-11). In the Bacariza Formation F_3 -folding is only sporadically observed. Here the folds are less isoclinal in nature. Near the Pozo de Agua F_3 -folds which were refolded by F_4 -folds can be recognized (Fig. III-12).

F_4 -deformation phase

The F_4 -deformation phase was contemporaneous with M_3 (amphibolite facies) metamorphism. This resulted in a growth of blue-green hornblende crystals with a

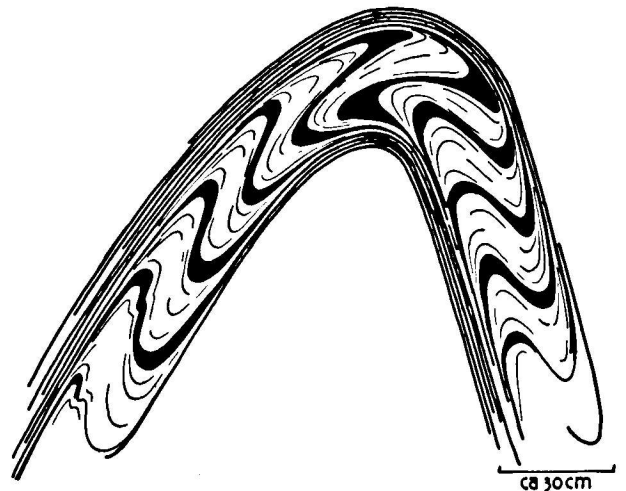


Fig. III-11. Sketch of a zone of F_3 -folding, refolded by an F_4 -fold, found in the Candelaria Granulite Formation, north of Trasmonte.

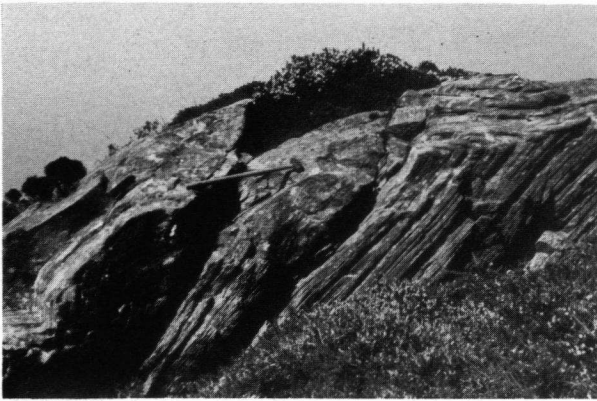


Fig. III-12. Refolding of an F_3 -fold by an F_4 -fold in the Bacariza Complex, east of the top of the Pozo de Agua.

markedly preferred orientation (see next chapter). The folding phase was also preceded by cataclasis of the rocks. This deformation phase created folds with steep to vertical axial planes and NNE–SSW axes that plunge gently (10° – 30°) to the north.

Large-scale structures such as the antiform in the Candelaria Formation, the antiform in the Agudo Formation and the synform in the southern end of the Bacariza Formation were caused by this deformation phase.

In the Bacariza Formation F_4 -folding occasionally produced folds with an amplitude of several decimeters. The major mechanism of folding seems to have been slip along the foliation plane (Class 1c in Ramsay's classification (1967)). Fig. III-13 shows such a fold, SW of the Pozo de Agua. The fold hinge can be followed for several hundred metres. Here the axial direction plunges 0° – 15° to the north. But usually F_4 -deformation of the Bacariza Formation was restricted to gentle folds with



Fig. III-13. F_4 -fold in the basic granulites of the Bacariza Formation, found SW of the Pozo de Agua. Looking N.



Fig. III-14. F_4 -folds in the basic granulites, N of Bacariza, just W of the eclogite ridge.

long wave lengths. In the northern part of the Bacariza Formation near Bacariza, F_4 -folds occur that resemble similar folds (Fig. III-14). The Candelaria Granulite Formation was folded into a large antiform structure during the F_4 -deformation phase. The hinge of the antiform can be seen on the peninsula of Sanxiao (Fig. III-15). Here the axial trace direction is ENE, the axis plunging 20° eastward and the axial plane dipping 50° SSE. To the north and south, the axial trace reverts to its normal NNE direction. The peninsula of Sanxiao must have been rotated in a dextral sense by a later deformation (F_5 ?), since all directions from previous phases rotated as well. At the hinge the axial plane is marked by the development of a weak s_4 -foliation (see Fig. III-16). On the limbs of the antiform structure, the

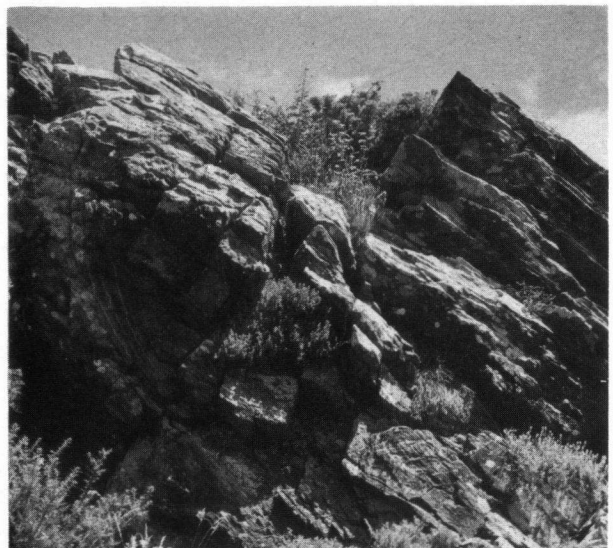


Fig. III-15. Antiform in the retrograded granulites just SW of the top of Sanxiao.



Fig. III-16. The centre of the fold hinge in Fig. III-15. A weakly developed s_4 -foliation is seen.

F_4 -folding produced parasitic folds of the leucocratic layers. The parasitic folds are generally no more than ripples on the foliation (s_2) plane, yielding a clear l_4 -lineation. The l_4 -directions form a small angle with l_3 -directions. These parasitic folds can only be seen if the leucocratic layers are thicker. These folds have a sinistral or dextral vergence (S- versus Z-folds) depending upon the limb of the macrofold. This makes it possible to determine which side of the hinge is involved even though the hinge itself is not exposed. In addition to these microfolds, isoclinal F_4 -folds with an amplitude of several dm are also frequently found, especially along the well-exposed coastal section near Cedeira. In the Cariñogneisses as well as in the Chimparragneisses, F_4 -folding of the paragneisses produced open to close folds such as seen in Fig. III-9. The difference in behaviour of the psammitic and pelitic layers under stress is seen in Fig. III-17.

Folding of eclogite. — The eclogite horizons were broken up into smaller lenses (brittle fracture of eclogite). These lenses surrounded by a matrix of banded gneisses formed large folds. The axial plane and axial direction can be reconstructed from the results of fabric analysis. These directions correspond to those of the F_4 -folding. In the centre of a large eclogite antiform on the Sierra de Moles (north of Campo del Hospital), folding of mafic granulites on a smaller scale is found (Fig. III-18). Fabric analysis of secondary hornblende suggests that these folds are of F_3 -origin. Later refolding by F_4 must



Fig. III-17. Small-scale parasitic folds in a pelitic layer between two psammitic layers.

have steepened the axial plane. The evidence is however not conclusive.

F₅-deformation phase

In a small area to the west in Cabo Ortegal near Pantin chevron folds developed, mainly in the Purrido amphibolites but also in the amphibolites of the Candelaria Formation (Fig. III-19). To the east the same kind of fold can be found near Abad in amphibolites and greenschists. Similar chevron folds are also found in the Paleozoic rocks which surround Cabo Ortegal to the east and south. It can be seen that the folds were formed by two sets of shear planes (conjugate folds). The direction of these folds is determined by the intersection of the shear planes with the layering. In the west most folds plunge moderately in a SE direction but in some places, axial directions plunge moderately in an ENE direction. Ramsay (1962b) describes a method to determine the

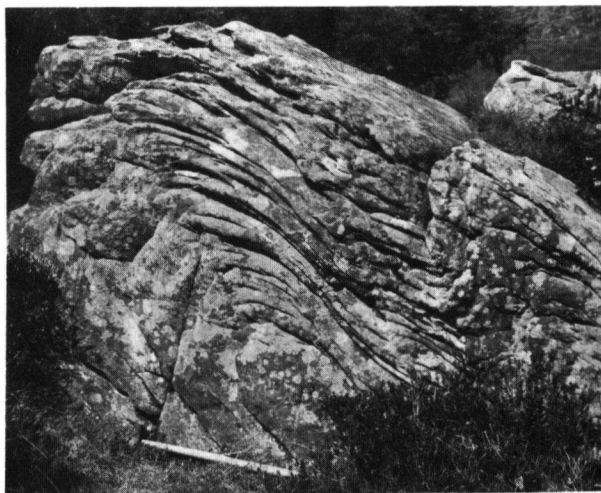


Fig. III-18. F_3 -folding of basic granulite cropping out in the centre of a large 'fold' of eclogite. Sierra de Moles, north of Campo del Hospital. Looking NE.

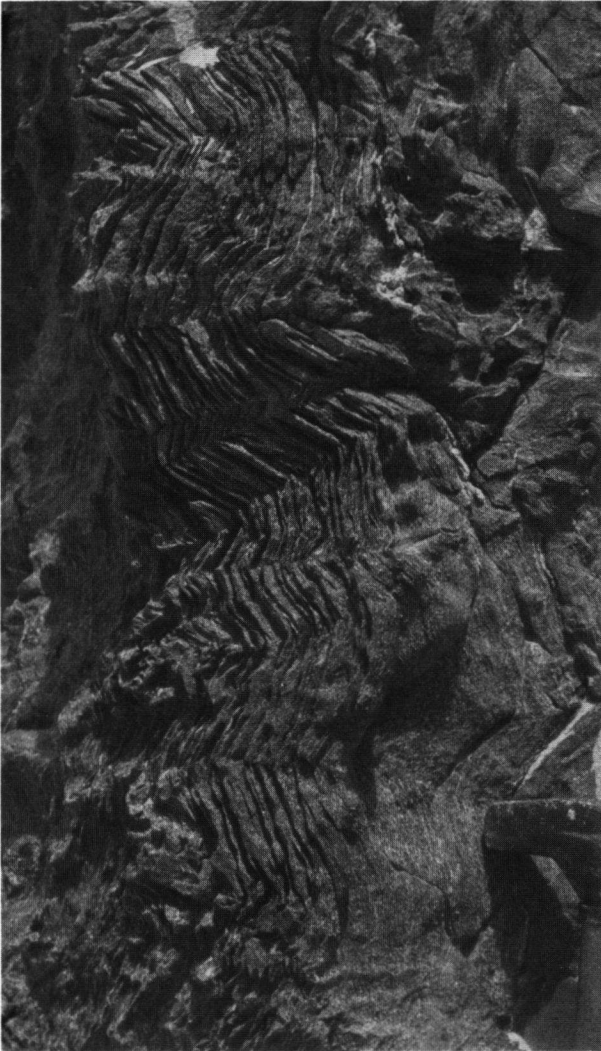


Fig. III-19. Chevron folding in the Purrido amphibolites along the coast near Freixo (Pantin).

principal axes of stress in such folds. This was done for a set of folds located near Pantin (Freixo). The results are shown in Fig. III-20. According to Ramsay (1962) chevron folds usually develop in thinly bedded or closely laminated rocks. They are formed at the end of an orogenic deformation when brittle rocks are subjected to stress. These folds are commonly associated with fault zones. The faults on the peninsula of Sanxiao which trace NW-SE, as well as the fault zone near Trasmonte to the north, can be attributed to the F_5 -deformation phase.

Structural map

The measured poles to the schistosity or foliation and linear directions are given on the structural map (enclosure I). The s_2 -poles are plotted, since s_1 is either not present in the high-grade metabasites and s_2 is parallel to s_1 as in the paragneisses. The Cabo Ortegal area has been divided into 15 subareas which are structurally more or

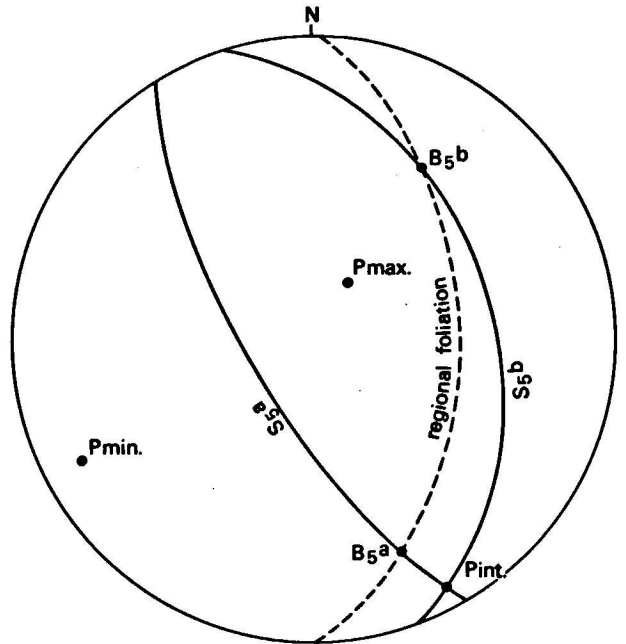


Fig. III-20. Stereographic plot of a set of conjugate folds found near Freixo (Pantin) and the constructed axes of stress.

less homogeneous. The s_2 -poles in each subarea have been plotted on a Schmidt's net and the densities contoured; directions of fold axes and lineations have been indicated in the same diagrams.

BEHAVIOUR OF THE METABASIC ROCKS UNDER STRESS

From the description of the folds it becomes evident that the metabasites in Cabo Ortegal behaved differently when subjected to stress. Deformation of the eclogite layers resulted in brittle fracture; the basic granulites show the formation of boudins and drag folds as well as concentric folding, while the amphibolites yielded flow folds mainly of the similar type.

Brittle rocks rupture without significant permanent strain. On the other hand a rock behaves in a ductile manner when deformation is without fracturing or faulting (cohesive flow). In rocks, flow is any deformation not instantly recoverable that occurs without permanent loss of cohesion (Handin and Hager, 1957). There are three principal flow mechanisms: 1. cataclasis, 2. intracrystalline gliding and 3. recrystallization (Griggs, 1940). Cataclasis and intracrystalline gliding are stress-induced; recrystallization is generally induced by an increase in temperature. The ductility of rocks is affected by factors such as pressure, temperature and strain rate, as well as composition, grain size and anisotropy (Handin and Hager, 1957, 1958; Griggs et al.; 1960, Heard, 1960; Donath and Parker, 1964; Donath and Fruth, 1971).

When there is a layering, the anisotropy commonly controls the geometry of flow (Donath, 1962). Flow

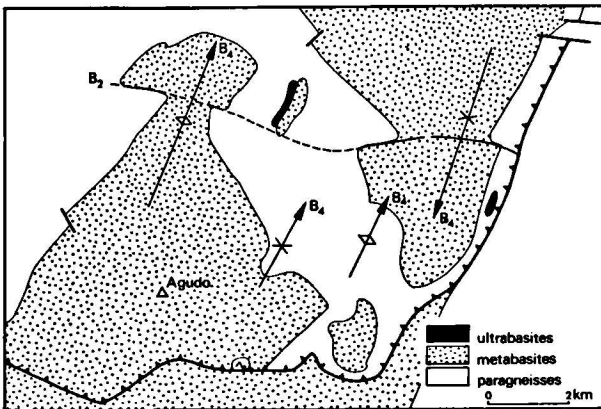


Fig. III-21. Large-scale 'mushroom' outcrop patterns formed in the metabasites and paragneisses in the centre of Cabo Ortegal (NE of Mount Agudo).

may be confined to individual layers or may be independent of the layering. As the ductility of the rock increases, the effect of layering decreases. Donath and Parker (1964) in their discussion of the mechanisms of folding state that: 'the mechanism of folding that will operate during deformation is therefore a function of (1) the nature of inherent anisotropy in the rocks and (2) the ductilities of the involved rocks'. In other words the mechanism of folding depends upon the mean ductility of the rock sequence and the contrast of ductilities within the sequence (Donath, 1963).

Returning now to the differences in deformational behaviour of the metabasites at Cabo Ortegal we must assume that differences in the water content of the rock played an important role because this affects the flow by recrystallization, while other factors such as temperature, pressure, strain rate and composition were nearly equal for all the rocks involved. The presence of water induces recrystallization and the water content has a pronounced influence on the position of the solidus in a P/T field. Rocks near their solidus are highly ductile. Of the metabasites amphibolite is the least 'dry' and under the metamorphic conditions prevailing in Cabo Ortegal, they must have been near their melting point. Apart from this the amphibolites are rather homogeneous. Thus the mean ductility as well as the ductility contrast was favourable for the formation of folds of the similar type (passive folds in the terminology of Donath and Parker, 1964). In the mafic granulites the presence of granatite layers might have caused a high ductility contrast. This combined with a moderate mean ductility of the rocks in question ('dry rocks') explains why mainly concentric folds were formed. The brittleness of the eclogite and the extreme ductility contrast between eclogite and banded gneiss caused the observed fracturing and 'folding' of the eclogite.

INTERFERENCE PATTERNS

Successive folding phases can result in the formation of characteristic interference patterns. Ramsay (1962,

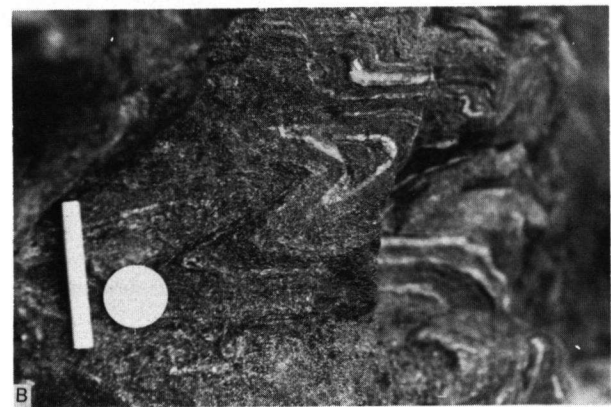


Fig. III-22. a. Type 2 interference pattern between F_2 and F_3 in the blastomylonites of the Carreiro zone resulted in an 'arrow-head'.

b. Crescent-shaped type 2 interference pattern between F_2 and F_4 in the banded gneisses along the northern coast of the Masanteo peninsula.

1967) demonstrated that only three fundamentally different patterns can exist. Which type is formed is determined by the angle between the first fold axis (B_1) and the axial plane of the second fold and the angle between the axial plane of the first fold and a_2 .* In addition to these relationships, the outcrop pattern (i.e. that part of the interference pattern that is actually seen) also depends upon the intensity of the second folding, the amount of flattening, the wave length and above all, the orientation of the outcrop surface.

From the above it is clear that the most easily recognized interference patterns develop when the axial planes of the two folds involved form large angles. This is the case in Cabo Ortegal where earlier phases (horizontal axial plane) were refolded by F_4 -folds (vertical axial plane). A look at the geological map reveals the presence of a type 2 (in Ramsay's classification) interference pattern in the Agudo antiform and to the east of it at the southern end of the Bacariza Formation (Fig. III-21). Type 2, on a small (cm) scale, is also found in

* Subscripts denote the sequence of the two folding phases involved; they do not refer to the folding phases in Cabo Ortegal.

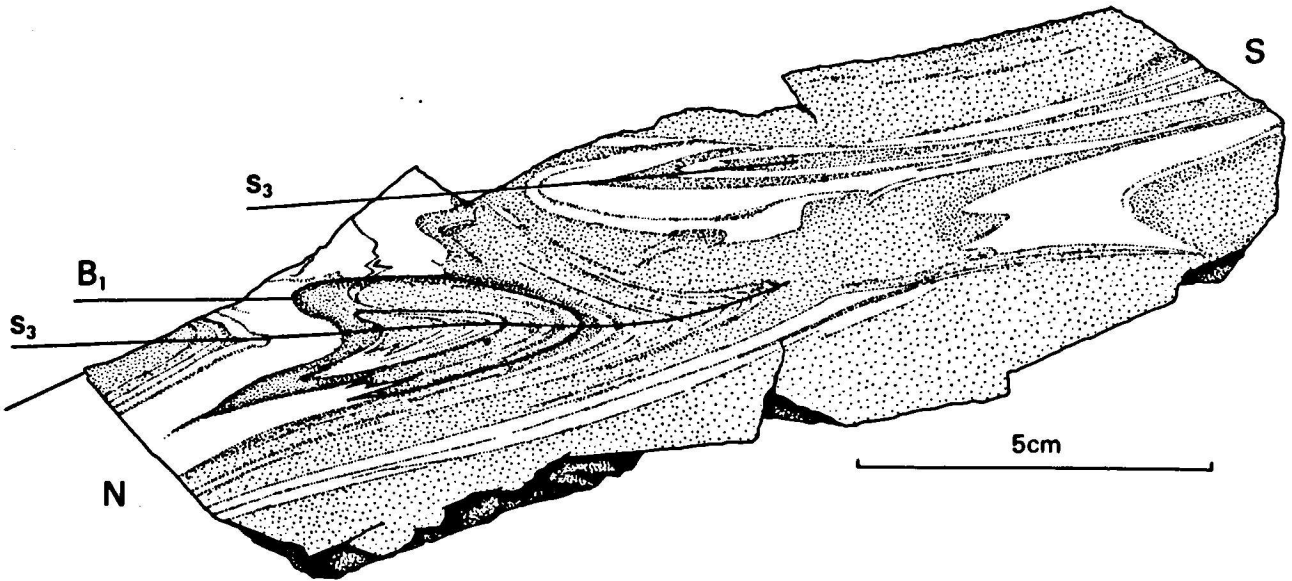


Fig. III-23. Refolding of F_1 by F_3 produced a type 2 interference pattern in a sample of Peña Escrita amphibolites.

the blastomylonites of the Carreiro zone of tectonic movement (Fig. III-22a) and in the gneisses along the northern coast of Masanteo (Fig. III-22b). These last two interference patterns are the result of the refolding of F_2 -folds by F_4 - and F_3 -folds, respectively. It proves that during F_2 the Carreiro zone was already an important tectonic movement horizon. An interference pattern is also seen in Fig. III-23, a sketch of a vertical, N-S trending cross-section in a hand-specimen of Peña

Escrita amphibolite (locality: near a small bridge over the rio do Porto, 1250 m SSW of the top of Mount Agudo). Besides small-scale horizontal F_3 -folds with N-S axial directions, a type 2 interference pattern is visible. Since the refolded B-axis lies almost in the plane of the section, this fold axis must have run almost N-S. Before F_3 , only B_1 -axes were N-S trending. Therefore it is concluded that the pattern has been produced by interference of F_1 and F_3 ; this means that the amphibolite already possessed an s-plane before F_2 .

The axial planes of F_3 and F_4 also form large angles but their axial directions intersect at low angles. The interference patterns are therefore of type 3. A good example of this type of interference is found in the outcrop S of Trasmonte (Fig. III-24) in the Candelaria amphibolites. A loose block of retrograde granulites found near Cedeira forms another example of this type of refolding (Fig. III-25). Refolding of F_3 -folds by F_4 is already demonstrated in Fig. III-8. Here the influence

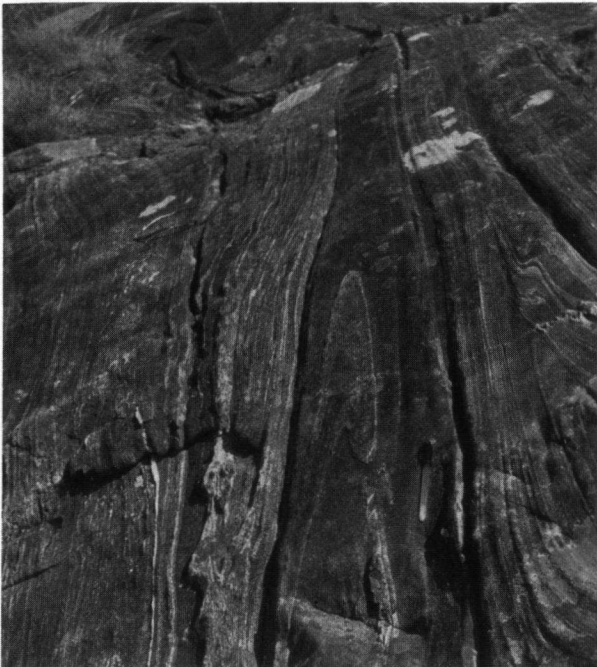


Fig. III-24. Outcrop pattern found in the amphibolites just S of Trasmonte resulting from the interference of F_3 and F_4 .

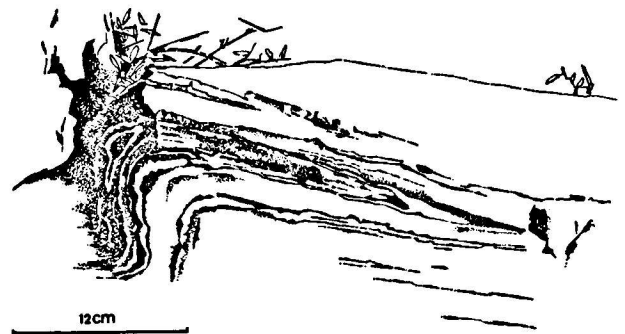


Fig. III-25. Interference pattern produced by an F_4 -fold refolding an F_3 -fold formed in a loose block of basic granulites, found near Cedeira. B_3 and B_4 have almost parallel axial directions. The sketch is a plane perpendicular to B_4 .

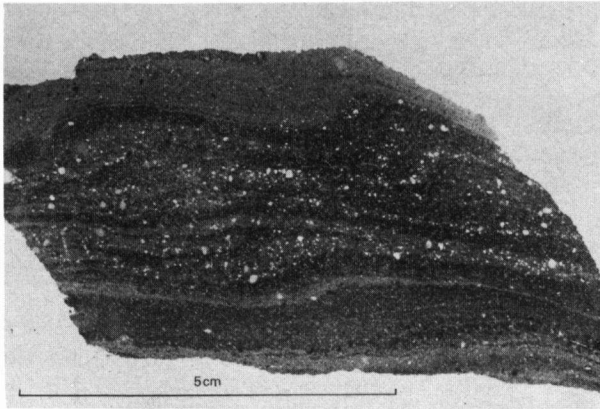


Fig. III-26. Photograph of a thin section of basic granulite showing the refolding of an F_3 -fold by F_4 -folds.

of the wave lengths of both folds on the interference pattern is evident. A thin section of a garnet-bearing hornblende gneiss from the Agudo Formation also shows the refolding of F_3 -folds by the F_4 -folding phase (Fig. III-26). Other instructive examples of refolding in the amphibolites of the Candelaria Amphibolite Formation

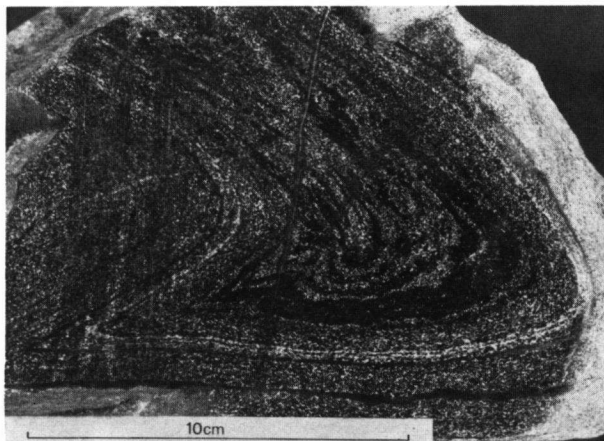


Fig. III-27. Profile plane of an F_4 -fold, refolding a pre-existing F_2 (?) -fold.



Fig. III-28. Refolding of an F_3 -fold by F_4 , seen in a block of Purrido amphibolite along the coast near Pantin.

are found in loose blocks, one on the Sanxiao peninsula and another along the coast near Porto do Carrizo (Figs. III-27 and III-28). Refolding of an F_4 -fold by chevron folding (F_5) can be found near Pantin (Fig. III-29) in the Purrido amphibolites.

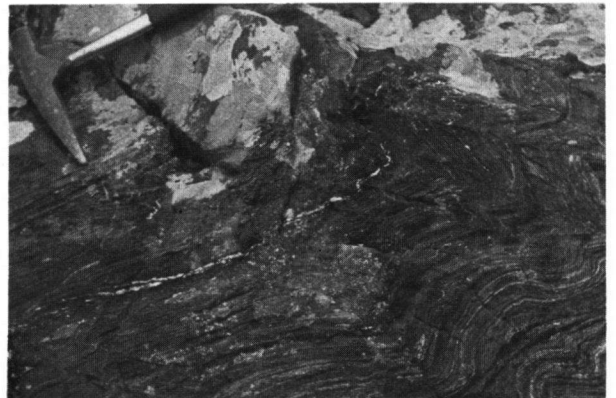


Fig. III-29. Chevron folds refolding an F_4 -fold in the Purrido amphibolites near Freixo (Pantin).

CHAPTER IV

PETROFABRICS

INTRODUCTION

Microscopical fabric analyses were carried out for clinopyroxene and amphibole from several metabasic rocks. The aim was to establish whether the preferred orientation patterns of these minerals can be correlated with the megascopic structures of the distinct deformation phases.

Procedure

All measurements of mineral orientation were carried out on a five-axis universal stage (Leitz UT5). The five-axis universal stage gives the orientation of the axes of the optical indicatrix, α , β and γ , in one setting. In the case of monoclinic minerals, such as clin amphiboles and clinopyroxenes, it is also important to establish certain crystallographic directions as well. If the orienta-

tions of the optical indicatrix and one $\{110\}$ -cleavage plane have been established, then the other crystallographic directions can be constructed (cf. van Zuuren, 1969, p. 45). Möckel (1969) has written a computer programme* requiring the readings of the universal stage setting and the orientation of one $\{110\}$ -cleavage plane as input-data; output is in the form of (rotated and) counted equal-area projection diagrams for α , β , γ , $[001]$, $\pi \{100\}$ and $\pi \{110\}$.

Unfortunately it is sometimes difficult to precisely locate the $\{110\}$ -cleavage plane required either because it lies beyond the maximum angle of tilt on the universal stage or because it is weakly developed (especially in clinopyroxene). In such a case another computer programme* is run beforehand, in which the setting of the optical indicatrix plus the angle between $[001]$ and γ are used to compute two sets of possible locations of the $\{110\}$ - and $\{100\}$ -planes; the $[001]$ -axis may be situated on either side of γ . When the grain in question is re-examined it is in most cases easy to decide which of the $\{110\}$ -cleavages is the one required.

The diagrams. — The diagrams have been drawn on the basis of the printed output of the IBM 360/50 computer of the 'Centraal Rekeninstituut' (Central Computer Institute) of the Leiden University. If s-planes were visible in the hand-specimen, their orientation is represented in the diagrams as solid lines. If relevant, the positions of the great-circle girdles normal to μ_1 or μ_3 are drawn using dashed lines. μ_1 , μ_2 and μ_3 are the eigenvectors of the matrix M (cf. Möckel, 1969, p. 101). When the distribution is a single point-maximum, μ_3 gives the estimated centre of this maximum; in the case of a great-circle distribution, μ_1 coincides with the estimated axis of this circle. The orientations of μ_1 and μ_3 are computed with FABRIC 6.*

Sampling

The sample of grains representing the mineral populations used in the preparation of the fabric diagrams was drawn according to a method described by Möckel (1969). On a photograph of a thin section, strips perpendicular to an s-plane (if present) are drawn and all grains lying in each strip are numbered and measured. It is understood that better but more time-consuming methods for drawing a sample exist (Möckel, 1969; van Zuuren, 1969).

How many grains are to be measured in order to obtain a representative sample is a question which is difficult to answer beforehand. It depends on the type of distribution, which can vary for the distinct types of

preferred orientation of a mineral (e.g. point-maximum for $[010]$ and a great-circle girdle for $\pi \{100\}$), and on the parameters of the distribution. Both type and parameters are unknown before the sample is measured. Stauffer (1966) suggested a method for obtaining the maximum sample size for a truly representative fabric. However, in practice the sample size (N) is determined mainly by the ratio time/information obtained. A factor that also may limit the sample size is the quantity of grains of a certain mineral present in the thin section. For the pronounced orientation patterns found in this study, a sample size between 100 and 200 grains is sufficient. In order to 'filter' the observed directions to some extent a 2% counting area ($A = 0.02$) is generally used for the construction of the diagrams.

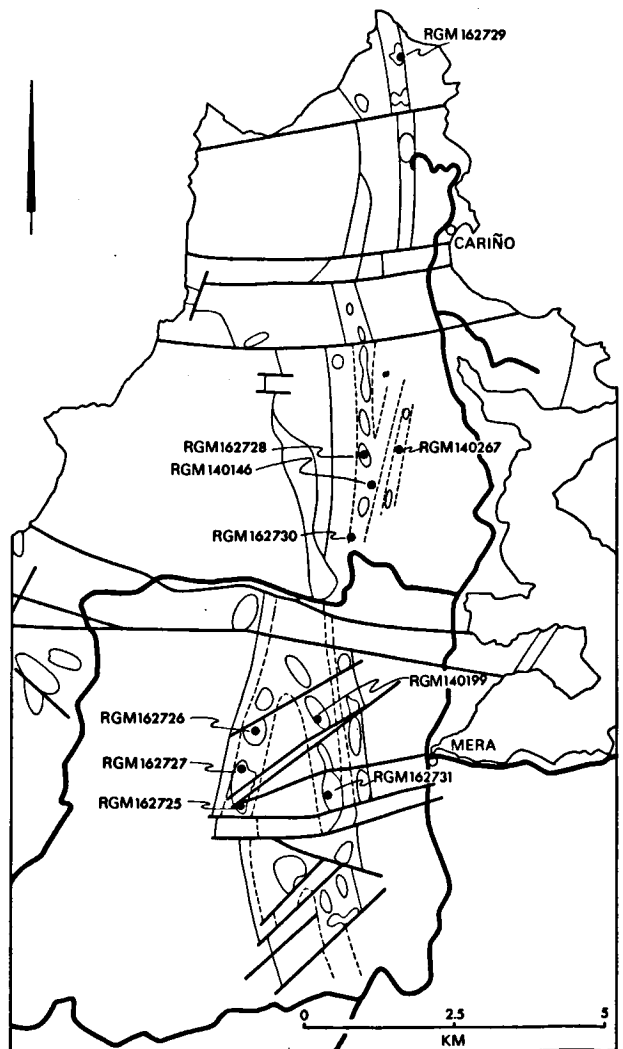


Fig. IV-1. Location of the eclogite samples mentioned in the text. The map covers the northeastern part of the Cabo Ortegal Complex.

*) FABRIC 2, FABRIC 3 and FABRIC 6 are computer programmes from a series of FORTRAN IV programmes written by J.R. Möckel for petrofabric data. These programmes are partly described in Möckel's thesis (1969, p. 91-102) and more completely in his roned laboratory manual 'Description and use of some FORTRAN IV computer programs for petrofabric analysis' (1970).

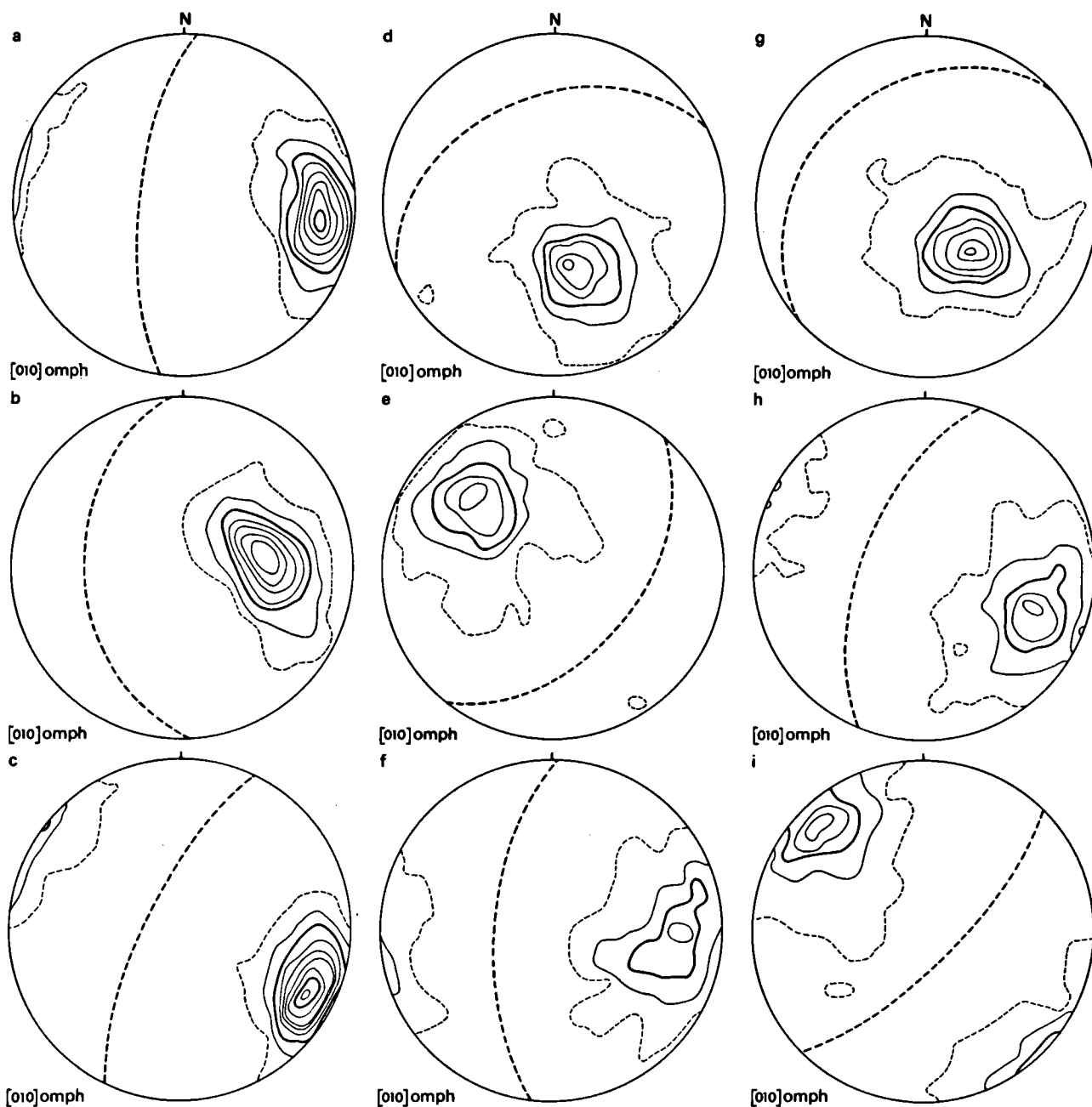


Fig. IV-2. Diagrams for [010] of omphacite in eclogites. Contours for densities 1, 3, 5, 7, 9, 11, 13, 15 and 17. ($N = 200$; $A = 0.02$). Great-circle girdles are drawn as dashed lines; their axes pass through the estimated centres of the point-maxima. a = sample RGM 162726; b = RGM 162727; c = RGM 162725; d = RGM 162728; e = RGM 162730; f = RGM-st. 140199; g = RGM 162729; h = RGM-st. 140267; i = RGM-st. 140146.

CLINOPYROXENE IN ECLOGITE

Fabric studies of eclogite-omphacites are made for two reasons: (1) to obtain general insight into the orientations of clinopyroxene in eclogites and (2) to see whether the orientation patterns observed provide added information on the nature of the apparently folded eclogite bodies forming the ridges. The locations of the

specimens used in the petrofabric study are shown in Fig. IV-1 and the orientations observed for [010], [001] and $\pi \{100\}$ are illustrated in Figures IV-2, IV-3 and IV-4. All diagrams on one page are for similar crystallographic directions to facilitate comparison.

The most characteristic feature of the omphacite fabrics is an unexpectedly strong preferred orientation of [010], around a point-maximum which is generally

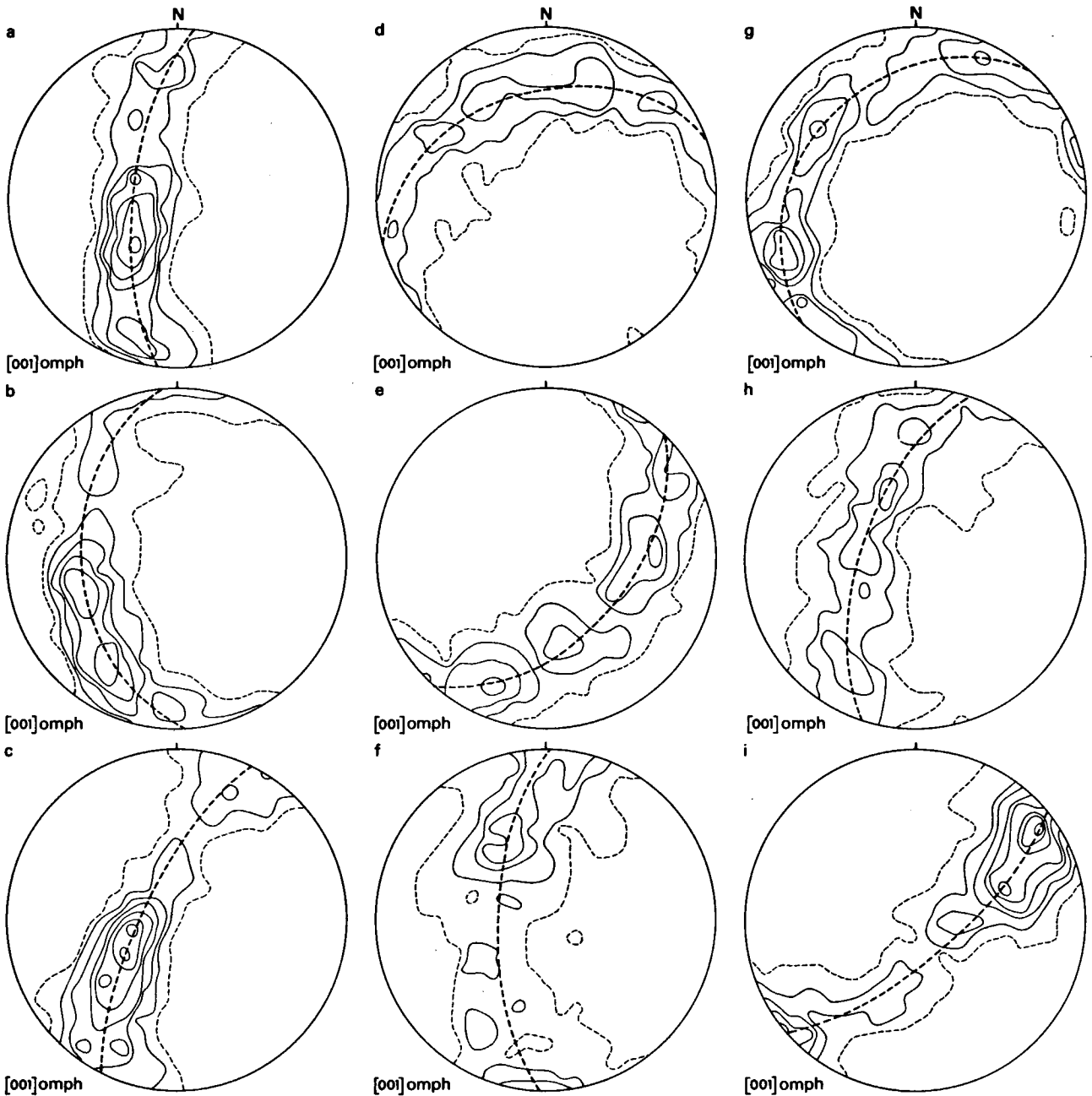


Fig. IV-3. Diagrams for [001] of omphacite in eclogite in the same samples as in Fig. IV-2. Contours for densities 1, 2, 3, 4, 5, 6, 7, and 8. ($N = 200$; $A = 0,02$). Great-circle girdles, drawn as dashed lines, coincide with those in Fig. IV-2.

elliptical in shape (Eigen values: 0.715–0.872). These maxima of [010] coincide with the pole to the foliation in each of the eclogite samples. This foliation is the result of a dimensional orientation of omphacite as well as zoisite and kyanite.

Assuming that the foliation of eclogite was originally horizontal and that it was rotated to its present position during folding, it should be possible to reconstruct the orientation of the fold axis involved. This is done by

drawing the great-circle which fits the [010]-maxima the best. The normal to this great-circle plunges 6° at 025° , which coincides with the general direction of the F_4 -folds.

Figures IV-3 and IV-4 also show that the great-circle girdles of [001] and $\pi \{100\}$ coincide. The girdles for [001] are narrower than those for $\pi \{100\}$ and perhaps for this reason, the sub-maxima within them are higher in value. This variation in the width of the girdles is at

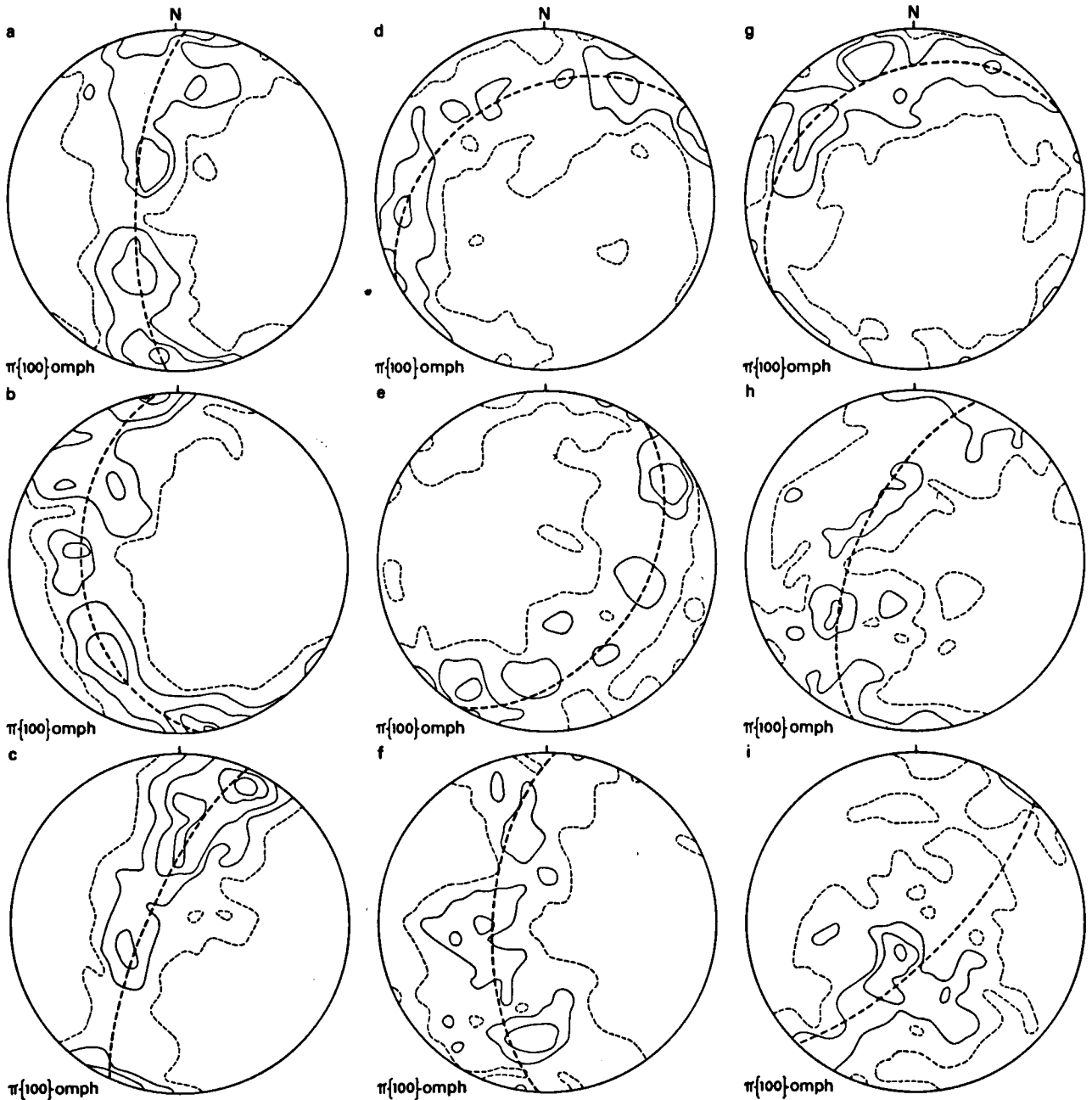


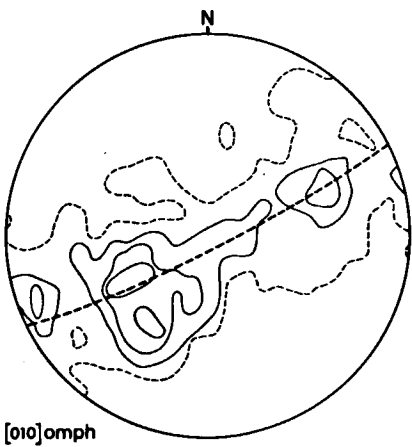
Fig. IV-4. Diagrams for $\pi \{100\}$ of omphacite in eclogite in the same samples as in Fig. IV-2. Contours for density 1, 2, 3, 4 and 5. ($N = 200$; $A = 0.02$). Great-circle girdles, drawn as dashed lines, coincide with those in Fig. IV-2.

least partly explained by the elongated shape of the [010]-maximum; the [001]-sub-maxima are normal to the spreading in the direction of the longest axis.

If the positions of the statistical maxima for [001] (calculated with the aid of FABRIC 6) are plotted, then one finds that these maxima plunge either to the northeast or to the southwest. A rather attractive explanation is to assume that one set belongs to steepened W-limbs and the other set to the overturned E-limbs of the almost isoclinal folds. The directions of the maxima for

[001] can be compared with an I_1 -lineation formed during the M_1 -metamorphism. If the foliation is rotated around the constructed fold axis back to its original horizontal position, the [001]-maxima cluster around a point situated 20° W of north.

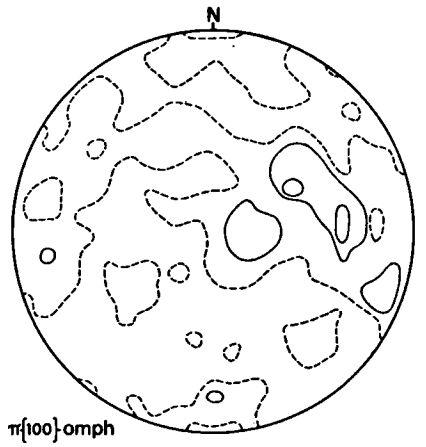
A contrast to the general orientation pattern observed for most of the omphacites is the omphacite fabric of sample RGM 162731 (Fig. IV-5). Under the microscope no difference in texture between the other eclogites and this sample can be observed. A point-maximum is now



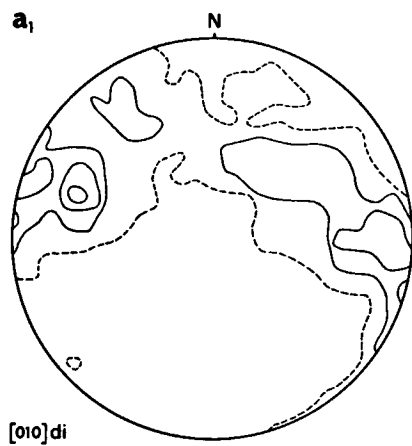
[010]omph



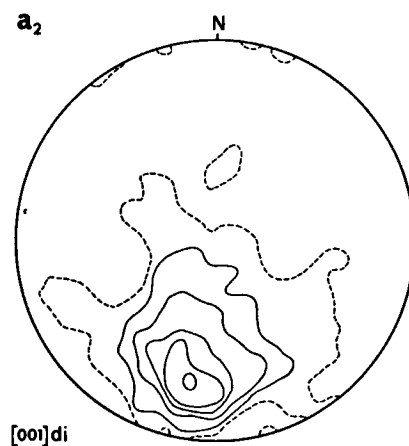
[001]omph



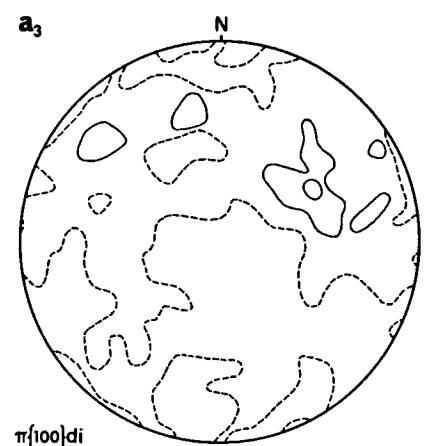
$\pi\{100\}$ omph



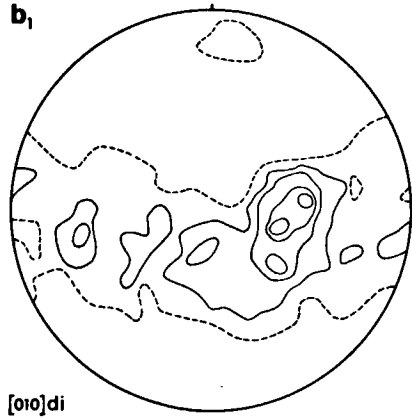
[010]di



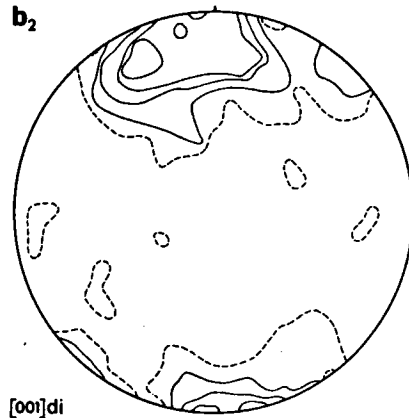
[001]di



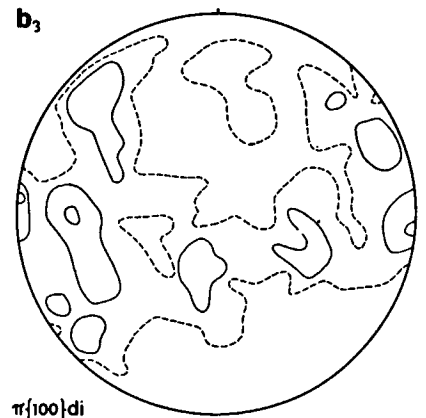
$\pi\{100\}$ di



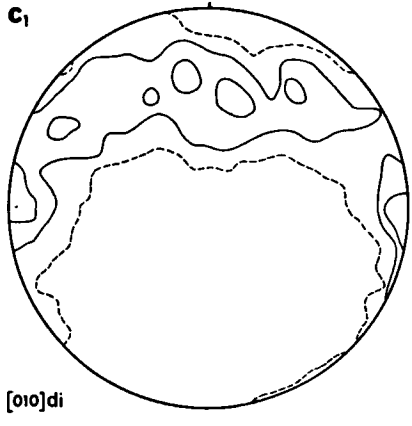
[010]di



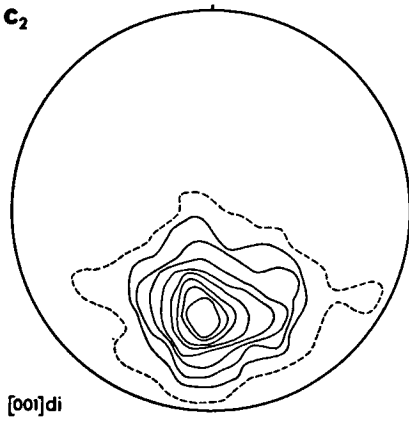
[001]di



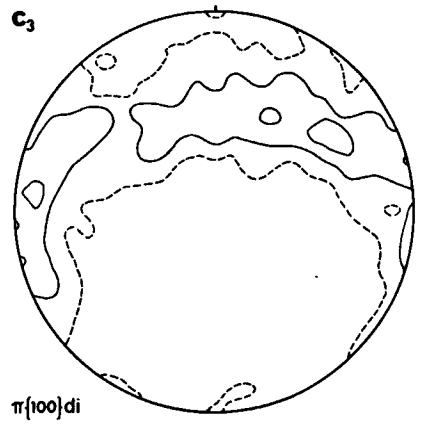
$\pi\{100\}$ di



[010]di



[001]di



$\pi\{100\}$ di

Fig. IV-5. Diagrams for the orientation of [010], [001] and π {100} of omphacite in eclogite sample RGM 162731. Contours for densities 1, 2, 3, 4, 5 and 6 ($N = 200$; $A = 0.02$). The axis of the great-circle passes through the estimated centre of the point maximum for [001].

formed by the [001]-axes and both [010] and π {100} are orientated in great-circle girdles. This orientation pattern shows close affinity to the orientation patterns of diopside in the basic granulites of Cabo Ortegal. Perhaps it is only accidental that the position of the [001]-maximum coincides with the original direction postulated for the sub-maxima of [001] in the previous samples (20° W of N). However, it should be noted that the F_1 -folds in the paragneisses also suggested roughly N-S trending axial directions.

CLINOPYROXENE IN BASIC GRANULITE

As previously stated, macroscopically the non-retrograded basic granulites (formed during M_1 synchronous with the eclogites, but on a somewhat higher structural level) are rocks which seem to lack any preferred orientation, i.e. granofelses (Goldsmith, 1959; Behr et al., 1971). Petrofabric analyses for diopside were carried out to establish whether such an apparent lack of preferred orientation also exists on a microscopic scale and also to provide a comparison with the fabrics of omphacite.

From inspection of the diopside fabrics in the three basic granulites shown in Fig. IV-6, it is evident that significant preferred orientation is undoubtedly present since all the samples demonstrate the same orientation pattern. The fabrics represent samples taken from the Bacariza Formation, an area which for the most part was not steepened by later folding. The diagrams prove that the distinct preferred orientation of the diopsides differs markedly from that of the omphacites. In the basic granulites the [001]-directions cluster around a point-maximum and crystallographic directions normal to [001] are oriented along great-circle girdles. The point-maxima for [001] have a NS azimuth and plunge gently. Again it seems warranted to assume that these point-maxima lie in the direction of B_1 .

Fabrics of F_2 -folds

In order to ascertain whether or not this fabric was formed by syntectonic recrystallization during M_1 , i.e. before the impact of the second deformation phase when cataclastic flow was active and E-W fold axes were formed, the diopside fabric of an F_2 -fold was studied. The orientations of the diopside grains in both limbs of an F_2 -fold were measured (samples RGM 162735, Fig. IV-7). In contrast to the M_1 fabric, the patterns of preferred orientation in the F_2 -fold are very weak. A weak and irregular point-maximum for [001], accompanied by π {100} oriented along a girdle, can

be discerned in Fig. IV-7a; however in Fig. IV-7b the reverse can be observed: a point-maximum for π {100} and the c -axes in a girdle around it. No connection can be established between the macroscopic fold and the fabric.

Fabrics of F_3 -folds

Two analyses of the orientation of clinopyroxene in the fold hinges of F_3 -folds were also carried out (Figs. IV-8 and IV-9). One is from the hinge zone of an F_3 -fold (sample RGM 162736) with a well-developed horizontal schistosity. The schistosity is especially pronounced in the leucocratic layers (here a quartz fabric with the strong preferred orientation so characteristic of felsic granulites is present). In the mafic parts new biotite flakes are oriented parallel to the schistosity. The diopside grains are relics of the M_1 -phase surrounded by partly recrystallized stable hornblende. The other sample (Fig. IV-9) is from a fold with a vertical axial plane although it is likely that the fold is a steepened F_3 -fold. Here the cataclastic effect on the diopside grains is less obvious (sample RGM 162737). Both samples show point-maxima for [001]. In sample RGM 162736 the maximum is elongated parallel to the schistosity.

From the diagrams for [010] and π {110} a preference for the orientation of an 110 -plane parallel to the axial plane can be deduced. The {100}-planes are without sub-maxima and are regularly dispersed in a great-circle girdle normal to the schistosity. Sample RGM 162737 shows a similar orientation except that the sub-maximum for [010] is more pronounced.

DESCRIPTION OF OTHER CLINOPYROXENE FABRICS RECORDED IN LITERATURE

Clinopyroxene fabrics are remarkably scarce in literature; they are generally given as a supplement to the study of the preferred orientations of olivine in ultramafic rocks.

Brothers (1964) analysed the orientation of 40 grains of clinopyroxene from the Skaergaard intrusion; he believed that the strong point-maximum observed for [001] (parallel to the current direction) could be attributed to the action of convection currents during settling (deposition fabric).

Clinopyroxene fabrics from the ultramafic and associated eclogite rocks in the Higashiakaishiyama district (Japan) have been described by Yoshino (1961 and 1964) and by Banno and Yoshino (1965), but unfortunately only the optical directions for α , β and γ are

Fig. IV-6. Diagrams for [010], [001] and π {100} of diopside in basic granulite. Contours for densities 1, 2, 3, 4, 5, 6, 7, 8 and 9 ($N = 200$; $A = 0.02$). a = RGM 162733; b = RGM 162734; c = RGM 162732.

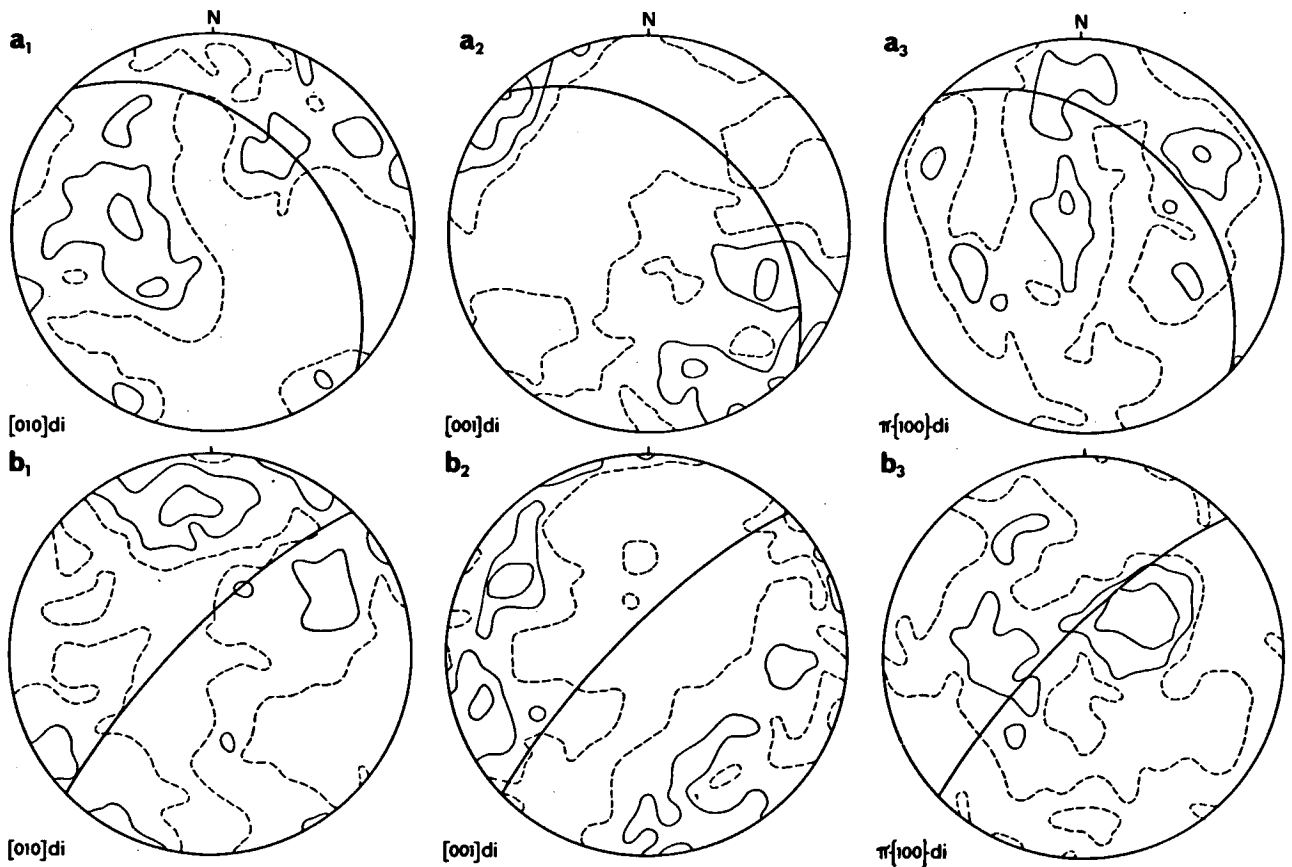


Fig. IV-7. Diagrams for $[010]$, $[001]$ and $\pi\{100\}$ of diopside in both limbs of an F_2 -fold. Contours for densities 1, 2, and 3 ($N = 200$; $A = 0.04$). Great-circles indicate the orientation of the layering. Sample RGM 162735.

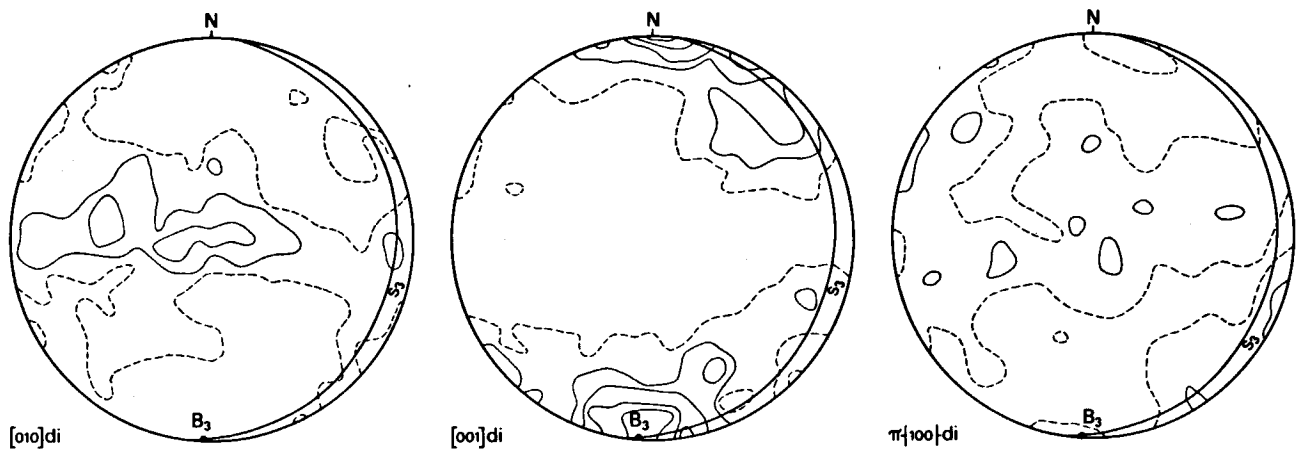


Fig. IV-8. Diagrams for $[010]$, $[001]$ and $\pi\{100\}$ of diopside in an F_3 -fold. Contours for densities 1, 2, 3, 4, and 5 ($N = 200$; $A = 0.02$). Sample RGM 162736.

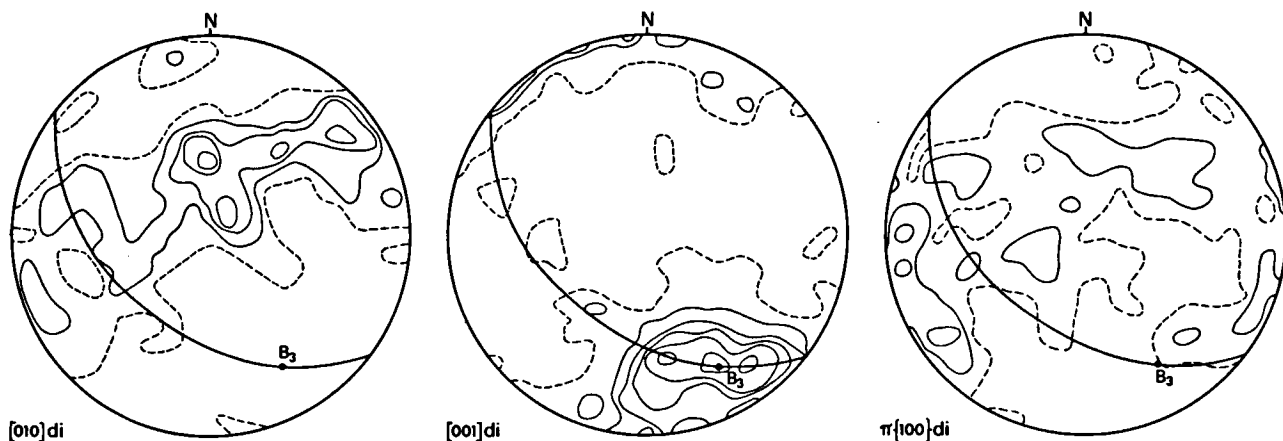


Fig. IV-9. Diagrams for $[010]$, $[001]$ and $\pi\{100\}$ of diopside in an F_3 -fold. Contours for densities 1, 2, 3, 4, 5, and 6 ($N = 100$; $A = 0.02$). Sample RGM 162737.

given. Their results indicate that in general $[010]$ is oriented normal to the plane of the eclogite streaks and they conclude that $[001]$ is concentrated parallel to a definite axis in this plane. However, in some cases $[010]$ is oriented along a great-circle girdle and γ is concentrated around a point-maximum of $[001]$ (cleft girdle). This seems to be the case when the surrounding dunite is mylonitized.

Clinopyroxene fabrics in peridotites have also been described by Avé Lallemant (1967) and Möckel (1969). Möckel recorded a strong point-maximum for $[001]$ in a schistose garnet-peridotite, whereas the preferred orientations found by Avé Lallemant for clinopyroxene are generally weak, except for the diopside fabric of a garnet-peridotite where α , β and γ show distinct point-maxima.

Kappel (1967) analysed the preferred orientation of omphacite from eclogite lenses in garnet-serpentinite from the granulite massif of the lower Austrian Moldanubicum: there the β -axes form a great-circle girdle while γ is oriented normal to this girdle. Kappel suggested that the centre of this γ -maximum is the direction of the $[001]$ -axes.

Kumazawa et al. (1971), in a paper dealing with the elastic properties of eclogite xenoliths, present orientation diagrams for $[001]$, β and γ . Their hand-specimens with a pronounced lineation (l-type) generally show a strong point-maximum for $[001]$, whereas foliated samples (s-type) have a point-maximum for the $[010]$ -axes.

Van Zuuren (1969) has recorded $[001]$ axes lying in a great-circle with two sub-maxima; the sample came from granulites on the periphery of the Ordenes 'basin' near Santiago (NW Spain). One of the point-maxima recorded by van Zuuren has the same orientation as the fold axis; the other is normal to the fold axis and lies in the foliation plane. Van Zuuren also measured the $[001]$ orientation for porphyroclastic pyroxene in mylonitic pyroxene-amphibolites; a strong point-maximum appears parallel to the lineation.

Inoue (1961) records the orientation of 150 $[010]$ -

axes of diopside grains in a pyroxene-bearing amphibolite from the Saburi Mountainland (Japan). Here a point-maximum for $[010]$ -axes is oriented parallel to the tectonic a-direction.

Kojima and Hide (1957) report the orientation pattern of aegirine-augite in the quartz-schists of the Sambagawa crystalline schists (Besshi-Shirataki district, Japan). The usual orientation is strong maxima for α , β and γ ; the α - and γ -maxima are contained within the bedding-schistosity plane (ab).

Kozłowski (1965) gives the orientation of α , β , γ and $[001]$ for dark granulite and an eclogite sample from the Granulite Complex of Stary Gieraltów (East Sudetes, Poland). In the eclogite sample, $[010]$ -axes form a strong point-maximum, whereas α and γ are oriented in great-circles normal to the $[010]$ -maximum; in the granulite sample $[001]$ -axes show the strongest preferred orientation, $[010]$ -axes tend to lie in a great-circle and the orientation for α and γ (in a cleft girdle?) is weak.

From this survey of the literature two patterns of preferred orientation clearly emerge: (1) a point-maximum for $[010]$ which is generally normal to the plane of the foliation; (2) a point-maximum for $[001]$ which lies in the foliation plane. In Cabo Ortegal the first is represented by the omphacites in eclogites (eclogite fabric), the latter occur in the basic granulites (granulite fabric).

AMPHIBOLE FABRICS

Amphiboles were measured in order to obtain an insight into the relationship between later deformations and the growth of new metamorphic minerals (mainly during M_2) as well as the relationship between the old and new metamorphic fabrics. A clear example of the latter is a secondary hornblende found in eclogite sample RGM 162727. The pattern of preferred orientation confirms the conclusion, drawn from textural relationships visible in thin sections, that the hornblende grew homoaxially at the expense of omphacite (Fig. IV-10). The point-



Fig. IV-10. Homoaxial growth of hornblende (hbl) at the expense of eclogitic omphacite (cpx). gt = garnet; zo = zoisite; r = rutile. Thin section RGM 162726.

maximum for [001] of hornblende (Fig. IV-11) coincides with the point-maximum for [001] of omphacite which it replaces (Fig. IV-3b). Therefore it appears that the hornblende orientation in eclogites is determined by the orientation of the pre-existing omphacite.

Hornblende in an F_2 -fold

Coarse-grained hornblende porphyroblasts in the fold hinge of an E-W trending F_2 -fold near San Andres (Fig. III-3) were measured to study the orientation of hornblende in an F_2 -structure; hornblende is believed to have grown during M_2 , that is after the F_2 -deformation phase, and synchronous with F_3 . From the diagrams (Fig. IV-12) it is clear that {100} is concentrated into two maxima. It is assumed that these maxima indicate

the positions of the poles to s_2 and s_3 . This may be confirmed by the orientation of the [001]-axes which also form submaxima within a girdle, one parallel to B_2 and one parallel to the regional direction of B_3 . Probably the submaximum for B_2 is due to mimetic growth of hornblende on pre-existing diopside with a preferred orientation and the submaximum for B_3 , to oriented growth in the F_3 -stress field. Macroscopically no indication of F_3 -folding is seen.

Hornblende in F_3 -folds

Hornblende (sample RGM 162736) from an F_3 -fold hinge was taken from a basic granulite for which the clinopyroxene fabric was already known (Fig. IV-8). Again the preferred orientations of [001] for pyroxene and amphibole coincide. A comparison of the crystallographic planes of clinopyroxene and hornblende (Fig. IV-9 and IV-13) reveals that the preferred orientation of {100}-hornblende (elongated maximum) is almost the same as that for [010]-diopside.

The orientation of hornblende within a garnet-pyroxene-hornblende-granulite has been measured. Sample RGM 162740 was taken from an F_3 -fold hinge which crops out in the Sierra de Moles between ridges of eclogite (an antiform structure which has been discussed earlier). The diagram (Fig. IV-14) shows a strong maximum for [001]-amphibole which coincides with the direction of the fold axes. An F_3 -origin is attributed to the fold since the brown-green colour of the hornblende is characteristic for M_2 .

Hornblende in F_4 -folds

Hornblende was measured in sample RGM 162739 which is a retrograded basic granulite of the Candelaria Granulite Formation and comes from the hinge of an F_4 -fold (Fig. III-15). The fabric diagram for the [001]-axes of hornblende shows a point-maximum that coincides with the direction of the fold axis (Fig. IV-15). However, it appears from diagram IV-15 that the {110}-planes of hornblende are oriented in the newly

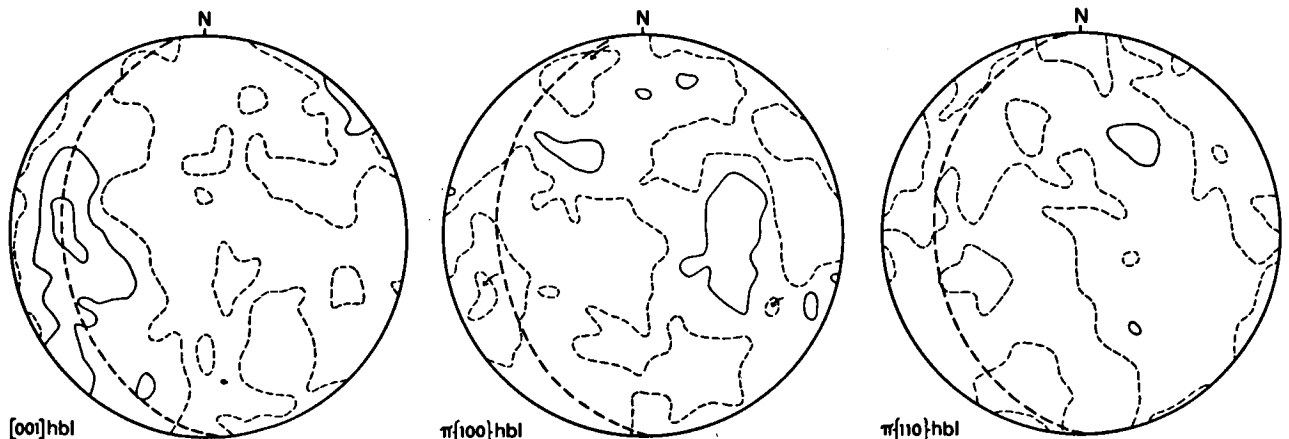


Fig. IV-11. Diagrams for [001], π {100} and π {110} of hornblende in eclogite sample RGM 162727. Contours for densities 1, 2, and 3 ($N = 100$; $A = 0.02$). Dashed line is the computed great-circle; its axis is the eigenvector μ_1 for the distribution of [001].

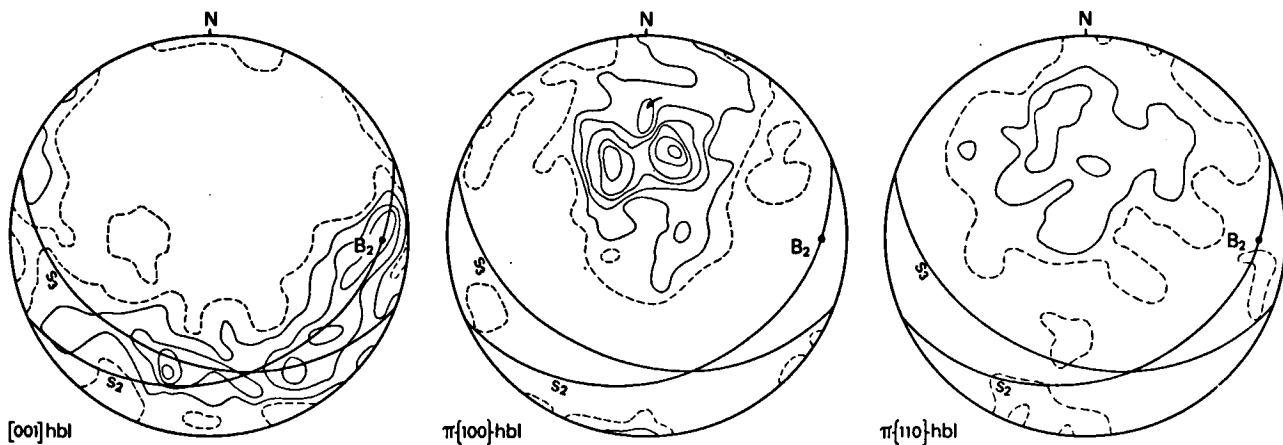


Fig. IV-12. Diagrams for $[001]$, $\pi\{100\}$ and $\pi\{110\}$ of hornblende in an F_2 -hinge. Sample RGM 162738. Contours for densities 1, 2, 3, 4 and 5 ($N = 100$; $A = 0.02$). Solid lines are drawn with the maxima for $\pi\{100\}$ as centre.

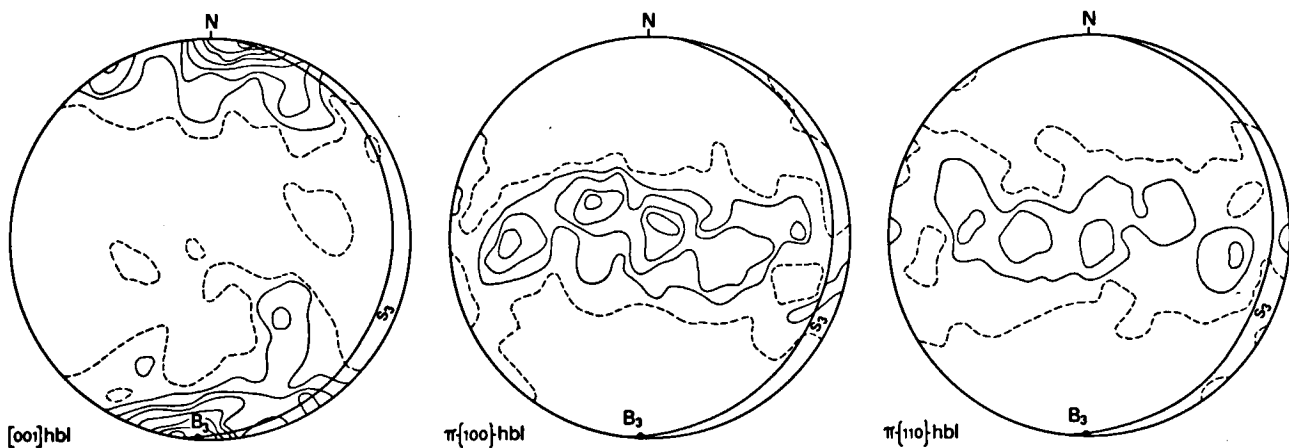


Fig. IV-13. Diagrams for $[001]$, $\pi\{100\}$ and $\pi\{110\}$ of hornblende in an F_3 -hinge. Contours for densities 1, 2, 3, 4, 5, 6 and 7 ($N = 100$; $A = 0.02$). Sample RGM 162736.

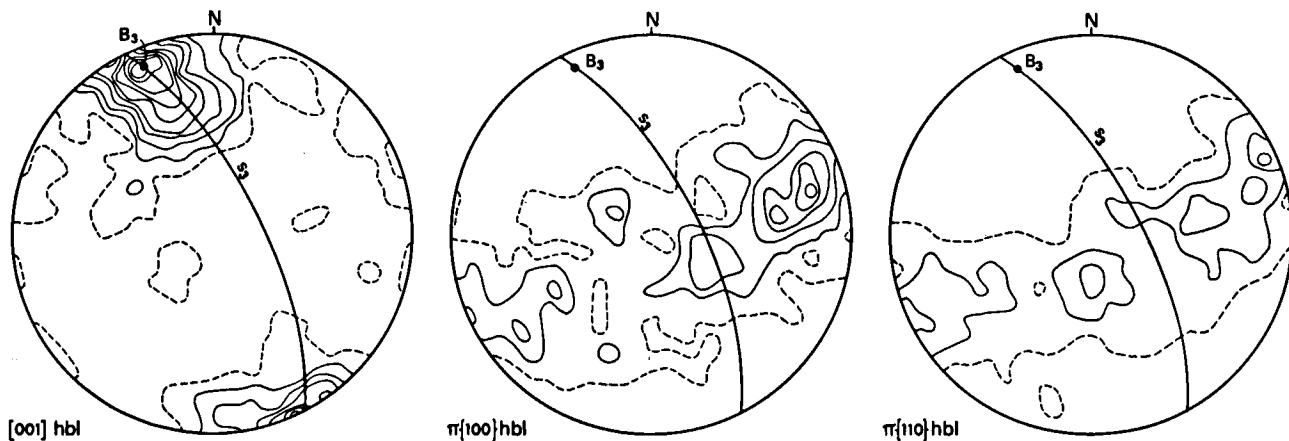


Fig. IV-14. Diagrams for $[001]$, $\pi\{100\}$ and $\pi\{110\}$ of hornblende in an F_3 -hinge. Contours for densities 1, 2, 3, 4, 5, 6, 7, 8 and 9 ($N = 100$; $A = 0.02$). Sample RGM 162740.

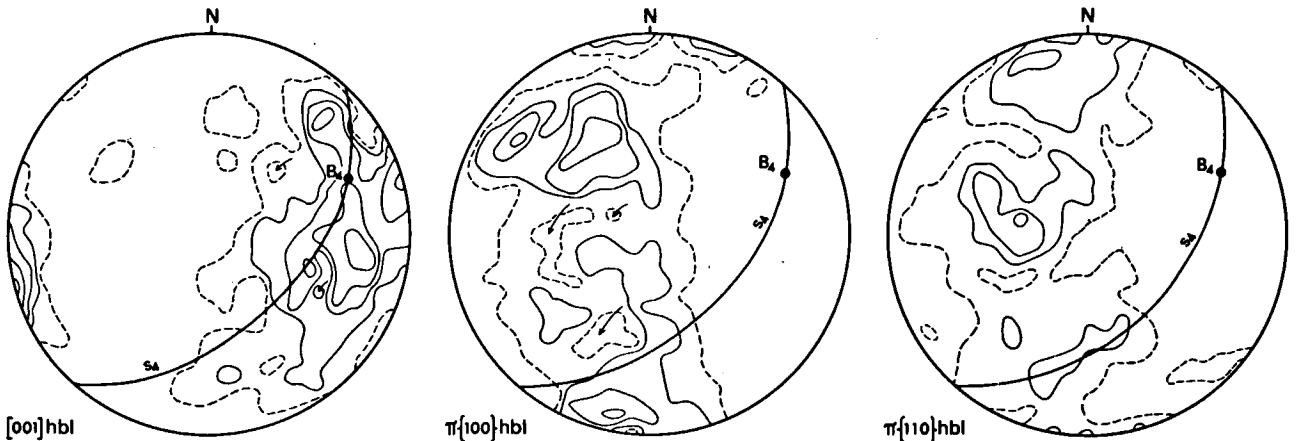


Fig. IV-15. Diagrams for $[001]$, $\pi \{100\}$ and $\pi \{110\}$ of hornblende in an F_4 -hinge. Sample RGM 162739. Contours for densities 1, 2, 3, 4 and 5 ($N = 100$; $A = 0.02$).

developed s_3 -schistosity plane and the poles to the $\{100\}$ -plane lie in a broad great-circle girdle.

The hornblende fabric in the amphibolites of the Candelaria Amphibolite Formation is typified by sample RGM 162741. This is a loose block found near the top of the Penedos Mountain; it contains several folds which are not mutually parallel. The orientations of the hornblende in these different folds, which are believed to represent F_2 -, F_3 - and F_4 -folds, are illustrated in Fig. IV-16. In all cases the orientation of the $[001]$ -axes is

parallel to the F_4 -fold axis (Fig. IV-17). It is also clear from the diagrams that throughout the block the $\{100\}$ -planes are oriented parallel to the s_4 -foliation. The preferred orientation for coarse-grained hornblende also gives a similar result (compare diagram IV-17c and IV-17d). This is especially evident in the case of the orientations of the $[001]$ -axes. This therefore means that during the F_4 -deformation phase a complete reorientation of the pre-existing hornblende fabrics (at least in the Candelaria Formation) probably took place.

In his description of other hornblende fabrics from literature van Zuuren (1969) points out that the pronounced preferred orientation of the $[001]$ -axes parallel to the fold axis or lineation is a commonly recognized phenomenon. In addition, submaxima are often found perpendicular to the fold axis and within the axial plane.

THE ORIGIN OF PREFERRED ORIENTATIONS

The origin of preferred orientation in rocks has been the subject of continuous study during the last decades. In an attempt to reproduce the preferred orientations observed in natural rocks, deformation experiments have been carried out using both silicates and metals. Several theories have been proposed to explain the preferred orientation produced by deformation; these theories are based on two different processes, namely intracrystalline slip and recrystallization.

Fig. IV-17. Diagrams for $[001]$, $\pi \{100\}$ and $\pi \{110\}$ of hornblende in several folds of sample RGM 162741. All samples are rotated into a plane normal to the F_4 -axis. a: hornblende in an F_2 -fold ($N = 100$; $A = 0.02$); b: hornblende in an F_3 -fold ($N = 100$; $A = 0.02$); c: fine-grained hornblende in an F_4 -fold ($N = 100$; $A = 0.02$) and d: medium-grained hornblende in the same F_4 -fold. ($N = 150$; $A = 0.02$). Contours for densities 1, 2, 3, 4, 5, 6, 7, 8 and 9.

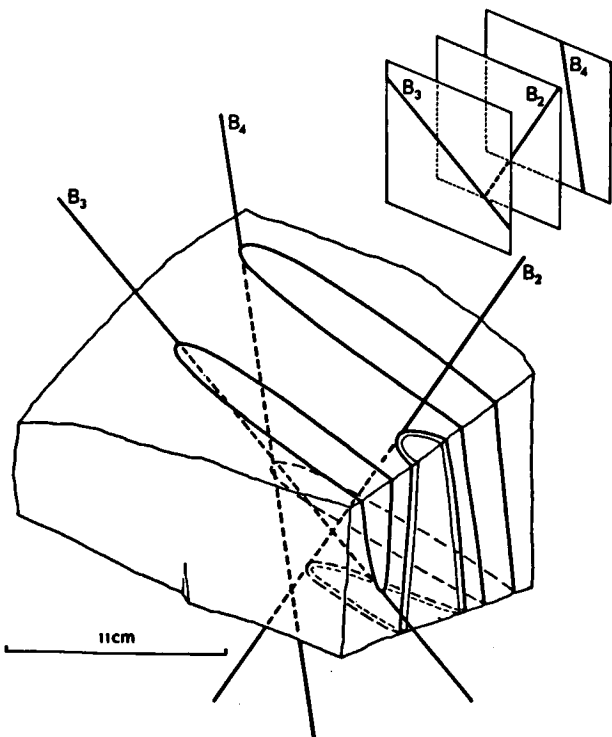
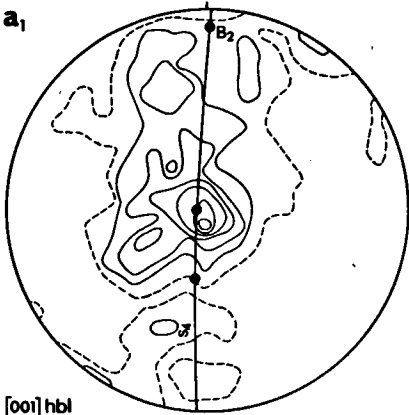
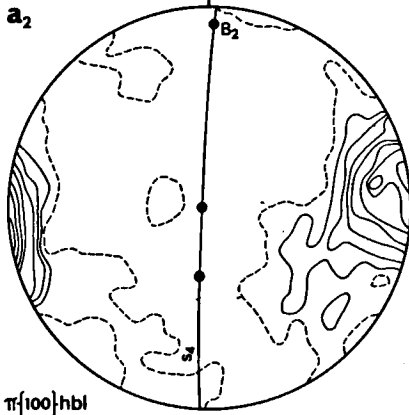


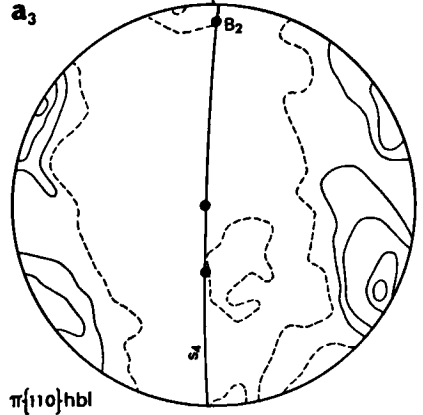
Fig. IV-16. Schematic picture of the orientation of fold axes in sample RGM 162741. Diagrams of the hornblende orientation in the folds are seen in Fig. IV-17.



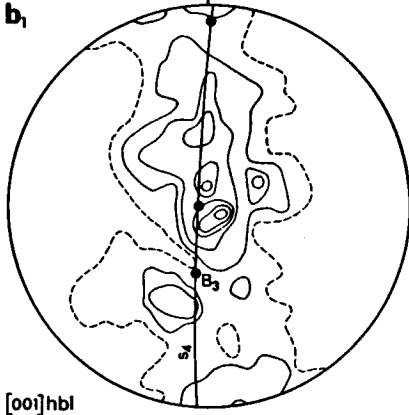
[001] hbl



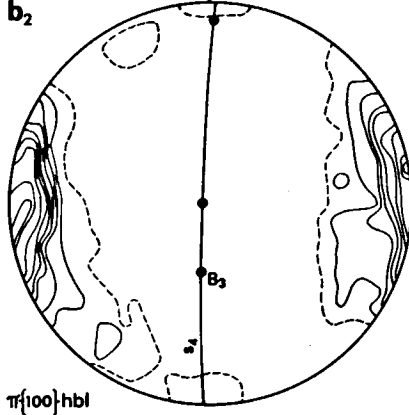
$\pi\{100\}$ hbl



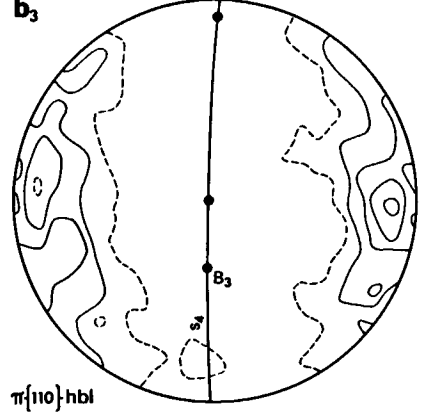
$\pi\{110\}$ hbl



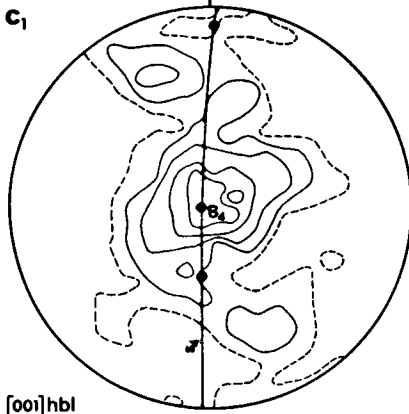
[001] hbl



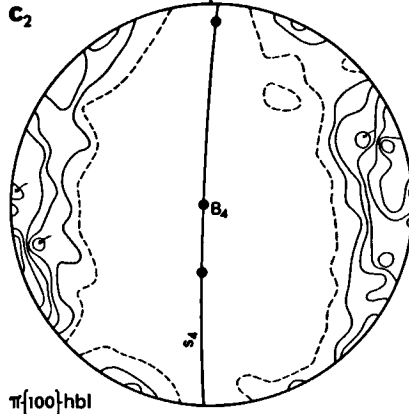
$\pi\{100\}$ hbl



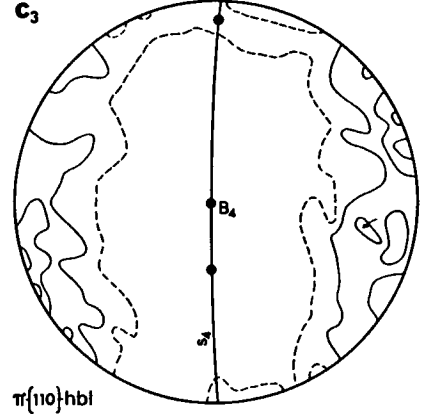
$\pi\{110\}$ hbl



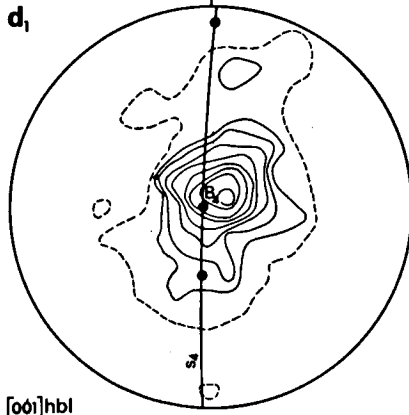
[001] hbl



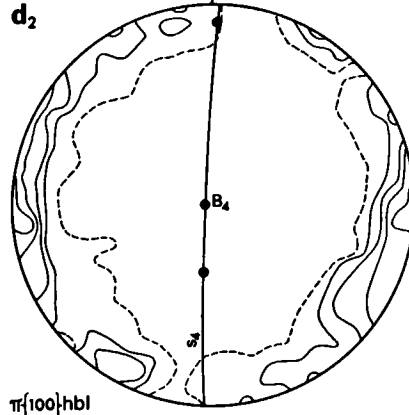
$\pi\{100\}$ hbl



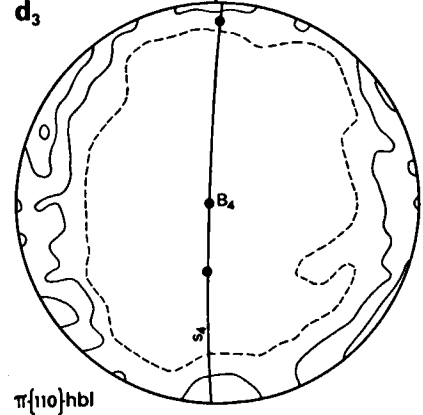
$\pi\{110\}$ hbl



[001] hbl



$\pi\{100\}$ hbl



$\pi\{110\}$ hbl

Intracrystalline slip

In this process the shape of any aggregate of grains can be changed by slip or twinning on a restricted number of rational slip planes; the planes involved are those oriented along the greatest resolved shear stress. This slipping produces a rotation of the axes of the crystal which may bring other planes into positions favourable for slip. When five independent slip systems are present any change in shape, without change in volume, may be produced by shear (Taylor, 1938; Bishop and Hill, 1951). This mechanism of deformation by intracrystalline slip can produce unique patterns of preferred orientation and it is possible to predict this preferred orientation for a certain amount of strain. Such predictions can be found in the work of Siemes (1970) and Saynisch (1970) for galena and sphalerite, respectively. Preferred orientation can also be produced by an appropriate combination of glide and climb (Hirth and Lothe, 1968); in this case the number of independent slip systems can be reduced from five to three. This mechanism of preferred orientation by glide and climb is especially important at high temperatures.

Recrystallization

There are several hypotheses which explain preferred orientation by a process of solid state recrystallization.

The theories based on thermodynamic equilibrium (The elastic anisotropy hypothesis). — Here preferred orientation is assumed to be a result of preferred grain growth. This preferred grain growth is correlated with the different elastic properties of individually oriented grains under non-hydrostatic stress (Kamb, 1959, 1961; MacDonald, 1957, 1960; Kumazawa, 1963). The thermodynamic approach to preferred orientation however neglects the stored energy of deformation and its influence on grain boundary migration during syntectonic recrystallization or the subsequent annealing, a process that has been demonstrated to be exceedingly important for quartz and metal microfabrics (Beck and Hu, 1966; Sellars and Tegart, 1968; Hobbs, 1968; Wilson, 1972).

The theory based on oriented nucleation. — Nucleation with restricted orientation is assumed to be the reason for the preferred orientation which develops when metals are annealed. The nuclei are thought to assume specific orientations during deformation; why nuclei of restricted orientation should form is still not clear and has recently been reviewed by Beck and Hu (1966). However because preferred orientation can sometimes develop after annealing in samples without an initial preferred orientation, oriented nucleation might be a possible origin of preferred orientations.

The theory based on oriented grain growth. — Grain boundary mobility depends on the relative orientation of crystals with respect to their mutual boundary. Experiments on metals have shown that low angle

boundaries are relatively immobile in contrast to high angle boundaries. New grains with high angle boundaries with respect to host grains which have a preferred orientation grow faster than new grains of other orientation and can in this manner produce a different preferred orientation. This mechanism is demonstrated by Hobbs (1968) in his experiments on deformation of single quartz crystals.

Preferred orientation observed within Cabo Ortegal

The contribution of these different processes to the formation of the preferred orientation of clinopyroxene and hornblende in the Cabo Ortegal Complex is difficult to evaluate, because two important factors are not taken into account in the theoretical and experimental studies but may have a pronounced influence on the actual preferred orientation patterns: (1) The fact that the rocks are not monomineralic in contrast to the samples used in the experimental studies and theories, and (2) the fact that transition into another metamorphic facies may involve the formation of hornblende at the expense of clinopyroxene.

Nevertheless under the P/T conditions assumed for the Cabo Ortegal Complex it is probable that intracrystalline deformation played a significant role but also that recrystallization accompanied or postdated the deformation since strained grains are not observed. If intracrystalline slip processes were active an explanation must be found for the differences in preferred orientation observed for eclogitic and granulitic clinopyroxenes. One explanation may be that omphacite and diopside crystallize in different space groups (Vogel, 1967, p. 198; Clark and Papike, 1966). The differences in symmetry may mean that omphacite and diopside do not have the same slip systems and therefore deformation will produce different preferred orientations. However as mentioned above the formation of preferred orientation by the process of intracrystalline slip can also be the result of a combination of glide, climb and cross slip. Climb processes are highly influenced by temperature and strain rate which may mean that the differences in preferred orientation reflect differences in temperature and/or strain rate. This could explain why a preferred orientation typical of the granulites was found in an eclogite sample. Experimental recrystallization of diopside at high P and T (1000°C, 15 Kb, $\dot{\epsilon} = 7.8 \times 10^{-7}$) resulted in a preferred orientation comparable to that of the Cabo Ortegal eclogites (N.L. Carter, pers. comm.). Therefore differences in temperature may be the determining factor rather than differences in space group.

Different preferred orientations for one mineral, such as the eclogite and granulite patterns of clinopyroxene, are also reported for olivine i.e. the α - and γ -maxima. Kumazawa (1968) attributes the different patterns to differences in the P/T conditions existing at the time of rock formation, whereas Hartman and den Tex (1964) state that the differences in olivine orientation can be explained by the thermodynamic theory of Kamb

assuming that recrystallization took place under dry (γ -maximum) versus wet (α -maximum) conditions.

The importance of the presence of water during the deformation of quartz is reported by Griggs (1967). Therefore the absence or presence of water in the 'dry' eclogites and 'wet' granulites may also have influenced the preferred orientation of the clinopyroxenes in these rocks.

From the preferred orientations of diopside and hornblende, it is clear that an important relationship exists between the observed preferred orientation and the mesoscopic structure, since [001]-axes lie parallel to the fold axes; however the orientation of younger hornblende, grown at the expense of clinopyroxene in a retrograded eclogite which shows no signs of later internal deformation, seems to be determined by the orientation of the clinopyroxene crystal. The fact that the

rock does not show signs of internal deformation does not mean that hydrostatic conditions reigned, as is proven by the synchronous plastic deformation of basic granulites. Therefore mimetic growth of hornblende seems to contradict the thermodynamic approach. The absence of a preferred orientation for clinopyroxene in an F_2 -fold where the strain was great (since the folds lie in a mylonitic horizon) may indicate that during low temperature deformation, syntectonic recrystallization played a minor role and that the end product was a weak preferred orientation. All other fabric analyses are from rocks that were deformed during or immediately after a metamorphic phase. The similarity in the preferred orientation patterns for [001] of hornblende and clinopyroxene is striking. This may indicate that the same deformation processes were responsible for the preferred orientation of clinopyroxene and hornblende.

CHAPTER V

CONCLUSIONS AND SYNTHESIS OF THE RESULTS IN THE GEOLOGICAL FRAMEWORK OF THE NW IBERIAN PENINSULA

The geological history of the Hesperian massif of the NW Iberian peninsula can be deduced from: (1) the study of catazonal complexes, which reveal the Precambrian history, such as the Cabo Ortegal Complex in Galicia and the Bragança-Vinhais and Morais-Lagoa Complexes in NE Portugal and (2) the study of rocks which were not metamorphosed before the Hercynian orogeny.

Geological history in the Precambrian

During an eugeosynclinal phase, sedimentation (graywackes, pelites, etc.) was accompanied by the emplacement of an ophiolitic suite (gabbros, basic lavas or tuffs and ultramafics).

Prograde metamorphism (M_1) of the above-mentioned sequence, caused by deep burial and tectonization, can be concluded from the metamorphic zoning; metamorphism passed through the almandine-amphibolite and granulite facies before the eclogite facies. The prograde nature is supported by the presence of kyanite enclosing staurolite in eclogitic rocks. The inferred thermal gradient of $17^\circ\text{C}/\text{km}$ and the low water pressure during metamorphism fix the eclogite facies conditions at a depth of about 40 km. The assumed Precambrian age of this phase was recently substantiated by one K/Ar age determination of an eclogitic kyanite that yielded an age of 900 ± 30 m.y. (Vogel and Abdel-Monem, 1971). This metamorphic phase was accompanied by folding of the paragneisses along N-S trending axes; the fabric of the clinopyroxenes in the homogeneous metabasites is consistent with the stress field that caused the folding of the paragneisses (pronounced maxima for [001] in the granulites and for [010] in the eclogites).

Later the orogen was uplifted and the Cabo Ortegal

Complex was upthrust in several stages, accompanied by extensive mylonitization of the rocks. Metamorphic readjustment to the changing physical conditions can be recognized in the development of hornblende-granulite (M_2) and amphibolite (M_3) facies parageneses. Recumbent folds along E-W trending axes were formed before M_2 and along N-S trending axes during M_2 . During the third metamorphic phase (amphibolite facies conditions), N-S trending folds with subvertical axial planes were formed. A final upthrust brought the complex into its present position between the almost non-metamorphic Paleozoic rocks. Similar sequences of metamorphic phases have been recognized in the catazonal complexes of NE Portugal (Anthonioz, 1969) and along the perimeter of the Ordenes Basin (Warnaars, 1967; van Zuuren, 1969), but only in the Cabo Ortegal Complex is the eclogite facies so clearly exposed. If the metamorphic histories of these isolated remnants of a Precambrian orogen can be correlated, then a correlation of the deformation phases in these complexes which can be linked to the metamorphic phases also seems warranted, although den Tex (1963) points out that the relationship between deformation and metamorphic phases in an orogen may differ from place to place. A tentative correlation between the catazonal complexes is given in Fig. V-1.

The uplifting of the Precambrian orogen was accompanied by sedimentation of rocks that were only metamorphosed during the Hercynian. The geological history in E Galicia is known from the studies of Matte (1968) and Capdevila (1969). Geosynclinal sedimentation started in the Upper Precambrian on or near the basement with the 'Ollo de Sapo' porphyroid Formation and

ORDENES COMPLEX van Zuuren 1969			CABO ORTEGAL			BRAGANÇA AND MORAIS Anthoiz 1969			
	axial direction	axial plane		axial direction	axial plane		axial direction	axial plane	
M ₁	granulite facies amphibolite facies	F ₁ NNW-SSE	subhorizontal	M ₁	eclogite facies granulite facies amphibolite facies	F ₁ N-S	subhorizontal	M ₁	eclogite facies granulite facies amphibolite facies
						F ₂ E-W	cataclasis subhorizontal	F ₁ E-W	cataclasis subhorizontal
M ₂	amphibolite facies	F ₂ ENE-WSW	cataclasis subhorizontal	M ₂	hbl granulite facies	F ₃ N-S	subhorizontal	M ₁	granulite facies amphibolite facies greenschist facies
		F ₃ E-W	subvertical						
M ₃	amphibolite facies greenschist facies	F ₄ N-S	cataclasis subvertical ?	M ₃	amphibolite facies	F ₄ N-S	cataclasis subvertical	M ₂	amphibolite facies greenschist facies
		F ₅ E-W	subvertical (N-S strike)					F ₂ N-S	cataclasis subvertical
M ₄	greenschist facies	F ₆ N-S	subvertical	M ₄	greenschist facies	F ₅	chevron folding	M ₃	greenschist facies
								F ₄ NW-SE	subvertical
								F ₅ NE-SW	subvertical

Fig. V-1. Correlation of metamorphic and deformation phases for the catazonal complexes in Galicia and NE Portugal.

the pelitic Villalba Formation. After the Precambrian a minor assyntic folding phase is recorded by Matte. During the Cambrian the zone of the 'Ollo de Sapo' formed a geanticlinal cordillera; during the Ordovician sedimentation on this ridge was limited. The presence of an Ordovician basal conglomerate in N Portugal suggests the presence of the Sardinian phase (Capdevila, 1965).

Paleozoic rocks younger than Silurian are rare in E Galicia. The geological history in W Galicia, which formed the axial zone, is discussed by van Zuuren, 1969; Arps, 1970; den Tex and Floor, 1967, 1971; Capdevila and Floor, 1970 and Floor et al. (in press). There the Ordenes schists are probably the equivalent of the Upper Precambrian Villalba Formation. Some of the western Galician schists are assumed to be of Paleozoic age insofar as they form a continuation of the Cambrian and Ordovician-Silurian rocks in N Portugal.

Intrusion of granitic rocks occurred during the Upper Ordovician (460–430 m.y.; Priem et al., 1970) and thin basic dykes are also known from the Lower Paleozoic in eastern Galicia (Capdevila, 1969). Rocks belonging to a second ophiolitic suite (ultramafics, gabbros and spilitic volcanites) are reported in the Silurian near the catazonal complexes (Ho Len Fat et al., in press).

Hercynian orogeny

The Hercynian orogeny started in E Galicia with the formation of recumbent folds on N-S trending axes. This folding phase was followed by a second phase with axes parallel to the first, but with vertical axial planes. Hercynian metamorphism started during the first folding

phase and reached its climax during the interphase. In E Galicia Hercynian metamorphism is centered on several thermal domes. The metamorphism is of the low-pressure or intermediate-low-pressure type with andalusite and sillimanite as the characteristic alumina-silicates. Locally the facies series passed through the kyanite stability field but where the temperatures were the highest, sillimanite was formed (thermal gradients of 20°–30°C/km).

In the axial zone anatexis and intrusion of granitic rocks were widespread. Intrusion of a gabbro stock is considered Hercynian by Warnaars (1967). Generally it is assumed that the Precambrian M₃-phase in the catazonal complexes is the equivalent, but at a deeper level, of the main Hercynian metamorphic phase.

For the Cabo Ortegal Complex, Vogel bases this hypothesis on the assumption that the orthogneisses found in the Chimparragneisses are of the same age as the monometamorphic orthogneisses E of Vigo (Floor, 1966) and on the fact that the fold axes run parallel to the Hercynian directions. However, other facts point to a Pre-Hercynian age for M₃: (1) Although sillimanite is the characteristic alumina-silicate in the Hercynian metamorphosed sediments in the axial zone, only kyanite is found in the Cabo Ortegal Complex and other catazonal complexes. (2) The Upper Precambrian 'Ollo de Sapo' Formation deposited on or near the Precambrian basement was not metamorphosed in the same facies. (3) Although the axial directions coincide, the first Hercynian folds have subhorizontal axial planes and the folds synchronous with M₃ have subvertical planes

though they are supposed to have been formed at a deeper level. According to Anthonioz (1969), the first Hercynian folding phase folded only the acid series ('Ollo de Sapo' and Villalba Formations) and not the catazonal rocks. Therefore the catazonal complexes may have behaved as rigid blocks during folding.

The emplacement of the catazonal massifs in or on the almost non-metamorphic Silurian has been explained on the assumption that the complexes are remnants of a large nappe (Anthonioz, 1969, 1970; Ribeiro et al., 1965; Ries and Shackleton, 1971). As rootzone for this nappe Anthonioz suggested the Sierra Segundera, NE of the massifs. Although the Sierra Segundera may be part of the Precambrian soele, the absence of catazonal metabasic rocks makes it unlikely as rootzone. In contrast to the nappe hypothesis is the mechanism of emplacement by extrusion of the complexes into and over the Paleozoic (den Tex and Vogel, 1962; Matte and Ribeiro, 1967; Ribeiro, 1970). This mechanism does not explain the fact that some of the complexes (Cabo Ortegal, Bragança and Morais) are so widely separated and yet lie together in Silurian strata, nor the fact that they are circular or oval in shape since straight fault traces are to be expected. The extrusion hypothesis is hardly supported by the results of the gravimetrical survey of Cabo Ortegal since it predicts a prolongation of the complex to the east.

The following alternative is proposed: As stated by den Tex and Floor (1971) 'a, probably deep reaching NNW striking fault forms the boundary between crystalline Western Galicia and (meta) sedimentary-cum-igneous Eastern Galicia'. Although this fault has been mapped only as far as Guntin, it perhaps continues to the south-east masked by younger intrusions. The catazonal complexes in NE Portugal lie west and the Cabo Ortegal

Complex east of this fault. If it is assumed that this fault originated as a wrench fault with a sinistral movement, horizontal movements over about 200 km may have carried the Cabo Ortegal Complex away from its original position opposite the complexes of NE Portugal to its present position. The NW-SE direction of the strike-slip fault is consistent with the Hercynian stress field. The advantage of this hypothesis is that it facilitates the explanation of certain observed facts:

- 1) The axial directions in the three complexes originally coincided.
- 2) The striking similarity between the rock types in the complexes is easier to understand, e. g. the Purrido amphibolites and the amphibolites of Remondes (Morais).
- 3) All complexes lie on Silurian rocks.
- 4) The increase in metamorphic grade to the N (absence of eclogites in Morais, their local presence in Vinhais and their abundance in Cabo Ortegal).
- 5) The reversal of the metamorphic zoning in the complexes.
- 6) The presence of the acid series of Lagoa on top of the amphibolites of Morais. These amphibolites represent the highest levels in the Precambrian stratigraphy.
- 7) The continuation of the Cabo Ortegal Complex to the east.

Similar large strike-slip movements are also proposed by Le Pichon et al. (1970) as a mechanism for the rotation of Spain. Although 200 km is a large displacement, it is small compared with the movement along the San Andreas Fault in the last 20-30 m.y. Therefore the overthrust of a large sliver of Precambrian basement over the Silurian does not seem impossible.

SAMENVATTING

De petrografie van het zuidelijk deel van het Cabo Ortegal Complex wordt in het kort behandeld. Een petrologisch en chemische studie aan soortgelijke gesteenten in het noordelijk deel is reeds verwerkt in een proefschrift van D. E. Vogel (1967). Hieraan wordt thans een onderzoek naar de structurele geschiedenis toegevoegd. Het volgende beeld komt hieruit tevoorschijn: de gedurende een geosynclinale fase afgezette sedimenten werden tezamen met de zich in deze sedimenten bevindende basische stollingsgesteenten in het Precambrium gemetamorfoseerd. Deze metamorfose heeft een prograad karakter waarbij de eclogiet faciës bereikt werd via de amfiboliet en de granuliet faciës. Een metamorfe zonerings kan uitgekarteerd worden. De isograad 'stauroliet-uit' is in de paragneisen te vervolgen, terwijl de grens tussen de granuliet faciës en de eclogiet faciës in de basische gesteenten bepaald wordt door de isograad 'plagioklaas-uit'.

Het feit dat de paragneisen weinig en de basische gesteenten geen opsmeltingsverschijnselen vertonen, zelfs niet in de hoogste metamorfe faciës, kan slechts verklaard worden wanneer zeer lage waterdamp drukken geheerd hebben. Een lage P_{H_2O} maakt de vorming van granuliet en eclogiet in de aardkorst mogelijk. Verondersteld wordt dat de fysische omstandigheden, waaronder de gesteenten in de verschillende faciës zijn gemetamorfoseerd, slechts weinig van elkaar verschilden. Dit is daar het geval waar de curven, die de verschillende faciës begrenzen, samenkomen. De plaats van dit 'tripelpunt' moet op de grenscurve, die de granuliet-eclogiet faciës scheidt, liggen en wordt verder bepaald door het stabiliteitsveld van hoornblende bij de heersende P_{H_2O} . Dit gekombineerd met het feit dat de omphaciet in de eclogiet een jadeïet-gehalte van ongeveer 33% bezit, stelt de fysische omstandigheden voor de eclogietvorming vast op $T = 700^{\circ} - 750^{\circ}C$ en $P = 11 - 13$ Kb. De metamorfose

geschiedde derhalve bij een thermische gradiënt van ca. $17^{\circ}\text{C}/\text{km}$; een gradiënt die ongeveer samenvalt met die voor de oceanische korst. Slechts het omlaag brengen van de gesteenten tot voldoende diepte kan de metamorfose veroorzaakt hebben.

Tijdens deze metamorfose werden in de paragneisen plooien met een horizontaal assenvlak en N-S strekkende assen gevormd; de homogene basische gesteenten ondergingen slechts een vormverandering, doch de maakselanalyse van de clinopyroxen in deze gesteenten toont aan dat een duidelijke voorkeursorientatie tijdens deze eerste metamorfe fase is gevormd.

Na deze eerste fase van metamorfose en deformatie werd het complex stapsgewijs omhoog gebracht, waarbij elke keer de metamorfe aanpassing aan de veranderde omstandigheden in de gesteenten herkend kan worden. Sterke kataklase onder vorming van dikke pakketten mylonitische gesteenten, geassocieerd met de vorming van plooien met E-W gerichte assen en de daarmee mogelijk samenhangende omkering van de metamorfe zonerings, gaat aan de tweede metamorfe fase vooraf. De groei van bruinroene hoornblende stabiel naast granaat, clinopyroxen en plagioklaas wijst op granuliet faciës omstandigheden bij een hogere $\text{P}_{\text{H}_2\text{O}}$. Deze metamorfe fase wordt vergezeld door een plooingsfase (F_3), waarbij plooien met horizontale assenvlakken en N-S gerichte ploi-assen gevormd worden.

Verder omhoog schuiven van het complex waarbij

wederom mylonitisatie van de gesteenten optreedt, maakt hernieuwde metamorfe aanpassing aan de veranderde fysische omstandigheden noodzakelijk. Deze metamorfe fase (M_3) vindt plaats in de amfiboliet faciës, en is gekenmerkt door de groei van blauwgroene hoornblende en het vervangen van rutiel door titaniet en zoisiet door clinozoisiet. Granaat is nog slechts stabiel in basische gesteenten van geschikte chemische samenstelling. Tijdens deze fase vormden zich isoclinale plooien (F_4) met verticale assenvlakken en horizontaal N-S gerichte assen. Aan de randen van het complex worden lokaal nog chevron-plooien gevonden (F_5) die ook in het omliggende Paleozoïcum voorkomen.

Op grond van de gelijkenis van de plooingsrichtingen in het Paleozoïcum kan eventueel verondersteld worden, dat de derde metamorfe fase (M_3) van Hercynische ouderdom is. De opeenvolging van de plooingsfasen werd vastgesteld door hun relatie ten opzichte van de metamorfose via de maakselanalyse te onderzoeken, en door de bestudering van de interferentie-patternen die de relatieve ouderdom van de fasen onthult.

De maakselanalyse van clinopyroxen in granuliet en eclogiet toont dat de omphaciet een sterke voorkeursorientatie van [010] en de diopsied van [001] bezit. Hoornblende en diopsied rekristalliseerden met [001] parallel aan de plooias richting. De mogelijke mechanismen die deze voorkeursorientatie veroorzaakten worden kort behandeld.

REFERENCES

- Althaus, E., 1967. The triple point andalusite-sillimanite-kyanite. An experimental and petrologic study. *Contr. Min. Petr.*, 16, pp. 29-44.
- Althaus, E., Karotke, E., Nitsch, K. H. & Winkler, H. G. F., 1970. An experimental re-examination of the upper stability limit of muscovite plus quartz. *N. Jb. Min. Mh.*, pp. 325-336.
- Anthonioz, P. M., 1968. Considérations sur le métamorphisme blastomylonitique dans l'unité de Bragança (Tras-os-Montes, Portugal). Position tectonique des complexes granulitiques nord-portugais. *An. Univ. et A. R. E. R. S.*, 6, pp. 71-76.
- , 1969. Etude petrographique et structurale des régions de Morais et Bragança (NE du Portugal). Thèse, Université de Poitiers, 311 pp.
- , 1970. Etude des complexes polymétamorphiques précambriens de Morais et Bragança (NE du Portugal). *Sci. de la Terre*, 15, pp. 145-166.
- Arps, C. E. S., 1970. Petrology of a part of the Western Galician basement between the Rio Jallas and the Ria de Arosa (NW Spain) with emphasis on zircon investigations. *Leidse Geol. Med.*, 46, pp. 57-155.
- Avé Lallement, H. G., 1965. Petrology, petrofabrics, and structural geology of the Sierra de Outes-Muros region (Prov. La Coruña, Spain). *Leidse Geol. Med.*, 33, pp. 147-175.
- , 1967. Structural and petrofabric analysis of an 'Alpine-type' peridotite: the Iherzolite of the French Pyrenees. *Leidse Geol. Med.*, 42, pp. 1-57.
- Banno, S. & Yoshino, G., 1965. Eclogite-bearing peridotite mass at Higasiakaisiyama in the Bessi area, Central Sikoku, Japan. *The Upper Mantle Symposium New Delhi, 1964*, pp. 150-160.
- Beck, P. A. & Hu, H., 1966. The origin of recrystallization textures. In: H. Marolin (ed.), *Recrystallization, Grain Growth and Textures. Seminar Am. Soc. Metals*, pp. 393-433.
- Behr, H. J., Tex, E. den, Waard, D. de, Mehnert, K. R., Scharbert, H. G., Sobolev, V. S., Watznauer, A., Winkler, H. G. F., Wynne-Edwards, H. R., Zoubek, V. & Zwart, H. J., 1971. Granulites - Results of a discussion. *N. Jb. Min. Mh.*, pp. 97-123.
- Berthelsen, A. 1960. Structural studies in the Pre-Cambrian of Western Greenland. *Meddel. Grøn.*, 123, 233 pp.
- Bishop, J. F. W. & Hill, R., 1951. A theory of the plastic distortion of a polycrystalline aggregate under combined stresses. *Phil. Mag.*, 42, pp. 414-427.
- Bonhomme, M., Mendès, F. & Viallette, Y., 1961. Ages absolus pas la méthode au strontium des granites de Sintra et Castro Daire au Portugal. *C. R. Acad. Sci., Paris*, 252, pp. 3305-3306.
- Brothers, R. N., 1964. Petrofabric analysis of Rhum and Skaergaard layered rocks. *Jour. Petr.*, 5, pp. 255-274.
- Brown, G. C. & Fyfe, W. S., 1970. The production of granitic melts during ultrametamorphism. *Contr. Min. Petr.*, 28, pp. 310-318.
- Bryhni, I., Bollingberg, H. J. & Graff, P. R., 1968. Eclogites in quartzofeldspathic gneisses of Nordfjord, West Norway. *Norsk Geol. Tidsskr.*, 49, pp. 193-225.
- Bryhni, I., Green, D. H., Heier, K. S. & Fyfe, W. S., 1970. On the occurrence of eclogite in Western Norway. *Contr. Min. Petr.*, 26, pp. 12-19.
- Capdevila, R., 1965. Sur la géologie du Précambrien et du Paléozoïque dans la région de Lugo et la question des plissements

- assyntiques et sardes en Espagne. *Notas Comuns. Inst. Geol. Min. Esp.*, 80, pp. 157–174.
- , 1969. Le métamorphisme regional progressif et les granites dans le segment hercynien de Galice Nord Orientale (NW de l'Espagne). Thèse, Univ. de Montpellier, 430 pp.
- Capdevila, R. & Vialette, Y., 1965. Premières mesures d'âge absolu effectuées par la méthode au strontium sur des granites et micaschistes de la province de Lugo (Nord-Ouest de l'Espagne). *C. R. Acad. Sci., Paris*, 260, pp. 5081–5083.
- Capdevila, R. & Floor, P., 1970. Les différents types de granites hercyniens et leur distribution dans le nord ouest de l'Espagne. *Boletín Geol. Min.*, 81, pp. 215–225.
- Carey, S. W., 1962. Folding. *Jour. Alberta Soc. Petroleum Geol.*, 10, pp. 95–144.
- Carlé, W., 1945. Ergebnisse geologischer Untersuchungen im Grundgebirge von Galizien, N.W. Spanien. *Geotekt. Forsch.*, 6, pp. 13–36.
- Carter, N. L., 1971. Static déformation of silica and silicates. *Jour. Geophys. Res.*, 76, pp. 5514–5540.
- Coleman, R. G., Lee, D. E., Beatty, L. B. & Brannock, W. W., 1965. Eclogites and eclogites: Their differences and similarities. *Bull. Geol. Soc. Am.*, 76, pp. 483–508.
- Clark, J. R. & Papike, J. J., 1966. Eclogite pyroxenes ordered with P2 symmetry. *Science*, 154, pp. 1003–1004.
- Dawes, P. R., 1970. The plutonic history of the Tasiussaq area, South Greenland, with special reference to a high-grade gneiss complex. *Grønlands Geol. Undersøg.*, 88, pp. 1–125.
- Dobretsov, I. L., Sobolev, V. S. & Khlestov, V. V., 1970. Principles of identification and classification of regional metamorphic formations. *Internat. Geol. Rev.*, 12, pp. 1159–1171.
- Donath, F. A., 1962. Role of layering in geologic deformation. *New York Acad. Sci. Trans.*, 24, pp. 236–249.
- , 1963. Fundamental problems in dynamic structural geology. In: T. W. Donnelly (ed.), *The earth sciences: problems and progress in current research*. Univ. Chicago Press, Chicago, pp. 83–103.
- , 1964. Strength variation and deformational behavior in anisotropic rock. In: W. R. Judd (ed.), *State of Stress in the earth's crust*. Elsevier, New York, pp. 281–301.
- Donath, F. A. & Parker, R. B., 1964. Folds and Folding. *Bull. Geol. Soc. Am.*, 75, pp. 45–62.
- Donath, F. A. & Fruth, L. S., 1971. Dependence of strain-rate effects on deformation mechanism and rock type. *Jour. Geol.*, 79, pp. 347–371.
- Emmons, R. C., 1943. The universal stage (with five axes of rotation). *Mem. Geol. Soc. Am.*, 8, 205 pp.
- Engels, J. P. & Vogel, D. E., 1966. Garnet reaction rims between plagioclase and hypersthene in a metanorite from Cabo Ortegale (NW-Spain). *N. Jb. Min. Mh.*, pp. 13–19.
- Eskola, P., 1921. On the eclogites of Norway. *Videns. Skr. Math. Naturv. kl., Kristiania*, 8, pp. 1–118.
- , 1952. On the granulites of Lapland. *Am. Jour. Sci., Bowen Vol.*, pp. 133–172.
- Essene, E. J. & Fyfe, W. S., 1967. Omphacite in Californian metamorphic rocks. *Contr. Min. Petr.*, 15, pp. 1–23.
- Essene, E. J., Hensen, B. J. & Green, D. H., 1970. Experimental study of amphibolite and eclogite stability. *Phys. Earth Planet. Interiors*, 3, pp. 378–384.
- Fleuty, M. J., 1964. The description of folds. *Proc. Geol. Ass.*, 75, pp. 461–493.
- Flinn, D., 1965. Deformation in metamorphism. In: W. S. Pitcher and G. W. Flinn (editors), *Controls of Metamorphism*. Oliver & Boyd, Edinburgh, pp. 46–72.
- Floor, P., 1966. Petrology of an aegirine-riebeckite gneiss-bearing part of the Hesperian Massif: The Galifeiro and surrounding areas, Vigo, Spain. *Leidse Geol. Med.*, 36, pp. 1–204.
- , 1970. Session de travail consacrée à la subdivision des roches granitiques hercyniennes dans le nord-ouest péninsulaire. *Boletín Geol. Min.*, 81, pp. 245–248.
- Frey, M., 1969. Die Metamorphose des Keupers vom Tafeljura bis zum Lukmanier-Gebiet. *Beitr. Geol. Karte Schweiz, N. F.* 137, pp. 1–160.
- Fry, N. & Fyfe, W. S., 1969. Eclogites and waterpressure. *Contr. Min. Petr.*, 24, pp. 1–6.
- Gjelsvik, T., 1952. Metamorphosed dolerites in the gneiss area of Sunnmøre on the West coast of Southern Norway. *Norsk Geol. Tidsskr.*, 30, pp. 30–134.
- Goldsmith, R., 1959. Granofels, a new metamorphic rock. *Jour. Geol.*, 67, pp. 109–110.
- Green, D. H. & Ringwood, A. E., 1967. An experimental investigation of the gabbro to eclogite transformation and its petrological applications. *Geochim. Cosmochim. Acta*, 31, pp. 767–833.
- Green, H. W., Griggs, D. T. & Christie, J. M., 1970. Syntectonic and annealing recrystallization of fine-grained quartz aggregates. In: P. Paulitsch (ed.), *Experimental and Natural Rock Deformation*. Springer-Verlag, Berlin, pp. 272–335.
- Greenwood, H. J., 1960. Waterpressure and total pressure in metamorphic rocks. *Carnegie Inst. Yearb.*, 59, pp. 58–63.
- Griggs, D. T., 1940. Experimental flow of rocks under conditions favoring recrystallization. *Bull. Geol. Soc. Am.*, 51, pp. 1001–1022.
- , 1967. Hydrolytic weakening of quartz and other silicates. *Geophys. Jour. Royal Astr. Soc.*, 14, pp. 19–31.
- Griggs, D. T., Turner, F. J. & Heard, H. C., 1960. Deformation of rocks at 500° to 800° C. In: D. Griggs and J. Handin (editors), *Rock Deformation*. *Mem. Geol. Soc. Am.*, 79, pp. 39–104.
- Handin, J. & Hager, R. V., 1957. Experimental deformation of sedimentary rocks under confining pressure: tests at room temperature on dry samples. *Bull. Am. Assoc. Petrol. Geol.*, 41, pp. 1–50.
- Handin, J. & Hager, R. V., 1958. Experimental deformation of sedimentary rocks under confining pressure: tests at high temperature. *Bull. Am. Assoc. Petrol. Geol.*, 42, pp. 2892–2934.
- Hartman, P. & Tex, E. den, 1964. Piezocrystalline fabrics of olivine in theory and nature. XXII Internat. Geol. Cong. Proc. section 4, pp. 84–114.
- Haüy, R. J., 1822. *Traité de minéralogie*, 2nd ed., Delance, Paris.
- Heard, H. C., 1960. Transition from brittle fracture to ductile flow in Solenhofen limestone as a function of temperature, confining pressure, and interstitial fluid pressure. In: D. Griggs and J. Handin (editors), *Rock Deformation*. *Mem. Geol. Soc. Am.*, 79, pp. 193–226.
- Hietanen, A., 1967. On the facies series in various types of metamorphism. *Jour. Geol.*, 75, pp. 187–214.
- Hirth, J. R. & Lothe, J., 1968. *Theory of dislocations*. McGraw-Hill, New York, 780 pp.
- Ho Len Fat, A. G., Koning, H. and Meer Mohr, C. G. van der, (in press). The association of fossil bearing limestones, spilitic and ultramafic rocks in the SE border-group of the Cabo Ortegale Complex, Galicia, Spain. *Geol. & Mijnbouw*.
- Hobbs, B. E., 1968. Recrystallization of single crystals of quartz. *Tectonophysics*, 6, pp. 353–401.
- Holland, J. G. & Lambert, R. St. J., 1969. Structural regimes and metamorphic facies. *Tectonophysics*, 7, pp. 197–218.
- Hotz, P. E., 1953. Petrology of granophyre in diabase near Dillsburg, Pa. *Bull. Geol. Soc. Am.*, 64, pp. 675–704.
- Hoschek, G., 1967. Untersuchungen zum Stabilitätsbereich von Chloritoid und Staurolith. *Contr. Min. Petr.*, 14, pp. 123–162.
- , 1969. The stability of staurolite and chloritoid and their significance in metamorphism of pelitic rocks. *Contr. Min. Petr.*, 22, pp. 208–232.
- Howard, K. A., 1968. Flow direction in triclinic folded rocks. *Am. Jour. Sci.*, 266, pp. 758–765.

- Hsu, K. J., 1955. Granulites and mylonites of the region about Cucamonga and San Antonio canyons, San Gabriel mountains, California. *Univ. California Publ. Geol. Sci.*, 30, pp. 223–352.
- Inoue, T., 1961. Structural-petrological studies of metamorphic complex of the Seburi mountainland, with special reference to its bearing on the metamorphism of the Sangun metamorphic zone in northern Kyūshū. *Jour. Sci. Hiroshima Univ.*, C, 3, pp. 403–424.
- Kamb, W. B., 1959. Theory of preferred crystal orientation developed by crystallization under stress. *Jour. Geol.*, 67, pp. 153–171.
- , 1961. The thermodynamic theory of nonhydrostatically stressed solids. *Jour. Geophys. Res.*, 66, pp. 259–271.
- Kappel, F., 1967. Die Eklogite Meidling im Tal und Mitterbachgraben im niederösterreichischen Moldanubikum Südlich der Donau. *N. Jb. Min. Abh.*, 107, pp. 266–298.
- Knorring, O. v. & Kennedy, W. Q., 1958. The mineral paragenesis and metamorphic status of garnet-hornblende-pyroxene-scapolite gneiss from Ghana (Gold Coast). *Min. Mag.*, 31, pp. 846–859.
- Kojima, G. & Hide, K., 1957. On new occurrence of aegirine augite-amphibole-quartz-schists in the Sambagawa crystalline schists of the Besshi-Shirataki district, with special reference to the preferred orientation of aegirine augite and amphibole. *Jour. Sci. Hiroshima Univ.*, C, 2, pp. 1–20.
- Koning, H., 1967. Les types des roches basiques et ultrabasiques qu'on rencontre dans la partie occidentale de la Galice (Espagne). *Leidse Geol. Med.*, 36, pp. 235–242.
- Kozłowski, K., 1965. The granulitic complex of Stary Gieraltów – East Sudetes. *Archiwum Min.*, 25, pp. 5–123.
- Kumazawa, M., 1963. A fundamental thermodynamic theory on nonhydrostatically stressed solids. *Jour. Geophys. Res.*, 66, pp. 3981–3984.
- , 1968. Nonhydrostatic thermodynamics, basic concepts in theory and application (Abstract). *Trans. Am. Geophys. Union*, 49, p. 303.
- Kumazawa, M., Helmstaedt, H. & Masaki, K., 1971. Elastic properties of eclogite xenoliths from diatremes of the east Colorado Plateau and their implication to the mantle structure. *Jour. Geophys. Res.*, 76, pp. 1231–1247.
- Kushiro, I., 1965. Clinopyroxene solid solutions at high pressures. *Carnegie Inst. Wash. Yearb.*, 64, pp. 112–117.
- Lambert, I. B. & Wyllie, P. J., 1968. Stability of hornblende and a model for the low velocity zone. *Nature*, 219, pp. 1240–1241.
- Lange, H., 1965. Zur Genese der Metabasite im Sächsischen Erzgebirge. *Freib. Forsch. H.*, C 177, 136 pp.
- Lappin, M. A., 1960. On the occurrence of kyanite in the eclogites of the Seljo and Åheim districts, Nordfjord. *Norsk Geol. Tidsskr.*, 40, pp. 289–296.
- Le Pichon, X., Bonnin, J. & Sibuet, J. C., 1970. La faille nord-pyrénéenne: faille transformante liée à l'ouverture du Golfe de Gascogne. *C. R. Acad. Sci.*, série D, 271, pp. 1941–1944.
- Lovering, J. F. & White, A. J. R., 1964. The significance of primary scapolite in granulitic inclusions from deep-seated pipes. *Jour. Petrol.*, 5, pp. 195–218.
- Maaskant, P., 1970. Chemical petrology of polymetamorphic ultramafic rocks from Galicia, NW Spain. *Leidse Geol. Med.*, 45, pp. 237–325.
- MacDonald, G. J. F., 1957. Thermodynamics of solids under nonhydrostatic stress with geological applications. *Am. Jour. Sci.*, 255, pp. 266–281.
- , 1960. Orientation of anisotropic minerals in a stress field. *Mem. Geol. Soc. Am.*, 79, pp. 1–8.
- Marcos, A., 1971. Las deformaciones Hercinianas en el occidente de Asturias: la segunda fase de deformación y su extensión en el NW de la península. *Breviora Geol. Asturica*, 15, pp. 1–6.
- Matte, P., 1968. La structure de la virgation hercynienne de Galice (Espagne). *Géol. Alpine*, 44, pp. 157–280.
- Matte, P. & Ribeiro, A., 1967. Les rapports tectoniques entre le Précambrien et le Paléozoïque dans le Nord-Ouest de la Péninsule Ibérique; grandes nappes ou extrusions? *C. R. Acad. Sci.*, D, 264, pp. 2268–2271.
- Mehnert, K. R., 1968. Migmatites and the origin of granitic rocks. Elsevier, Amsterdam, 393 pp.
- Miller, C., 1970. Petrology of some eclogites and metagabbros of the Oetzal Alps, Tirol, Austria. *Contr. Min. Petr.*, 28, pp. 42–56.
- Möckel, J. R., 1969. Structural petrology of the garnet-peridotite of the Alpe Arami (Ticino, Switzerland). *Leidse Geol. Med.*, 42, pp. 61–130.
- Naumann, C. F., 1950. *Lehrbuch der Geognosie*, I. Engelmann, Leipzig, 1000 pp.
- Newton, R. C. & Kennedy, G. C., 1963. Some equilibrium reactions in the join $\text{CaAl}_2\text{Si}_2\text{O}_8\text{-H}_2\text{O}$. *Jour. Geophys. Res.*, 75, pp. 2967–2983.
- Parga-Pondal, I., 1966. La investigación geológica en Galicia. *Leidse Geol. Med.*, 36, pp. 207–210.
- Parga-Pondal, I. et al., 1967. Carte Géologique du Nord-Ouest de la Péninsule Ibérique (1 : 500.000), Serv. Géol. Portugal, Lisboa.
- Pistorius, C. W. F. T., Kennedy, G. C. & Sourirajan, S., 1962. Some relations between the phases anorthite, zoisite and lawsonite at high temperatures and pressures. *Am. Jour. Sci.*, 260, pp. 44–56.
- Piwinskii, A. J. & Wyllie, P. J., 1968. Experimental studies of igneous rocks series: A zoned pluton in the Wallowa batholith, Oregon. *Jour. Geol.*, 76, pp. 205–235.
- Platen, H. von, 1965a. Kristallisation granitischer Schmelzen. *Contr. Min. Petr.*, 11, pp. 334–381.
- , 1965b. Experimental anatexis and genesis of migmatites. In: W. S. Pitcher & G. W. Flinn (editors), *Controls of metamorphism*. Oliver & Boyd, Edinburgh, pp. 203–218.
- Priem, H. N. A., Boelrijk, N. A. I. M., Verschure, R. H., Hebeda, E. H. & Floor, P., 1966. Isotopic evidence for Upper Cambrian or Lower Ordovician granite emplacement in the Vigo area, North-Western Spain. *Geol. & Mijnbouw*, 45, pp. 36–40.
- Priem, H. N. A., Boelrijk, N. A. I. M., Verschure, R. H., Hebeda, E. H. & Verdurmen, E. A. Th., 1970. Dating events of acid plutonism through the Paleozoic of the western Iberian Peninsula. *Eclogae Geol. Helvet.*, 63, pp. 255–274.
- Raleigh, C. B., 1965. Glide mechanisms in experimentally deformed minerals. *Science*, 150, pp. 739–741.
- , 1967. Plastic deformations of upper mantle silicate minerals. *Geophys. Jour.*, 4, pp. 45–49.
- Raleigh, C. B. & Talbot, J. L., 1967. Mechanical twinning in naturally and experimentally deformed diopside. *Am. Jour. Sci.*, 265, pp. 151–165.
- Ramsay, J. G., 1962a. The geometry and mechanics of formation of 'similar' type folds. *Jour. Geol.*, 70, pp. 309–327.
- , 1962b. The geometry of conjugate fold systems. *Geol. Mag.*, 99, pp. 516–526.
- , 1962c. Interference patterns produced by the superposition of folds of similar type. *Jour. Geol.*, 70, pp. 466–481.
- , 1967. *Folding and fracturing of rocks*. McGraw-Hill, New York, 568 pp.
- Ribeiro, A., 1970. Position structurale des Massifs de Morais et Bragança (Trás-os-Montes). *Com. Serv. Geol. Portugal*, 104, pp. 115–138.
- Ribeiro, A., Medeiros, A. & Almeida Rebelo, J. A., 1965. Estado actual dos conhecimentos sobre a geologia de Trás-os-Montes oriental. *Bol. Soc. Geol. Port.*, 16, pp. 93–110.
- Richardson, S. W., 1968. Staurolite stability in a part of the system Fe-Al-Si-O-H. *Jour. Petrol.*, 9, pp. 467–488.
- Richardson, S. W., Gilbert, M. C. & Bell, P. M., 1969. Experimental determination of kyanite-andalusite and andalusite-

- sillimanite equilibria; the aluminum silicate triple point. *Am. Jour. Sci.*, 267, pp. 467–488.
- Ries, A. C. & Shackleton, R. M., 1971. Catazonal complexes of north-west Spain and north Portugal, remnants of a Hercynian thrustplate. *Nature*, 234, pp. 65–68.
- Ringwood, A. E. & Green, D. H., 1966. An experimental investigation of the gabbro-eclogite transformation and some geophysical implications. *Tectonophys.*, 3, pp. 383–427.
- Russell, W. L., 1955. *Structural geology for petroleum geologists*. McGraw-Hill, New York, 427 pp.
- Saynisch, H. J., 1970. Festigkeits- und Gefügeuntersuchungen an experimentell und natürlich verformten Zinkblendeeisen. In: P. Paulitsch (ed.), *Experimental and Natural Rock Deformation*. Springer-Verlag, Berlin, pp. 209–252.
- Scheumann, K. H., 1924. Prävariskische Glieder der Sächsisch-Fichtelgebirgischen Kristallinen Schiefer; I. Die magmatisch orogenetische Stellung der Frankenger Gneissgesteine. *Abh. math.-phys. Kl. Sächs. Akad. Wiss.*, 39, H.1, pp. 1–61.
- Schreyer, W., 1968. A reconnaissance study of the system $MgO-Al_2O_3-SiO_2-H_2O$ at pressures between 10 and 25 kb. *Carnegie Inst. Wash. Yearb.*, 66, pp. 380–392.
- Siemes, H., 1970. Experimental deformation of galena ores. In: P. Paulitsch (ed.), *Experimental and Natural Rock Deformation*. Springer-Verlag, Berlin, pp. 165–208.
- Sellars, C. M. & Tegart, W. J. M., (editors), 1968. *Deformation under hot working conditions*. Iron and Steel Inst. Pub., 108, 189 pp.
- Sobolev, V. S., Dobretsov, N. L., Reverdatto, V. V., Sobolev, N. V., Ustrakova, E. N. & Khlestov, V. V., 1967. Metamorphic facies and series of facies in the U.S.S.R. *Medd. Dansk Geol. For.*, 17, pp. 458–472.
- Stauffer, M. R., 1966. An empirical-statistical study of three-dimensional fabric diagrams as used in structural analysis. *Can. Jour. Earth Sci.*, 3, pp. 473–498.
- Storre, B. & Karotke, E., 1971. An experimental determination of the upper stability limit of muscovite + quartz in the range 7–20 kb water pressure. *N. Jb. Min. Mh.*, pp. 237–240.
- Sturt, B. A., 1970. Exsolution during metamorphism with particular reference to feldspar solid solutions. *Min. Mag.*, 37, pp. 815–832.
- Taylor, G. I., 1938. Plastic strain in metals. *Jour. Inst. Metals*, 62, pp. 307–324.
- Tex, E. den, 1961. Some preliminary results of petrological work in Galicia (N.W. Spain). *Leidse Geol. Med.*, 26, pp. 75–91.
- , 1965. Metamorphic lineages of orogenic plutonism. *Geol. & Mijnbouw*, 44, pp. 105–132.
- , 1967. Aperçu pétrologique et structural de la Galice cristalline. *Leidse Geol. Med.*, 36, pp. 211–222.
- , 1971a. The facies groups and facies series of metamorphism and their relation to physical conditions in the earth's crust. *Lithos*, 4, pp. 23–41.
- , 1971b. The poly-orogenic, catazonal terrain at Cabo Ortegal (NW Spain) and its bearing on the granulite problem. *Freib. Forschungshefte*, C 268, pp. 41–58.
- Tex, E. den & Vogel, D. E., 1962. A 'Granulitgebirge' at Cabo Ortegal (NW Spain). *Geol. Rundschau*, 52, pp. 95–112.
- Tex, E. den & Floor, P., 1967. A blastomylonitic and polymetamorphic 'Graben' in Western Galicia (NW Spain). In: *Etages Tectoniques. Colloque de Neuchâtel*, 18-24 Avril 1966, pp. 169–178.
- Tex, E. den & Floor, P. (in press). A synopsis of the geology of western Galicia.
- Tilley, C. E., 1936. The paragenesis of kyanite-eclogites. *Min. Mag.*, 24, pp. 422–432.
- , 1937. The paragenesis of kyanite-amphibolites. *Min. Mag.*, 24, pp. 555–567.
- Turner, F. J., 1968. *Metamorphic petrology – mineralogical and field aspects*. McGraw-Hill, New York, 403 pp.
- Turner, F. J. & Weiss, L. E., 1963. *Structural analysis of metamorphic tectonites*. McGraw-Hill, New York, 545 pp.
- Tuttle, O. F. & Bowen, N. L., 1958. Origin of granite in the light of experimental studies in the system $NaAlSi_3O_8-KAlSi_3O_8-SiO_2-H_2O$. *Mem. Geol. Soc. Am.*, 74, pp. 1–153.
- Vogel, D. E., 1966. Nature and chemistry of the formation of clinopyroxene-plagioclase symplectite from omphacite. *N. Jb. Min. Mh.*, pp. 185–189.
- , 1967. Petrology of an eclogite- and pyrogarnite-bearing polymetamorphic rock complex at Cabo Ortegal, NW Spain. *Leidse Geol. Med.*, 40, pp. 121–213.
- , 1969. Catazonal rock complexes in the poly-orogenic terrain at Cabo Ortegal. *Spec. Pap. Geol. Assoc. Canada*, 5, pp. 83–88.
- Vogel, D. E. & Abdel-Monem, A. A., 1971. Radiometric evidence for a Precambrian metamorphic event in N.W. Spain. *Geol. & Mijnbouw*, 50, pp. 749–750.
- Vogel, D. E. & Bahezre, C., 1965. The composition of partially zoned garnet and zoisite from Cabo Ortegal, NW Spain. *N. Jb. Min. Mh.*, pp. 140–149.
- Vogel, D. E. & Warnaars, F. W., 1967. Meta-olivine gabbro from Cabo Ortegal (NW Spain): a case of incipient eclogitization? *N. Jb. Min. Mh.*, pp. 110–115.
- Voll, G., 1960. New work on petrofabrics. *Lpool. Manch. Geol. Jour.*, 2, pp. 503–567.
- Waard, D. de, 1965. A proposed subdivision of the granulite facies. *Am. Jour. Sci.*, 263, pp. 455–461.
- Warnaars, F. W., 1967. Petrography of a peridotite-, amphibolite- and gabbro-bearing poly-orogenic terrain NW of Santiago de Compostela (Spain). Ph. D. thesis, Leiden Univ., 208 pp.
- White, A. R. J., 1964. Clinopyroxenes from eclogites and basic granulites. *Am. Min.*, 49, pp. 883–888.
- Wilson, C. J. L., (in press). The prograde microfabric in a deformed quartzite sequence. Mount Isa, Australia.
- Winkler, H. G. F., 1961. Genesen von Graniten und Migmatiten auf Grund neuer Experimente. *Geol. Rundschau*, 51, pp. 347–364.
- , 1966. Der Prozess der Anatexis: Seine Bedeutung für die Genese der Migmatite. *Tsch. Min. Petr. Mitt.*, 11, pp. 266–287.
- , 1967. Die Genese der metamorphen Gesteine. Berlin, Springer-Verlag, 2nd ed., 237 pp.
- , 1970. Abolition of metamorphic facies, introduction of the four divisions of metamorphic stage, and of a classification based on isograds in common rocks. *N. Jb. Min. Mh.*, pp. 189–248.
- Winkler, H. G. F. & Platen, H. von, 1961a. Experimentelle Gesteinsmetamorphose IV. Bildung anatektischer Schmelzen aus metamorphosierten Grauwacken. *Geochim. Cosmochim. Acta*, 24, pp. 48–69.
- Winkler, H. G. F. & Platen, H. von, 1961b. Experimentelle Gesteinsmetamorphose V. Experimentelle anatektische Schmelzen und ihre petrogenetische Bedeutung. *Geochim. Cosmochim. Acta*, 24, pp. 250–259.
- Winkler, H. G. F. & Platen, H. von, 1962. Experimentelle Gesteinsmetamorphose VI. Einfluss von Anionen auf metamorphe Mineralreaktionen. *Geochim. Cosmochim. Acta*, 26, pp. 145–180.
- Wyllie, P. J. & Tuttle, O. F., 1959. Effect of carbon dioxide on the melting of granite and feldspars. *Am. Jour. Sci.*, 257, pp. 648–655.
- Wyllie, P. J. & Tuttle, O. F., 1961. Experimental investigation of silicate systems containing two volatile components; part II. *Am. Jour. Sci.*, 259, pp. 128–143.
- Wyllie, P. J. & Tuttle, O. F., 1964. Experimental investigation of silicate systems containing two volatile components; part III. *Am. Jour. Sci.*, 262, pp. 930–939.
- Yoder, H. S., 1952. The $MgO-Al_2O_3-SiO_2-H_2O$ system and the related metamorphic facies. *Am. Jour. Sci.*, Bowen vol., pp. 569–627.
- , 1955. Role of water in the metamorphism. *Spec. Pap. Geol. Soc. Am.*, 62, pp. 505–524.

Yoder, H. S. & Tilley, C. E., 1962. Origin of Basalt Magmas; An experimental study of natural and synthetic rock systems. *Jour. Petr.*, 3, pp. 342-532.

Yoshino, G., 1961. Structural-petrological studies of peridotite and associated rocks of the Higashi-akaishi-yama district, Shikoku, Japan. *Jour. Sci. Hiroshima Univ.*, C, 3, pp. 343-402.

-, 1964. Ultrabasic mass in the Higashiakaishiyama district, Shikoku, Southwest Japan. *Jour. Sci. Hiroshima Univ.*, C, 4, pp. 333-364.

Zuuren, A. van, 1969. Structural petrology of an area near Santiago de Compostela (NW Spain). *Leidse Geol. Med.*, 45, pp. 1-71.

Localities of the samples mentioned in the text
(in Lambert coordinates)

sample number	sheet	x	y	sample number	sheet	x	y	direction of dip/dip
RGM 162682	7	255.075	1009.975	RGM 162714	7	248.600	1005.680	
RGM 162683	7	255.675	1010.657	RGM 162715	7	248.960	1005.630	
RGM 162684	7	255.300	1009.300	RGM 162716	7	245.250	1006.750	
RGM 162685	7	254.102	1010.375	RGM 162717	7	244.700	1013.995	
RGM 162686	7	254.102	1010.375	RGM 162718	7	244.300	1012.400	
RGM 162687	7	253.390	1009.725	RGM 162719	7	243.625	1013.010	
RGM 162688	7	258.250	1013.275	RGM 162720	7	247.330	1013.740	
RGM 162689	7	256.560	1012.255	RGM 162721	7	244.475	1015.220	
RGM 162690	7	259.775	1013.800	RGM 162722	7	250.400	1004.450	
RGM 162691	7	257.350	1010.750	RGM 162723	7	251.275	1011.390	
RGM 162692	7	251.223	1011.210	RGM 162724	7	251.275	1011.390	
RGM 162693	7	244.725	1010.825	RGM 162725	1	256.570	1015.880	115/90
RGM 162694	7	251.975	1007.950	RGM 162726	1	257.225	1016.875	283/76
RGM 162695	7	252.406	1011.825	RGM 162727	1	256.790	1016.450	275/34
RGM 162696	7	252.406	1011.825	RGM 162728	1	260.320	1019.980	30/65
RGM 162697	7	248.135	1008.450	RGM 162729	1	263.075	1025.860	315/35
RGM 162698	7	244.790	1010.300	RGM 162730	1	259.375	1019.075	340/20
RGM 162699	7	253.840	1012.020	RGM 162731	1	257.750	1015.575	260/20
RGM 162700	7	253.560	1009.375	RGM 162732	1	255.020	1017.560	155/50
RGM 162701	1	254.850	1019.800	RGM 162733	1	254.875	1017.475	175/48
RGM 162702	7	247.220	1013.715	RGM 162734	1	254.420	1015.475	280/10
RGM 162703	7	249.060	1015.000	RGM 162735	7	252.265	1015.340	315/78
RGM 162704	7	251.560	1010.690	RGM 162736	1	252.230	1017.020	104/74
RGM 162705	7	246.450	1011.280	RGM 162737	1	253.275	1016.520	75/80
RGM 162706	7	247.670	1010.040	RGM 162738	1	254.725	1019.800	315/80
RGM 162707	7	244.310	1013.760	RGM 162739	7	244.470	1013.700	300/80
RGM 162708	7	250.400	1004.450	RGM 162740	7	256.755	1014.150	50/45
RGM 162709	7	251.150	1004.600	RGM 162741	7	243.975	1011.200	
RGM 162710	7	251.025	1004.825	RGM-st. 140146	1	269.350	1019.630	250/75
RGM 162711	7	254.680	1009.650	RGM-st. 140199	1	258.040	1017.300	275/30
RGM 162712	7	245.075	1013.975	RGM-st. 140267	1	260.720	1019.930	172/40
RGM 162713	7	247.875	1005.950					

SAMPLE MAP

